UNIVERSITEIT GENT

FACULTY OF APPLIED SCIENCES

Department of Electronics
and Information Systems

BETA

a-SiN:H X – Ray Sensor

Igor A. Popov

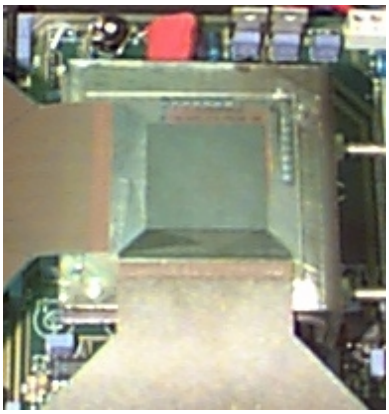

Promotor: Prof. Dr. ir. A. Van Calster
Co-promotor: Prof. Dr. ir. H. De Smet
Thesis submitted for obtaining the
Degree of Doctor in Applied Sciences

Academic year 2000 - 2001

Acknowledgements

I would like to thank all the people who were involved with this work. It was a long undertaking and now it is finally over. And may be it is time to admit, only this once, that I was not the easiest person to work and live with during these years.

I would like to express my deepest gratitude to Andre Van Calster and Jan Vanfleteren for giving me the possibility to join TFCG and for encouraging my continuous work here. The fact that at this stage of my life I am still working with something I like and draw enormous satisfaction from should be attributed to them.

"X-ray Discussion club" is the entity which had a big impact on the results of this work. It draw together Herbert De Smet, Johan De Baets, Geert Van Doorselaer with the sole goal of tackling all x-ray sensor and array related problems. I would like to extend my thanks to them. And especially Geert who's contribution to the development of functioning prototype includes all the driving / read out electronics and can not be overestimated.

Actual field measurements would be impossible without Prof. E.Boesman, Prof. F. Callens from the Solid State Crystallography Group. I would like to thank them for their long term co-operation and useful discussions through all these years.

Thanking people directly involved in everyday x-ray way-of-life I cannot but mention Herbert De Pauw and Jean Van Den Steen. Volunteering to help once brought them into misery of regular transportation and redeployment of equipment at x-ray measurement site. I would quite understand if they have had some words they meant to say to me for all the time they have spent and I am grateful they never did.

This work would not be brought to the successful finish without great atmosphere and co-operation in our TFCG clean room. I would like to express my deepest gratitude to Dieter Cuypers and Nadine Carchon for all their help and understanding when I could not live up to my own planning.

And in this closing part I would like to thank all my friends, including people I already mentioned. I can not name every one here without running into risk that this will look like credits to some Hollywood movie but I want you to know that I am very grateful. Wherever you are now, I am grateful for discussions, nice, though sometimes naïve, questions, going through my English, having a shoulder or cold shower always ready, occasional chess games, atmosphere, letters and e-mails, parties and quiet times. Thank you. And, yes, I mean you.

And last but not least I would like to thank my mom and dad, my dear brothers, and, sure, Da Shura.

Sometimes the best answer is more interesting question…
T. Prattchet

Foreword

This thesis consists of 118 pages, 43 figures and 31 tables divided between four chapters and three appendixes. Information given in appendixes is considered useful but not critical in achieving the goal of the work. Also while discussing different research / analysis methods I have limited myself to practical implementation of those, always referring to the sources containing full description of the methods. I hope that such approach has allowed me to present a comprehensive work with clearly seen core.

The ultimate goal of this work is to demonstrate the possibility of realising of an "all a-Si" direct x-ray sensor array. I think everyone would agree with the statement such as "if it *can* be done in silicon, it *will* be done in silicon eventually" but unfortunately there is quite strong opposition to the fact that *it* actually *can* be done in silicon. Naturally, before any discussion and research work on the topic can be started we have to assert our standpoint. This is the subject of the *Chapter I: Problem definition*.

Chapter I can be subdivided into three closely connected parts. First of all, it is an analysis of the current trends in the area of digital radiography in the context of the state-of-the-art systems. Such an analysis helps to understand advantages and disadvantages of the different systems as well as to answer the question on why there are so many approaches to a task of substituting "simple photo film". At the same time the role of a-Si alloys in digital radiography starts to become visible. And it is not much of a role, far too small for such a potential material as a-Si alloys. Quite naturally in the second part of the Chapter we have an in-depth look on (i) the radiation we have to deal with, (ii) why Si was never considered a real contestant for the task and (iii) what can be done to alter the current state of affairs. While dealing with these questions it becomes clear that problem is indeed not trivial, with severe, sometimes contradictory requirements to the material properties. Fortunately we are working with amorphous silicon, material of unique properties. And in order to reach our goal we will have to use these properties. This is why the third part of the Chapter is devoted to structure modification of a-Si alloys with the use of a-Si:H as a model material. a-Si is the most used material in thin-film electronics, and TFT is the most used device. This is the reason we used those to demonstrate the power of the approach. At the end of the Chapter amorphous hydrogenated silicon rich silicon nitride is introduced as a material of probable interest for us. The attractive sides of a-SiN:H includes its structural properties and its use in Thin Film Diode arrays both as a switching and sensing elements.

Before processing with x-ray sensing applications one wishes to have total understanding of a-SiN:H TFD, its performance limits and to which extent one can influence these limits. This is the subject of *the Chapter II: a-SiN:H thin films for TFD array applications*, chapter which lays technological foundation for our future work. So it starts with the overview of a-SiN:H technology. This overview includes description of the hardware used for the a-SiN:H deposition as well as selection of the film's characteristics we are going to control and respective measurements techniques. Description of the "TFD test cell" - test vehicle developed especially for a-SiN:H TFD study concludes technology overview.

The common problem of the technological experiments is the overwhelming amount of experimental data that needs to be obtained and analysed. Even for the simple PECVD reactor like one used in this work we will need thousands depositions in order to get basic understanding of the process. And yet our main goal will not be achieved. This is why the next part of the Chapter is devoted to mathematical aspects of the material science. *System of Experimental Design* and *Taboo search* are chosen to help us solve the problem of enormous amount of experimental data. Practical aspects of implementation of these methods are given in the *Appendix A*.

But the core of the Chapter II is the technology of a-SiN:H TFD. Sub-goal of this part is to develop technology processing of state-of-the-art a-SiN:H TFD. And before a-SiN:H TFD direct x-ray arrays become commercially available - state-of-the-art is LCD driven by a-SiN:H TFD. This sub-goal is reached through two level technological experiments. At the first level we select PECVD process window on the base of existing experience and reference data, keeping in mind that we want structurally stable thin films (the main goal is TFD working under x-ray irradiation, so lifetime is one of the biggest problems we will face). On the base of the first approach experiments we are able to refine our process window and tune electrical characteristics of the TFD. This tuning is achieved through modification of material as well as with optimising design aspects of the TFD. Spin-off of the work presented in this Chapter is the technology of LC display controlled by matrix of a-SiN:H TFDs - given in *Appendix B*.

Now that we have a state-of-the-art a-SiN:H TFD it is the time to return to the source of this work and have an in-depth look at the subject of the *Chapter III: a-SiN:H TFD in x-ray environment*. Chapter starts with the discussion of the experiment setup, including the available x-ray source and what and how we can measure. New test vehicle - "X-ray test cell" is also described. Special feature of this test vehicle is that it already includes different hardware simulators of pixel for x-ray sensing.

Two principally different approaches to study of a-SiN:H behaviour under x-ray irradiation are used. Firstly, there is static radiation damage experiments

in which TFD is exposed to radiation without any controlled voltage on its terminals. Such experiments allow to judge on the lifetime of the TFD (quality judgement). This is quite important because electrical measurements under direct x-ray irradiation is quite difficult and time consuming exercise. Conducting such measurements on the TFD that is not fit from the lifetime point of view is just a waste of valuable time. So the study of the electrical performance of the TFDs under direct x-ray irradiation is done on the TFDs that passed first “screening” stage of experiments.

Knowledge of the a-SiN:H TFD accumulated during the work described in Chapters two and three has allowed us to start optimisation of the TFD. Although there is little that can be done with TFD operating as a switching element there is a lot we can do with sensing TFD. And this is the subject of the last part of the Chapter three. All aspects of a-SiN:H TFD, such as design, material properties, nature of the sensing effect are being analysed in order to create TFD with maximum response to x-ray irradiation. Some theoretical ideas - such as enhancing a-SiN:H x-ray stopping efficiency - could not be realised in full in the frame of this work due to lack of hardware. Yet we discuss this though we do not use it. In this work we are looking for integral approach to problem - the only possible approach. And leaving out possible answers only because of “right here right now“ hardware problem just does not seem right.

Chapter IV: a-SiN:H TFD x-ray sensor array is devoted to the practical implementation of the results obtained in the course of this work. We have seen that the strongest point of a-SiN:H TFD in x-ray environment is its sensing effect. If one would like to use such TFD as a switching element, one would need to shield it from x-rays. Such an approach can not be accepted because it complicates the sensor array build -up process. This is why we have chosen to use driving strategy that is novel for digital radiography. With use of this driving strategy switching element in the pixel becomes obsolete.

New test vehicles are designed and produced in order to test our approach to the “array” and make necessary adjustments. Experimental results on pixel and array layouts, judgement on feasibility of suggested driving strategy constitute the core of this Chapter. Also 2D a-SiN:H TFD x-ray sensor prototype with customary driving and read-out electronics is described.

The *Conclusion* summarises the major results. The key points of this work that contribute to the current knowledge in the field are:

- introduction of a-SiN:H as a competitor to the “conventional x-ray sensing materials” for digital radiography;

- development of the technology processing of a-SiN:H TFD as a sensing element for the low energy 20 - 60 keV x-rays;

- introduction of the novel driving strategy that allows to utilise the unique characteristics of a-SiN:H TFD in the large area array applications

Other significant points include:

- practical application of structure modification to a-SiN:H thin films;

- development of a-SiN:H technology suitable for TFD driven LCD;

- integration of System Experimental Design with Taboo Search into real life technology process

The results of this work were discussed at:

- Society for Information Display meetings in 1995 - 1996,

- The International Society for Optical Engineering (SPIE) meeting in 1998

- International Congress on Imagine Science in 1998

- Material Research Society meeting in 1998 - 2000

- International seminar on Noise and Degradation processes in Semiconductor Devices, in 1997 - 1999

The list of published papers on the subject is given in the next section.

List of publications

I.A.Popov, L.D. Nazarova, *Predicting the stability of the characteristics of thin-film transistors on the basis of fundamental characteristics of a-Si:H films*, Semiconductors 28 (6) June 1994 pp 564-566

I.A.Popov , A. Van Calster, J. Lernout, *Stable a-SiN:H TFD for use in X-ray environment*, Proc. AsiaDisplay'95, Hamamatsu, Japan, 1995, pp. 297-300

I.A.Popov, *Structural modification of films of amorphous hydrogenated silicon using ultraviolet radiation*, Semiconductors 30 (3) March 1996 pp 258-261

I.A.Popov, A. Van Calster, BP Tchernorotov, *Production of stable a-SiN:H TFD for use in x-ray image sensor*, Proc. Int. Sem. Noise and degradation processes in semiconductor devices, Moscow, Russia, 1996, pp. 314 - 320

I.A.Popov, A. Van Calster, H. De Smet, E. Boesman, F.Callens, *2D direct X-ray sensor array on the base of a-SiN:H thin films*; Proc. EuroDisplay'96, Birmingham, England, 1996, pp.431-433

I.A.Popov, G. Van Doorselaer, A. Van Calster, H. De Smet, F. Callens, E.Boesman, *Prototype of 2D direct X-ray a-SIN:H sensor array*; Proc. SPIE Solid State Sensor Arrays: Development and Applications II, V3301, 1998, pp.126 - 130

I.A.Popov, G. Van Doorselaer, A. Van Calster, H. De Smet, F. Callens, E.Boesman, *a-SiN:H TFD sensor array for digital radiography*, Proc. ICPS (International congress on digital radiography) Antwerp, Belgium, 1998, pp. 315 - 319.

I.A.Popov, G. Van Doorselaer, A. Van Calster, H. De Smet, F. Callens, E.Boesman, *Material aspects of a-SiN:H based 2D direct X-ray sensor array*; Proc. MRS Amorphous and Microcrystalline Silicon Technology, V. 507, 1998, pp.231 - 236.

I.A.Popov, G. Van Doorselaer, A. Van Calster, H. De Smet, F. Callens, E.Boesman, *a-SiN:H thin films for x-ray sensor array*, Proc. Int. Sem. Noise and degradation processes in semiconductor devices, Moscow, Russia, 1999, pp. 123 - 129

I.A. Popov, G. Van Doorselaer, A. Van Calster, H. De Smet, J. De Baets, F. Callens, E. Boesman *a-SiN:H thin film diode for digital radiography*, to be published MRS 2000 Spring meeting proceedings “Amorphous and Microcrystalline Silicon Technology 2000”.

I.A. Popov, A. Van Calster, J. De Baets, H. De Pauw, *Implementation Of The System Of Experiment Design And Taboo Search Into SiON Thin Film Technology*, III SIAM conference on Mathematical aspects of material science, Philadelphia, 2000

A.I. Popov, V.A. Voronchov, I.A. Popov, Applications of the different levels of structure modification of non-crystalline semiconductors, Proc. II Int. conference on Amorphous and Microcrystalline Semiconductors, St.Pietersburg, 2000 (in Russian), pp. 11 – 12

I.A. Popov, H. De Pauw, A. Van Calster, J. De Baets, *SixNy Based Active Devices For Array Applications*, submitted for MRS 2001 Spring meeting.

TABLE OF CONTENT

Chapter One : Problem definition.

Digital radiography.

Digital radiography attracts a lot of attention for a long time already but until lately a little progress could be observed. Screen/film systems were and until now are the major media used in radiography for medical and industrial (non destructive testing) purposes. So why one wishes to exchange this screen/film systems that have been in use for almost 100 years with something totally new? To answer this let us compare screen/film radiography system with digital (*film-less*) radiography system.

- Digital radiography is silver-less technology. This may be not the most actual problem of today, but it reflects the irreversible trend in imagine science and gains more importance with every year.

- Images acquired with digital technology do not need to be post processed, meaning steps like developing for the film systems, that involve toxic and dangerous solutions.

- Although film is almost perfect media for displaying image it is far from perfect from the point of view of x-ray absorption, thus one has to use screens (intensifiers), that leads to the poorer image quality (decrease of the image contrast mainly) due to the photon scattering.

- Time between image acquisition and displaying for the digital system is few seconds and the existing trend is to go to the real time video signal. At this characteristic digital system is far more superior to the screen/film system. Practical implementations of this is that amount of re-takes due to various reasons such as faulty film, wrong positioning of the x-ray source/area of investigation will be reduced greatly with the use of digital systems.

- But the main reason of growing interest in digital radiography is that such systems has potentially higher sensitivity than screen/film systems. In everyday life this means lower radiation doses for medical/industrial applications or higher quality picture.

Whenever one speaks about x-ray image acquisition, screen/film or digital system, the main steps are the same: x-ray photon absorption and registration of the amount of x-ray photons absorbed. The difference between *indirect*

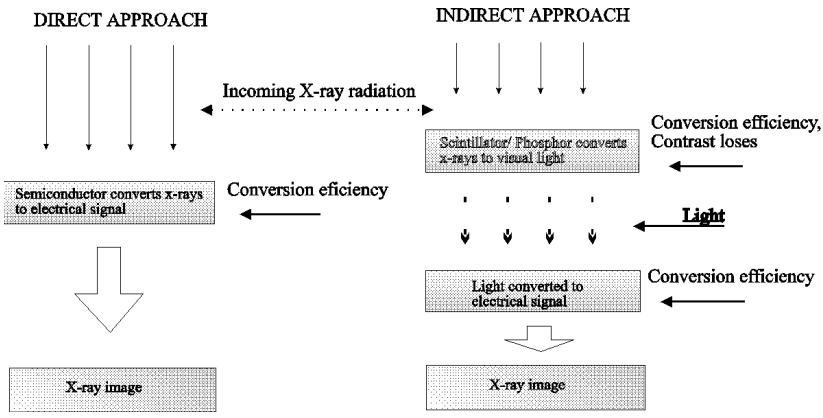

Figure 1-1 X-ray image acquisition flow for direct and indirect approaches

and *direct* solid state x-ray sensors is originated from how one deals with these two steps. If one chooses to use different materials for x-ray photon absorption and registration we talk about indirect approach. If the same medium (atomic network) is used for x-ray photon absorption and delivery of the proportional electrical signal we talk about direct approach. There are certain advantages and disadvantages in both of the approaches that originate from the nature of x-ray imagining.

The main parameter which characterise the overall performance of any radiographic system is quantum efficiency of the system DQE. System's DQE is the product of the quantum efficiency of the x-ray photon absorption multiplied by quantum efficiency of the conversion of absorbed photons into the electric charge carriers and multiplied by charge collection efficiency. By definition any of the three parameters with the lowest value will limit overall system's performance. The basic difference between indirect and direct approach now can be described as: indirect approach is based on increasing of x-ray photon absorption efficiency while direct approach is looking for increasing of charge collection efficiency.

The difference between direct and indirect approach is illustrated in Figure 1-1, where limiting factors are also mentioned. For the direct approach this x-ray photon absorption efficiency. Primarily it is the function of atomic weight and density of the material, and for the given material it decreases with the increase of x-ray photon energy. Normal range of x-ray energy used in radiography (medical or industrial) covers the range of at least 10 - 1000 keV and it is virtually impossible for the direct approach cover this range. In indirect approach one uses some kind of x-ray-to-less-energetic-radiation (visual light for example) conversion layer that provides high x-ray absorption efficiency over the whole range of x-ray photon energies. Being far

more effective than direct approach for the high x-ray photon energies indirect approach faces strong competition at the low -to-moderate x-ray energies.

The advantages and disadvantages of the different approaches could be best discussed on the real life state-of-the-art systems. In my believe these are:

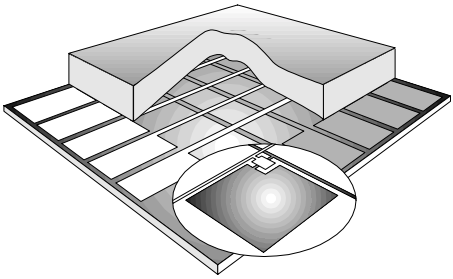

Figure 1-2 Digital radiography system utilising indirect approach (dpiX)

- Indirect approach: system of dpiX (USA)

- Direct approach: systems of Sterling (USA), Phillips (ND), University of Waterloo (Canada).

Indirect approach.

Typical system for digital radiography utilising indirect approach is shown in the Figure 1-2 [1,2]. It includes CsI based scintillator for conversion of the incoming x-ray radiation into the green light and 2D array of pixels, each of them consisting of the photodiode and thin film transistor (TFT). Photodiode is used for conversion of the light energy into electrical form and for storage of proportional electrical charge between frames. TFT is used for reading out particular pixel. On the insert the pixel layout is shown with the photodiode occupying the biggest part of the pixel. The question of the system optimisation now is separated into two different tasks:

- optimisation of scintillator - including subtasks to (a) increase of x-ray absorption efficiency, (b) decrease of generated light absorption in scintillator, (c) decrease light dispersion, (d) optically couple the scintillator and a-Si:H photodiodes.

- optimisation of the active matrix and sensing photodiodes includes mainly design aspects such as “useful” pixel area and so on. On material (both TFT and photodiode are build on a-Si:H) side there are very few problems - it is the well established technology for flat panel displays and scanners. Since the scintillator is designed to absorb 100 % of incoming x-ray irradiation active matrix (AM) underneath it sees no x-rays whatsoever. In this way the conditions of its operation differ not from the scanner conditions of operation.

Described indirect sensing system use low (< 5 V) voltage. But there are two basically different technologies (a-Si:H and CsI) involved into production of the final system.

Use of the additional conversion step - x-rays to light - and photodiode as a sensing element[1] are the limiting factors to the efficiency of the whole system. Nevertheless such systems are in the stage of clinical testing nowadays and perform on the level of the film/screen systems in similar conditions [3].

Direct approach.

Development of the digital radiography systems using direct approach was fuelled up by the wish to delete the intermediate x-ray - to - light step and problems and limitations which existing of such step impose. Thus, the strategy of the image read out stays the same - AM of a-Si:H TFTs. But system of scintillator plus a-Si:H photodiode is changed to system of the direct x-ray-to-electrical signal layer plus storage capacitor. Different research groups investigate the possibility of using different materials for a x-ray-to-electrical-signal layer. The most pronounced examples are a-Se (Sterling) and PbO (Phillips). Typical pixel structure is shown in Figure 1-3. As for pixel layout it differs from system to system depending on the developer's priorities such as aspect ratio, lifetime etc. [1,4,5,6]

Physics of the sensing process in direct approach is that conversion layer is reversed biased (depleted). Absorption of x-ray photon in depleted region leads to electron-hole pair generation which are immediately separated by

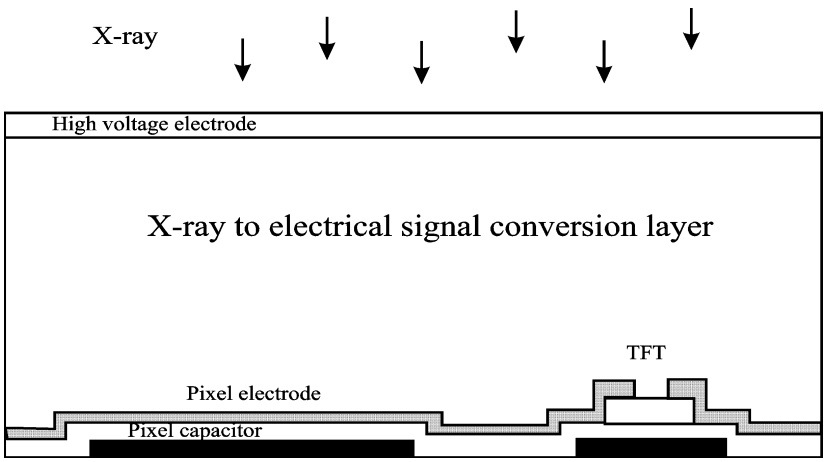

Figure 1-3 Typical pixel structure of the direct approach system

[1] Quantum efficiency of light conversion for the a-Si:H photodiode is below 20 %

external field. Charge proportional to the amount of absorbed photons is stored on the storage capacitor until read out. Such sensing process has some positive and negative sides.

First of all, using external field to separate charge carriers drastically improves image contrast compare to indirect systems. But the other side of the coin is that additional power supply is needed.

Secondly, one wishes to absorb as much x-ray photons as possible and keep the depletion region as wide as conversion layer thickness. This leads to the thickness of conversion layer comparable to that of scintillator in indirect systems. In it's own turn the use of such thickness leads to the need of high voltage external source in order to create sufficient depletion.

As well as in case of indirect approach such system uses well established technology for the a-Si:H TFT active matrix formation. Then, the x-ray to electrical signal conversion layer with the high voltage electrode is formed.

Naturally, the need of high voltage[2] is the major disadvantage of the system in discussion comparing to the indirect approach. So the major efforts are being taken to decrease needed value of the high voltage. One of the suggestions [5] is to use PbO instead of a-Se. As it claimed by Philips Research laboratories "it would be highly attractive to operate a 280 μm thick PbO layer at 1000 V rather than a 500 μm thick selenium layer (the same absorption) at 5000 V". There is no place to go into the details of "the same absorption" definition [7], but two major moments should be pointed out:

- Firstly, favourable estimation of PbO properties is based on the use of PbO as photoconductor in plumbicon camera tubes [5]. There is a technological challenge to produce thick PbO layers in a versatile process and keep the desired physical properties of the material.

- Secondly, a-Se based X-ray sensors operating at voltage 500 V are commercially available already now.

Basically different approach to the direct sensing at low voltage was demonstrated by the group of [8] (Waterloo University, Canada). In this approach an a-Si:H Schottky diode is used as a sensing element. Basic pixel structure is shown in
Figure 1-4 . Image acquisition is based on the next process: high energy x-ray photons are absorbed in thick Mo top electrode leading to injection of high energy electrons in to a-Si:H. These electrons (as well as secondary) are separated in reverse biased Schottky diode.

[2] Up to few kV in a early systems

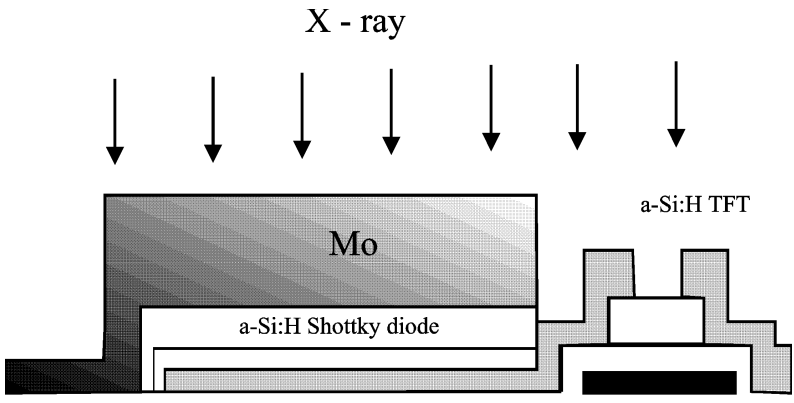

Figure 1-4 Pixel structure of a-Si:H based x-ray sensor

One of the strongest points of approach in the discussion is that for the first time both active matrix and sensing element are produced in the frame of the same, well developed a-Si:H technology. Technological challenge of producing thick (~500 nm) Mo layers is not as hard as one for PbO. One of the problems that did not exists in indirect approach, shows itself in approach with uniform a-Se or PbO conversion layer and reaches it's maximum in the current approach is that switching TFT is exposed to x-rays as well. Now the lifetime of the system is determined not only by lifetime of x-ray sensing element but also by lifetime of the TFT under the direct x-ray irradiation, whichever is worse.

The short summary of the current state of development of solid state x-ray sensor arrays for medical purposes is presented in Table 1 - 1.

Table 1-1 Data sheet on the digital radiography systems currently under development

	INDIRECT APPROACH	**DIRECT APPROACH**		
	dpiX	***OIS***	***PHILIPS***	***UnW****
Structure	TFT + scintillator + a-Si photodiode	TFT + a-Se	TFT + PbO	TFT + a-Si:H Shottky diode
Voltage	Low voltage	1000 V	450 V	Low voltage
Charge storage	a-Si photodiode	Storage capacitor	Storage capacitor	Shottky diode
Output signal	-	-	*n* nA on single cell	10th nA
Problems	Commercially available	Commercially available	PbO technology	Mo technology, aspect ratio
Lifetime	a-Si / scintillator	a-Se		Shottky diode, TFT**

* - University of Waterloo, Canada
** - Mostly solved, the group has impressive record in the field of stability of a-Si:H TFTs

Role of a-Si:H in digital radiography.

As we saw from the above any solid state digital radiography system consists of two major parts:

- part responsible for the detection of the electrical signal proportional to the x-ray dose (two step conversion for indirect approach and one step conversion for the direct approach);
- part responsible for retrieval of the obtained information.

Speaking about the role of amorphous hydrogenated silicon or it's alloys in digital radiography one will focus on "information retrieval" part. Indeed, any of the systems discussed above is using a-Si:H TFTs in active matrix to control information flow from the pixel to peripheral electronics. More than twenty years experience in the AM LCD gives a-Si:H TFTs the first place in the race. Large area applications, TFT size, lifetime issues, radiation resistance - these topics were worked at by numerous researches all over the world.

This is basically it - "role of a-Si:H in digital radiography". Any other than this application would face the fact that Si is not a very effective medium to absorb x-ray radiation. This can be clearly seen from the Table 2, where data on x-ray absorption efficiency for the most popular materials is presented[3]. In fact, low x-ray absorption is additional plus to a-Si:H TFT. It does not matter for indirect approach, where TFT does not see x-rays whatsoever and shielded from the visual light. But it does determine the lifetime of the systems that use direct approach. It may vary from system to system and from one a-Si:H technology to another but one is always keeping eye on his a-Si:H TFT performance in x-ray environment.

Impossibility to use a-Si for effective absorption of x-rays (3 mm thick a-Si:H films are technological nonsense) and it's unchallenged superiority in AM fabrication is the reason why current digital radiography systems are using different materials and technologies in a system build up process.

Nevertheless there are motions to expand the field of application of a-Si:H films in digital radiography such as, for example, system of University of Waterloo (
Figure 1-4). Systems build up process is 100 % compliant with the thin film technology and a-Si:H film is used in sensing element. Although one can see a-Si:H Schottky diode as a x-ray sensor in a way of modification of indirect approach (conversion of x-rays into electrons in top electrode and injection of electrons into a-Si:H film) but both steps are taken place in the same device and the trend shows itself clearly.

[3] Selection of 30 kV for comparison will be clear later in this chapter

Table 1-2 Theoretical values of photoabsorption cross section and attenuation length for different materials at 30 kV

Material	Atomic weight	Density, gm/cm^3	Photoabsorption cross section, cm^2/gm	Attenuation length, μ
Se	78.960	4.5	15.77	140.9
Cs	132.905	1.87	8.823	605.1
Pb	207.2	11.4	28.60	30.80
Mo	95.940	10.2	27.69	35.33
Si	28.086	2.33	1.141	3762.0

There are certain moments in x-ray generation and application that allows us to expand the role of a-Si:H films in digital radiography.

X-ray source is characterised by material of anode (W anode x-ray tubes are most popular), voltage on the anode (starting from 20 kV and all the way up), current. Increase of the voltage will result in increase of the photon energy and increase of the current will result in increase of number of photons. Total dose then is the product of some constant, which is function of voltage, distance, material of anode, x-ray spectra) multiplied by voltage multiplied by current multiplied by time. Different x-ray investigation require different total doses and most of the time dose will be controlled by choosing either voltage or current. Direct sensing approach is focused on the low voltage end of spectra.

X-ray spectra is of extreme importance when one wishes to optimise response of the device to x-ray irradiation. Theoretically the intensity distribution of the continuum i.e. the number of photons as a function of their retrospective energy, is characterised by a short wavelength limit corresponding to the maximum energy of the exciting electrons (i.e. the kilovoltage kV employed). The distribution of the continuum can be expressed in terms of excitation conditions by means of Kramers formula:

$$I(\lambda)d\lambda = KZi\left|\frac{\lambda}{\lambda\min}-1\right|\frac{1}{\lambda^2}d\lambda \quad \lambda\min = \frac{12.4}{kV}$$

This formula relates the intensity I(λ) from an infinitely thick target of atomic weight *Z* with applied current *i* where *K* is constant. This expression does not correct for self-absorption by the target which in practice leads to some modification of the intensity distribution.

Exact measurements of spectra is a very hard task normally performed by developers of x-ray tubes and then distributed. As an example on the Figure 1-5 (courtesy of AGFA Gevaert n.v.) x-ray spectra at 80 kV is shown. Value

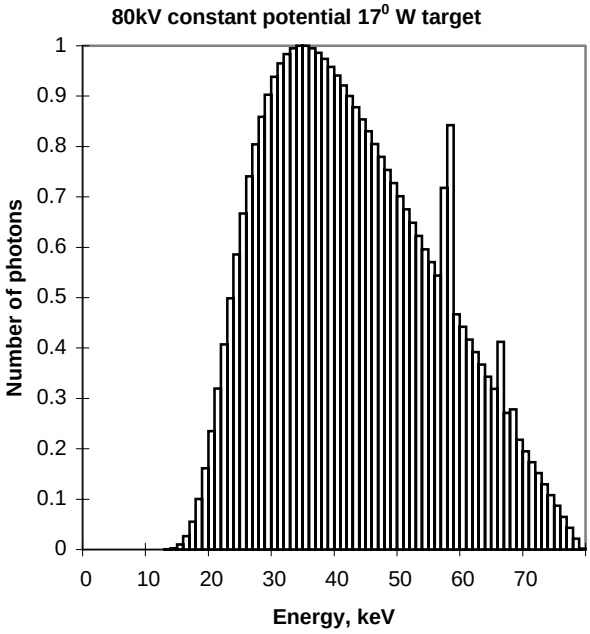

Figure 1-5 W anode X-ray spectra at 80 kV / 3 mm Al filter

Additional information to the Figure 1-5

Mean photon energy = 47.7 keV
Photon flux at 0.75 m = 2.88x10^{6} photons mA^{-1} s^{-1} mm^{-2}
Kerma in air at 0.75 m:
Mean energy 37.7 keV
Output = 137 μGy mA^{-1} s^{-1}
(Exposure 15.77 mR mA^{-1} s^{-1})

Table 1-3 Photon spectrum in 1.0 keV steps

keV	**1**	**2**	**3**	**4**	**5**	**6**	**7**	**8**	**9**	**10**
1-10	0	0	0	0	0	0	0	0	0	0
11-20	0	0	0	1	8	29	75	157	284	455
21-30	664	902	1154	1409	1655	1885	2092	2272	2426	2551
31-40	2651	2726	2778	2811	2825	2825	2811	2786	2751	2706
41-50	2658	2603	2543	2480	2413	2345	2274	2202	2129	2055
51-60	1981	1907	1833	1759	1684	1611	1537	2029	2380	1320
61-70	1249	1178	1108	1038	969	901	1164	766	786	616
71-80	551	490	429	367	306	245	183	122	61	5

of 80 kV is one of the most used in x-ray examinations and de facto is standard value for comparison of different systems performance.

In addition to the Figure 1-5 photon distribution by energies is shown in the Table 1-3, and some extra information on x-ray spectra is printed in italic on the previous page.

As can be seen from the data presented above, the most of generated photons have an energy in range 30 - 50 keV. After travelling distance of 0.75 m the original spectrum is modified due to absorption by air and the average photon energy drops to 37.7 keV. This data illustrates the fact that in x-ray radiography with energies below 100 keV the major part of information is delivered by photons with energies around 40 keV. In fact, one may focus on retrieving information from low energy photons (many photons, low penetration efficiency) accepting that information delivered by high energy photons (fewer photons, high penetration efficiency) will no be used efficiently. This draws a natural limit on maximum energy of incoming x-ray radiation.

Targeting to detection of photons with specific energy that have the most of information load is the niche for the full a-Si:H 2D x-ray sensor array. Field of radiography (medical and industrial - Non Destructive Examinations) is so wide that there always will be areas where use of a-Si:H array is appropriate. Using well established technology for the building up such an array will allow drastically increase the yield and decrease the cost of the system. Advantages are numerous and the goal of this work is to demonstrate the possibility to expand the role of a-Si:H in digital radiography beyond the use in pixel information retrieval.

Structure modification for a-Si:H alloys as a method of improvement of thin-film devices' performance.

Building the all a-Si:H x-ray sensor array includes different subtasks but the main subtask of them all is designing new material which will guaranty all needed properties. This is why this part is devoted to the structural properties of the non-crystalline semiconductors and how we can use them to engineer materials with required characteristics.

The idea behind the structure modification method is to control the material properties by altering its structure while the chemical composition stays constant. There are at least three possible levels at which structure could be altered:

- structure altered at the level of *close order* - influences all properties, determined by close order, electrical, optical, mechanical etc., example: a-C;

- structure altered at the level of *medium order* - influences macro properties, such as viscosity, density etc, example a-Se;

- structure altered at the *defect subsystem* level - influences electrical and optical properties, example a-Si:H alloys.

Let's us discuss the latter case somewhat more, because it is directly related to task of this work.

a-Si:H as a model material.

Electrical and physical parameters of non-crystalline materials are determined by the density of localised states (DOS) in the gap. In its turn the DOS depends strongly on the structure and "history" of the films. There are at least two kinds of disorder in hydrogenated amorphous silicon alloys which should be taken into account: (i) "deformation" disorder - deformation of chemical bonds length and angles and (ii) "composition" disorder - due to the existence of different structural units, containing two or more chemical elements, randomly distributed in the volume. Part of the dangling bond (DB) defects originating from "deformation" disorder are "stable" since breaking the Si-Si bond with high deformation energy leads to the decrease of full energy of the whole system. Such defects can be found in every a-Si alloy and their energy position is in the middle of the gap. Every other defect whose appearance is not connected to the relaxation of the whole system to the state with the minimal possible energy should be considered as "unstable". At the micro level one can separate the next potentially unstable defects: neutral and charged DB, weak Si-Si bonds, di- and tri-hydride bonds themselves and especially neighbouring to the DB. The behaviour of those "unstable" defects under the different influences will determine the changes in the electrical and physical properties of the films.

Thus, the main goal of the a-Si:H alloys technology processing is production of the thin films with the minimal concentration of "unstable" defects with the respect to the electrical requirements for the device and conditions of its operation. This can be either through careful control of a-Si:H alloys technology [9] or, as we going to show, the use of the structure modification method [10,11]. Technology of a-Si:H alloys is the key point. Once paid attention it is allow to achieve the performance of the state-of-the-art devices on the simplest designs.

Once again, the idea behind the structure modification method is to control the material properties by altering its structure while the chemical composition stay constant. Originally it has been developed and used for optimisation chalcogenide semiconductors properties [10]. As was found the theoretical possibility of properties' structure modification could be estimated using the coefficient of the structure modification efficiency:

$$Ksme = \frac{(Nos - Nc)}{Nc(1 - Ic - M)}$$

where Nc and Nos are the average coordination number and the average number of electrons in the outermost shells of the atoms respectively, Ic is an average coefficient of bond ionicity, M is the factor taking into account the metallisation of chemical bonds.

For the pure amorphous silicon with a rigid network of covalent bonds Ksme equals 0. Introduction in a such network of H, or H and N atoms leads to a decrease of the average coordination number for the Si network thus the Ksme value increases. However in "device quality" a-Si:H films its value is still only 0.02, which is negligible compared to chalcogenides.

So one can conclude that there is no use to implement the structure modification method for covalent non-crystalline alloys since it will not be effective. But, on the other hand, it is well known that manufacturing aspects and the "history" of the films greatly influence the properties of films, especially those properties which are determined by the electron sub-system. Hence one could suppose that structure modification of properties goes through the changes in concentration and types of defects due to local re-arrangement of neighbouring atoms but not through the modification of the whole network as in the case of chalcogenides. Accordingly, the requirements for the external influence which is supposed to cause structure modification must be reformulated - it must have greater effect on the defect sub-system than on the whole atomic network.

Disordered solids have not only different electrical and optical properties than crystals, but also specific phonon effects: localised phonons [12-15]. Existence of such phonons in a-Si:H alloys is strongly connected with the presence of hydrogen.

Thus, theoretically, the efficiency of structure modification of properties increases for hydrogenated a-Si. Introduction of hydrogen into the a-Si network also alter the phonon spectrum of the material - appearance of the energy- and space- localised phonons. Point absorption of such phonons in a cluster containing Si-H_n groups (as an example: a weak Si-Si bond or a dangling bond in the vicinity of a Si-H_n group) could lead to the local re- ar-

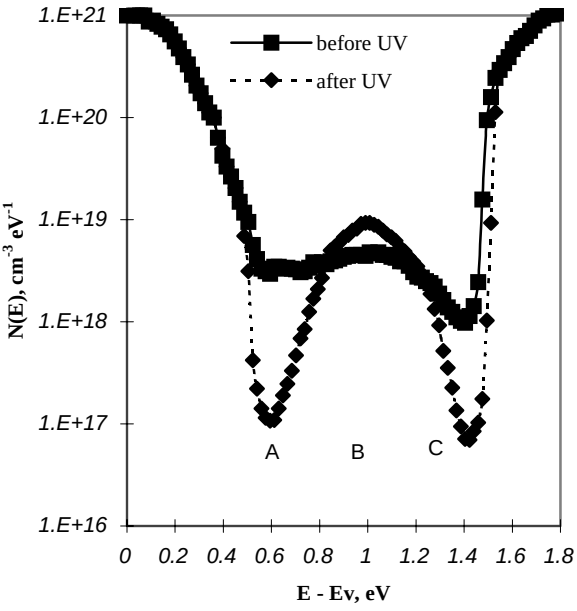

Figure 1-6 Density of localised states before and after x-ray irradiation build from: A-CPC; B-field effect,; C-SCLC

rangement of the neighbouring atoms and/or to a change in a state of the hydrogen atoms. Both of the processes will influence the electro-optical properties of the material.

The question of choosing an external influence which will allow to see the effects mentioned above could be solved on the base of existing data. Since one wants to see the effects caused by localised phonons there is no way of using annealing, white light, an electric field or additional hydrogenation because these alter the atomic network of the material rather than mostly defect centres. The use of UV irradiation [16] looks more attractive. Firstly, the regions of phonon generation and phonon absorption are separated. Secondly, there is no more doubt about what causes the changes in the field effect measurements - modification of the film or film/dielectric interface.

The experimental results of the structure modification of a-Si:H films are presented below. a-Si:H thin films used are these of “device quality” with about 10% of hydrogen content. The intensity of the UV irradiation is 6 mW/cm^2 with photon energy > 3.4 eV. Methods used for studying the DOS spectrum include: (i) temperature dependence of conductivity in the interval 100 - 400 K; (ii) field effect measurements; (iii) Space-Charge Limited Current measurements; (iv) Constant PhotoCurrent and IR spectroscopy. Such

a combination of methods allows to observe the changes in DOS almost over the entire forbidden gap.

SCLC measurements help to receive data about the DOS spectrum in a region between Fermi level and the bottom of the conductivity band. For the irradiated samples the energy interval, in which the obtained information is reliable, is getting much wider and a decrease of density of localised states in the global minimum is clearly observed. The CPC method allows to register changes in the DOS spectrum above the valence band and to estimate the Urbah energy from the absorption curves. For the irradiated samples a sharp (at least one order of magnitude) decrease of DOS at the level of 0.6±0.1 eV above the valence band is observed as well as a 10% decrease in Urbah energy.

The experimental data from the measurements mentioned above together with computer modelling leads to the DOS spectrum shown in Figure 1-6 before and after the UV irradiation with a dose of 10^{19} cm $^{-2}$. The major effect of the selected level of irradiation is in narrowing both band tails with the proportional increase of the deep states. It could be assumed from the above that the main effect of the structure modification in a-Si:H alloys is a transfer of defects from an “unstable” to a “stable” state.

Changes in the DOS spectrum in this interval must be seen on the IR spectra as well - in part of the hydrogen behaviour. The absorption peak at 500 - 700 cm^{-1} was approximated by superposition of the 3 Gaussians: 590 cm^{-1} - $Si-H_2$; 610 cm^{-1} - Si-H; 640 cm^{-1} - $Si-H_2$, $Si-H_3$ bonds. Dependence of the absorption integrals on the UV dose is shown on Figure 1-7. For the optimal UV doses the a-Si:H films also become about 5% more transparent in the range 400 - 2200 cm^{-1}. Thus it is possible to suppose that part of newly created “stable” DB are neutralised through a reaction like show below. Disintegration of the already existing $Si-H_2$ bond does not have a noticeable rate.

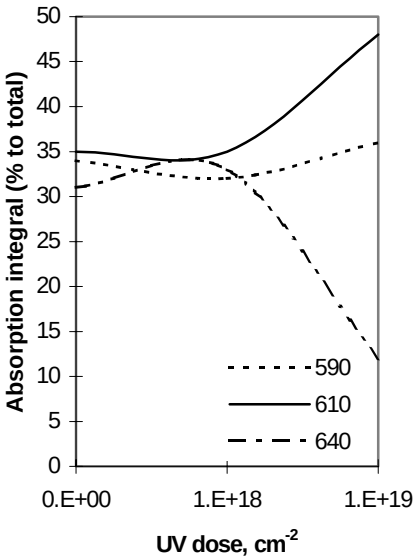

Figure 1-7 Hydrogen redistribution between different bond configurations after UV treatment

$$Si\text{-}Si_{weak} + Si\text{-}H_3 + UV \Rightarrow Si\text{-}H_2 + Si\text{-}H$$

Implementation of the structure modification method to the a-Si:H alloys is not only of theoretical interest but can drastically improve the performance of thin film devices. Let us look at the practical implementation. For this we will use a-Si:H as a model material - since behaviour of a-Si:H alloy is determined by behaviour of a-Si:H structural network in the great part. As a practical example we will use low and high voltage TFT - since *i*-type a-Si:H is used in TFT much more often than in any other device.

a-Si:H Thin-Film Transistor

TFTs used for demonstration of the influence of a-Si:H structure modification on their characteristics were simple bottom gate structures with L/W = 8/90 μm and with 0.15 μm SiO_xN_y as the gate insulator and 0.3 μm of active a-Si:H. No additional doping for source or drain contacts was used.

In Figure 1-8 one can find the dependence of the drain current vs. the gate voltage while the drain voltage is kept at 5V. The dose of UV irradiation is used as an external parameter. Under the optimal dose of 10^{19} cm^{-2} (for used thickness) there is a clear registration of (i) an increase of I_{on}; (ii) a decrease of I_{off}; (iii) an increase of $\Delta I_d/\Delta U_g$; (iv) an increase of U_{th}. It must be mentioned that changes in currents are at least 1 order of magnitude. These results are in perfect agreement with what one expects analysing the DOS spectra shown in Figure 1-6 Moreover these changes are permanent, unlike the Staebler-Vronsky effect. Results, published in [8] show a sharp decrease in degradation rate of irradiated TFT's IV characteristics under high temperature and electric field treatments, beyond the limits for control group TFTs.

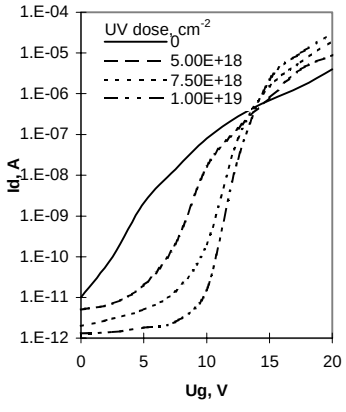

Figure 1-8 Change in TFT's IV characteristics with the UV dose

In case of exceeding the optimal dose on TFT structures all advantages steadily disappear and, at the limit, the TFT becomes not operational. This is mainly connected to the modification of the semiconductor/ insulator interface and the insulator itself.

Nevertheless this does not introduce a new critical point into the

processing since the tolerance limits for using a low power UV source are quite large.

a-Si:H High Voltage Thin Film Transistor

Let us consider a traditional high voltage thin film transistor with offset drain. Introduction of an un-gated region allows to increase the breakdown voltage compared to the conventional TFT and to decrease the off-state current. On the other hand a high series resistance negatively influences the on-state performance of the whole structure.

In other words the core of the problem is that, for the best performance, one has to have 2 areas within the same film which have totally different electrical properties. And this could not be solved through optimisation of the PECVD process, especially in the case of linear or two dimensional arrays. But there is still something what can be done with the help of structure modification in some broader meaning.

The Staebler-Vronsky effect is well known for a-Si:H films and should be defined as photon stimulated relaxation of the material's atomic network. Results of this relaxation are described elsewhere. Using this effect together with structure modification allows to optimise the performance of HV TFT with OD. An illustration of the process is shown as an inset in Figure 1-9. First the transistor is UV irradiated from the top side and after that it is irradiated with white light from the back side, using the gate as a shield. In this way one gets two different regions. The un-gated region has a high resistance providing a low off-state current and an increase of the breakdown voltage to about 50 V per µm length. Also the gated region has a high off-state resistance but it provides intensive injection of electrons in the un-gated region in the on-state. Thus, the on - off- state performance of an a-Si:H HV TFT with OD is at the level of the poly-Si HV TFT with Semi-Insulating field plate over the offset region reported lately [17]. The higher electron mobility in poly-Si is not utilised completely in the HV

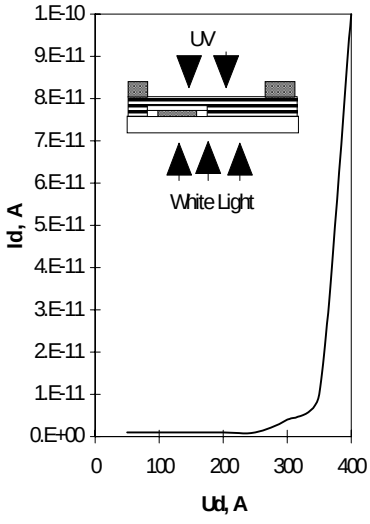

Figure 1-9 Typical IV characteristics of a-Si:H HV TFT

TFTSI because of additional capacitance introduced together with the additional field plate.

The structure modification of the material properties once again allows to improve the performance of the thin film devices without additional photolithographical steps. A major disadvantage of the suggested processing follows from the use of two different physical effects - an optimised a-Si:H HV TFT OD shows an increase of leakage current once operated at temperatures higher than 150 ^{o}C.

a-SiN:H in thin film electronics

Structural properties of the material can be modified by adding new chemical elements[4], and in case of a-Si:H alloys most pronounced example is nitrogen. a-SiN:H thin film alloys with different nitrogen content are used widely in thin film microelectronics nowadays. One of the major applications is TFD for LC displays. Not surprisingly the issue of maintaining the original current-voltage characteristics of the device over its entire operational lifetime attracts much attention.

Shanon et al [18] discuss the drift of electrical characteristics of the TFD under the operational conditions and suggest improved stable TFD basing on: (i) TFD's design optimisation (50% of entire improvement; (ii) a-SiN:H technology optimisation (30%); optimisation of the driving pulse shape (20%). But the technology processing of the a-SiN:H thin films is the key point and its role in increasing the stability is far higher than 30 %.

Structure modification with UV in the case of typical a-SiN:H films for TFD will complicate the process flow. The use of far UV will require vacuum chambers, and, what is even a greater disadvantage, it will require thicker films (a-SiN:H films used for TFDs nowadays are 35 -70 nm thick). But careful control of the different structural units existing in a film (as a pseudo-doping technique for a-Si:H [9]) can still be of a great help in optimisation the TFD parameters and stability.

A TFD's electrical parameters and stability depend on the chemical composition of the film (amount of hydrogen and nitrogen atoms) and on the structure (the way hydrogen and nitrogen atoms are build in the Si network as well as their volume distribution). In order to decrease the degradation rate, a-SiN:H films with hydrogen atoms incorporated mostly in the monohydride bonds and with nitrogen atoms substituting H atoms in Si-H_n groups at the grain boundaries are needed. Homogeneity of the films should be as

[4] Such procedure does not intend to change electrical properties of the material unlike doping

high as possible. The discussion on how exactly this goal can be achieved is the subject of the next chapter.

As an conclusion for the part on structural properties I would like to stress the next points:

- The performance of the thin film devices based on a-Si:H alloys could be improved in two principal ways: either by improving the device's design or by optimising the a-Si:H alloys. As it was experimentally demonstrated the latter allows to produce thin film devices of the basic designs which demonstrate state-of-the-art performance from the point of view of both the electrical properties and the long-term stability.

- One of the possible ways of a-Si:H alloys optimisation is the structure modification method. The principal difference between structure modification of chalcogenides and a-Si:H alloys is that in the latter case we observe a modification of the defect's sub-system but not of the whole atomic network. Thus, the changes caused by structure modification can be seen on electro-optical properties rather than on mechanical (such as density, etch rate and so on). The use of structure modification is demonstrated on a-Si:H Thin Film Transistor.

- a-Si:H alloys are known for a number of specific physical effects, one of which is the Staebler-Vronsky effect. The use of structure modification and Staebler-Vronsky together allows to produce areas, different from a structural point of view, within the same film. This is a headway to improvement of the electrical performance of High Voltage Thin Film Transistors with Offset Drain.

- Use of the external influences for a-Si:H alloys structural modification is not the only possible way. For some alloys, such as a-SiN:H for example, it is easier to ***produce*** films with a relaxed structure. All what is required is more attention to the structural composition of the films deposited on specific equipment. As we will demonstrate father on, once done this allows to produce simple crossover design a-SiN:H Thin Film Diodes exhibiting electrical performance of the more complicated double TFD design and outstanding stability.

- It must be mentioned once again that the methods of structure optimisation of a-Si:H alloys after/during production does not necessarily mean that processing of the final product is more complex, time consuming or expensive. All equipment one needs is already there. Deeper understanding of the material pays back not only in simpler device designs but also opens new application areas for existing technologies.

Summary

During the flow of this chapter the next few major aspects of possibility of all-a-Si:H alloy digital radiography were discussed:

- Current trends in digital radiography discussed in this chapter do not consider amorphous silicon alloys as a real contestant for anything in the field but “information retrieval” part.

- Careful consideration of the real life x-ray spectra and different fields of x-ray examination applications provide solid ground for these trends to be challenged.

- Amorphous silicon alloys for direct x-ray radiography can and will be optimised for the task by utilising its own unique properties rather than trying to make it to behave as “conventional x-ray sensing materials”. We have seen on the example of a-Si:H TFTs that performance of the device can be influenced greatly by controlling structural properties of the a-Si:H itself. We have also seen that performance of a-SiN:H (as a second to a-Si:H material in thin film electronics) is governed by the same laws.

Thinking of the all-a-Si:H alloy digital radiography system one can basically assume the use of a-Si:H TFT as a switching element for pixel and a-SiN:H TFD as a sensor. Even more, in some ideal case, one could try to use a-$Si_xN_{(1-x)}$:H TFDs both for switch and sensor thus drastically simplifying the processing and increasing the yield. These questions are the subject of the next chapters

.

Chapter Two : a-SiN:H thin films for TFD array applications.

There are certain reasons for choosing a-SiN:H as a base material and TFD as a base structure for the development of the novel cost effective 2D direct x-ray sensor array. These namely are:

- Diode structure, or, to make wide definition, metal-semiconductor /insulator-metal is the structure of the choice for the radiation sensitive device.

- More over, TFD can be used not only as a sensor but also as a switching element which allows to select a single element in a matrix. TFD based AM for control of liquid crystal displays are widely used now [19,20]. Their technology is much simpler than one for Thin Film Transistors and so TFD arrays have fewer defects and higher yield.

- Specific requirements to the TFD - operation under x-ray environments - lead to the special requirements to the material used in the device. In my believe choosing the a-SiN:H over a-Si:H is justified. Mainly because of the fact that device will be operated at the joint influence of hard radiation and strong electric fields, quite probable in avalanche multiplication region. This means that everything possible must be done to prevent/slow down any structural changes in the thin film, because structural changes will determine the lifetime of the sensor. Introduction of nitrogen shows stabilising influence on the atomic network of a-Si:H thin films [21,22].

- Nitrogen content in a-SiN:H films is easy controlled by the process gas flow ratio allowing to deposit films from pure a-Si:H to Si_3N_4.

- AM application aspects: (i) a-SiN:H films have low dielectric constant[5] what is positive thing from the point of view of matrix applications, (ii) With the increase of nitrogen content films become insensitive to the visual light, thus no light shielding would be needed, (iii) While used as a switching element in a matrix TFD is driven by low voltage.

The main goal of this chapter is not to demonstrate the possibility of building operational matrix of a-SiN:H TFDs but to study the behaviour of a-

[5] For a-SiN:H thin films dielectric constant is in the range ε~7 - 10

SiN:H films produced under the different conditions. It must be always kept in mind that we are looking for the most stable films, capable of withstanding operational conditions of x-ray environment. When such film are found their electrical performance will be paid attention to.

a-SiN:H technology overview

Table 2-1 Typical silane and ammonia decomposition reactions in PECVD

Reaction			Energy, eV
SiH_4	$\rightarrow$	$Si + 2H_2$	4.4
SiH_4	$\rightarrow$	$SiH + H_2 + H$	5.9
SiH_4	$\rightarrow$	$SiH_2 + H_2$	2.2
SiH_4	$\rightarrow$	$SiH_3 + H$	4.1
$SiH_2 + H$	$\rightarrow$	$SiH + H_2$	- 0.8
$SiH_4 + H$	$\rightarrow$	$SiH_3 + H_2$	- 0.4
NH_3	$\rightarrow$	$NH_2 + H$	4.5
NH_3	$\rightarrow$	$NH + H_2$	3.9
NH_3	$\rightarrow$	$N + H_2 + H$	7.7

Process equipment.

a-SiN:H thin films are deposited using Plasma Enhanced Chemical Vapour Deposition from the gas mixture of SiH_4 and NH_3.[6].Typical decomposition reactions are shown in the Table 2-1.

Which kind of the decomposition reaction is most probable, what radicals have higher concentration, what radicals are most important in a thin film growth process - such questions are the subject of the separate studies and are beyond of the frame of this work. For more information on the subject I would direct interested parties to the references [23,24,25] and references within.

PECVD reactor used in experiments is DP80 from “Plasma Technology”. This is the typical radial flow parallel plate rector, it’s schematic diagram is shown in Figure 2-1.

[6] There is long lasting discussion about what gas is better to use for SiN_x deposition. We suppose that NH_3, with all its disadvantages should be preferred from the point of view of dissociation energy: SiH_4 - 4.1, NH_3 - 4.7, N_2 - 9.8 eV

The main characteristics of the DP80 PECVD reactor are:

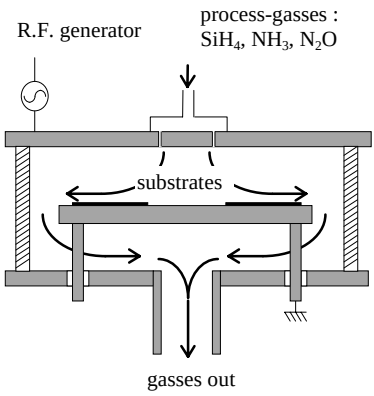

Figure 2-1 DP80 PECVD reactor shematic diagram

- RF power frequency - 13.56 MHz;
- 240 mm table with temperature range up to 400 ^oC;
- Gases are mixed before entering the deposition chamber, so the mass flows of the process gases can be controlled independently;
- gas shower located in centre of the top plate. Since the diameter of the shower is smaller than that of the table the uniformity of the film over the table suffer slightly ~ 10% non uniformity over 240 mm;
- Chamber walls - Pyrex glass

Control parameters of the DP 80 are set in arbitrary units so the system is independent from the type of mass flow controllers and a power of RF generator. In the configuration used for the experiments in the frame of this work the relation between real values and DP 80 settings is given by:

$$\text{a.u. RF} = 30.5 + 2.7 * [\text{Wt}]$$
$$\text{a.u. gas}_1\ (SiH_4)\ \text{flow} = -12 + 9.8 * [\text{sccm}]$$
$$\text{a.u. gas}_2\ (NH_3)\ \text{flow} = -21 + 5.3 * [\text{sccm}]$$

Measurement techniques

Probably the most important factor for us at the current stage is the atomic ratio N/Si in the a-SiN:H films. This can be clearly seen from the Figure 2-2. At the N/Si ratio ~ 0.9 it influences properties of the a-SiN:H films especially strongly. Thus the exact determination of N/Si is necessary. The best method for this, especially during the development of the new technology process, is Auger spectroscopy. The disadvantage of this method is the amount of time needed for Auger analysis. So this makes the use of the Auger spectroscopy as an atomic ratio control test far too complex for routine measurements.

Another possibility is the use of optical absorption as a control test for a-SiN:H films. It is based on the strong dependence of a-SiN:H optical band

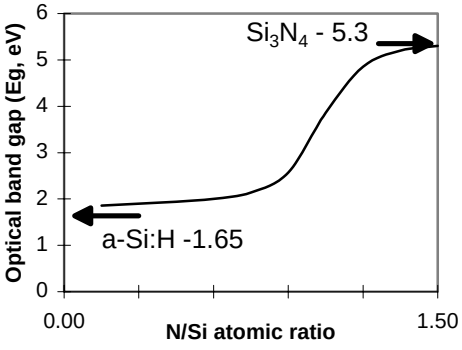

Figure 2-2 Optical band gap of a-SiN:H as a function of N/Si ratio

gap E_{opt} on N/Si ratio(Figure 2-2). Moreover those measurements could be used for the determination of the film's thickness - because of the difference between the index of diffraction of the PECVD a-SiN:H, **n**>1.9, and the glass substrate, **n** = 1.51, is high enough to produce interference fringes in the transmission spectrum. But for such calculations one needs, at least roughly, the value of the refractive index of the film [26].

A method that could be used for measuring both refractive index and thickness is ellipsometry. The refractive index changes from 1.46 for SiO_2 through 2.05 for Si_3N_4 to 3.9 for a-Si:H. The possibility of the use of ellipsometry silicon rich silicon nitride films will need careful consideration.

There are some comments on use of ellipsometry for the determination of the refractive index and thickness of non-stoichiometric silicon nitride. (See for example ref. 26). The main point is that the films have significant absorption at the measuring wavelength (546 nm) especially for the lower N/Si ratio. Nomograms which assume the transparent films give an overestimated result under this condition. In order to clear this we made an optical absorption analysis and in Figure 2-3 one can find the absorption spectra of the films with the low N/Si ratio. There are few moments which should be pointed out:

- For silicon rich silicon nitride films refractive index and thickness must be measured on the films less than 100 nm thick.

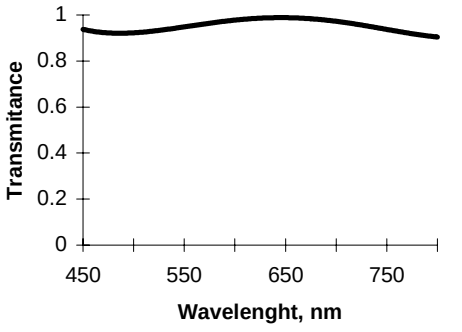

- However, when analysing the results for the different samples one will notice that lower uniformity of **n** causes bigger mistake in **n**.

Figure 2-3 Transmittance spectrum of silicon rich SiN

Table 2-2 Experimental and calculated frequencies of $HSiSi_{3-n}N_n$ stretching vibrations

Structure	Frequency values, (cm^{-1})		r_{max}
	experimental	calculated	
$HSiSi_3$	1985-2010	1992-2024	0
$HSiSi_2N$	2060	2061-2078	0.45
$HSiSiN_2$	2110-2120	2115-2124	0.90
$HSiSiN_3$	2172	2161	1.33

Table 2-3 Vibrational modes of chemical bonds being observed in IR spectra of a-SiN_r:H alloys

Absorption band (cm^{-1})	Local structure and type of vibrations	Peak position (cm^{-1})
600 - 700	Si-H, Si-H_2 wagging	630
700 - 1000	Si_3-Si-N stretching	790
	H-Si_2-Si-N stretching	850
	Si- $N_{Clustered}$ in Si_4N_9 stretching	970
1100 - 1200	Si - N bending	1150
1900 - 2300	see Table 2-2	
3300 - 3400	N-H stretching	3350

Based on the above one can say that in our N/Si ratio region (n ~ 1.9 - 2.1) ellipsometry can be used for the investigation of the n vs. N/Si ratio correlation[7]. On the other hand one has to be careful when transferring this correlation between refractive index and composition of the film to other equipment. It should be kept in mind that this correlation can be somewhat different for the different PECVD reactors.

Information on amount of nitrogen in the a-SiN:H films is important but described investigation methods give a little information about microstructure of the film i.e. about nitrogen distribution in volume, ways it is build in the structural network of Si. And discussed methods provide no information on the hydrogen content and its distribution in bonds with nitrogen and silicon. Analysis of Infra-Red absorption spectra provides answers to this questions. Although IR metrology is well developed for the a-Si:H there are certain complications in case when nitrogen is introduced.

The main absorption lines for a-Si:H are shown in the Table 2-4 together values of oscillator strength. Amount of hydrogen in different bonding configuration then can be calculated as:

[7] With the use of Auger spectroscopy data for the reference nods

$$X = \Gamma \int_{\nu\,\min}^{\nu\,\max} \frac{\alpha(\nu)}{\nu} d\nu$$

where Γ is the oscillator strength.

Problems occur with the increasing nitrogen content (Table 2-3, Table 2-2). Complexes like ***Si_3-N-H*** or ***N-Si_2- H*** (range 1900 - 2300 cm^{-1}) could not be very well separated from the IR spectrum. The existence of such complexes cause the shift of peaks and changes in absorption coefficient. Values of Γ are determined with an error of about 50 %. All those factors lead to a mistake in H concentration about 30 % [27,28,29].

Joining the discussion on correct determination of Γ is not the ultimate goal of this work. For our purposes of comparison of the different thin films the calculation of absorption integral is sufficient so in future analysis we will operate with absorption integral rather than absolute concentrations of nitrogen and hydrogen in the different bonding configurations. Absorption integrals are calculated according to the methodology suggested in [30] . Absorption integral is approximated as:

$$\int_{\nu\,\min}^{\nu\,\max} \frac{\alpha(\nu)}{\nu} d\nu = A\Delta\nu$$

Table 2-4 Position of the H related absorption bands and values of Γ (oscillator strength) for a-Si:H

Peak position, (cm^{-1})	Local structure	Γ, cm^{-3}
590	$Si\text{-}H_2$	
610	Si-H	$7.1\ 10^{21}$
630-640	$Si\text{-}H_2$	
	$(Si\text{-}H_2)_n$	
	$Si\text{-}H_3$	
845-850	$(Si\text{-}H_2)_n$	
862	$Si\text{-}H_3$	$2.1\ 10^{19}$
880	$Si - H_2$	$8.6\ 10^{19}$
890	$(Si\text{-}H_2)_n$	$8.6\ 10^{19}$
907	$Si\text{-}H_3$	$8.6\ 10^{19}$
2000-2050	Si-H	$1.72\ 10^{20}$
2090-2100	SiH_2	$1.72\ 10^{20}$
	$(Si\text{-}H_2)_n$	
2140	$Si\text{-}H_3$	

where A = log I_o/I = 2 log I_o/I' and I' = $(I_o\ I)^{1/2}$ .Procedure of the I, I', I_o, Δν determination is shown in Figure 2-4

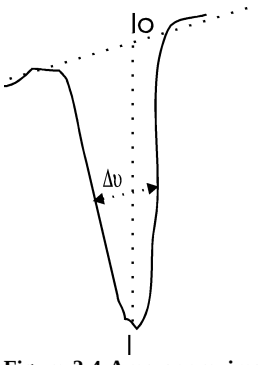

Figure 2-4 Area approximation method

IR spectra also can be used for the study of inhomogeneity of a-SiN:H films. Such a study is based on careful investigation of the Si-H_n and $HSiSi_{3-n}$ N_n stretching vibrations absorption band in the region 1900 - 2300 cm^{-1}. Unlike S-H wagging vibrations at 630 - 650 cm^{-1} , stretching vibrations are very sensitive to the local environment of the bond, thus making possible the estimation of the local inhomogeneities. The method for such estimation suggested in [31] is based on the decomposition of 1900-2300 cm-1 absorption band into four Gaussian bands:

$$\alpha(\nu) = \frac{A}{w\sqrt{2\pi}} \exp\left[-\frac{(\nu - \nu_1)^2}{2w^2} \right]$$

Fitting parameters are frequencies and peak amplitudes of subbands. The peak position of the highest frequency subband corresponds to the inhomogeneous structure of the films with clustered nitrogen atoms. Clustered hydrogen could be detected as well using the width of the stretching band at the half height (I').

a-Si:H alloys are known for a quite high values of the build in mechanical stress. This stress, even if it is not cause mechanical damage to the film, will influence electrical performance of the devices. Since we are looking for the thin film for large area applications with uniform electrical characteristics naturally we would like to monitor stress level in the films. This can be done by optical measurements as well by analysing the diffraction patterns from the naked Si substrate and the thin film on Si substrate under the laser illumination. Careful description of the theoretical basis and measurement installation can be found in [32].

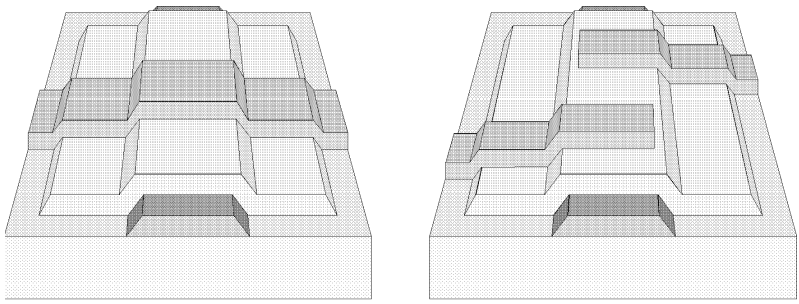

Figure 2-5 Single (a) and Bridge (b) TFD

Design of the photolithographic mask set: TFD test cell

Investigation of structural properties of the a-SiN:H described above do not need any special test vehicles - it is just thin film on the Si substrate. Need for specific tests structures comes when we talk about electrical measurements. Such measurements shall help to answer the next questions:

- TFD best layout;
- Satisfying capacitance requirements;
- Influence of “metal - a-SiN:H” interface on the performance of a TFD

so all the related structures must be included. Summary on the structures included in the test cell is given in Table 2-5.

There are two principally different TFD layouts included in the test cell: “single” (simple crossover structure) and “bridge” (which is in fact two TFD connected in series formed simultaneously). These layouts are shown in Figure 2-5 a and b respectively. The difference between “bridge” and “inverted bridge” mentioned in the Table 2-5 is in sequence in which electrodes are formed. For the “bridge” TFD common electrode formed in *metal 2* and for the “inverted bridge” - in *metal 1*. The shape of the common electrode in the bridge structure TFD differs from the normal rectangle shape in order to keep the same overlap areas in case of a slight misalignment. Total test cell layout is shown in Figure 2-7.

Processed substrate (Figure 2-6) includes 6 test cells, area for optical measurements and the structure for the Constant PhotoCurrent Measurements and

temperature dependence of conductivity. Combination of the a-SiN:H on silicon substrates and test substrates allow to study:

I. Fundamental parameters of the a-SiN:H :
   - A. N/Si ratio by the Auger spectroscopy;
   - B. Chemical composition of the films, influence of PECVD parameters on Si-N, Si-H_n (n=1,2,3) and N-H bonds concentration, inhomogeneity by the IR spectroscopy;
   - C. Thickness and refractive index **n** of the films by the ellipsometry;
   - D. Optical band gap E_{opt} and thickness estimation by the $\alpha(h\nu)$ measurements;
   - E. Structure relaxation processes by temperature dependence of the conductivity;
   - F. Density of states spectrum in the gap by the constant PhotoCurrent method.
   - G. Intrinsic stress measurements
   - H. Pinhole density

II. Electrical characteristics of the a-SiN:H in the different TFD's structures:
   - A. I_{on}, I_{off} currents;
   - B. Current-voltage characteristic's non-linearity coefficients;
   - C. Capacitance;
   - D. Energy activation in the dark and photoconductivity[8] in planar structures.

The use of such combination of different methods will allow us to find the optimal procedure for routine quality control of the a-SiN:H films.

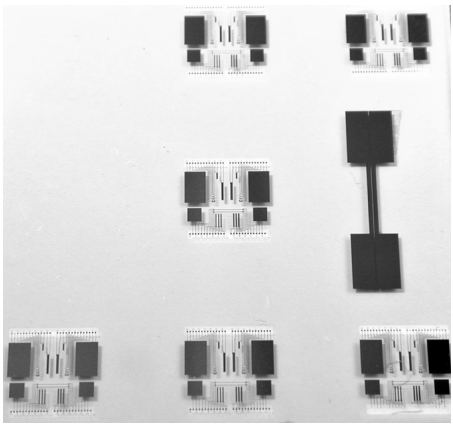

Figure 2-6 Processed substrate with TFD test cell

[8]It should be mentioned once more that "photo" sensitivity of the a-SiN:H is low. So everywhere we use "photo" related terms, we mean not white light but more energetic radiation (less than 200 nm wavelength)

Table 2-5 Description of the "TFD Test Cell"

Contacts	Type	Dimensions, μm	Comments
1 - 2	Capacitance	3540 x 2295	
3 - 4	TFD Bridge	100 x 100	See Figure 2-5
5 - 6	TFD Bridge	75 x 75	
7 - 8	TFD Bridge	50 x 50	
9 - 10	TFD Bridge	20 x 20	
11 - 12	TFD Single	700 x 15	See Figure 2-5Also could be used self-align technique
13 - 14	TFD Bridge	2000 x 15	Also could be used self-align technique
15 - 16	TFD Inverted Bridge	2000 x 15	Also could be used self-align technique
17 - 18	TFD Single	700 x 15	Also could be used self-align technique
19 - 20	TFD Inverted Bridge	20 x 20	
21 - 22	TFD Inverted Bridge	50 x 50	
23 - 24	TFD Inverted Bridge	75 x 75	
25 - 26	TFD Inverted Bridge	100 x 100	
27 - 28	Capacitance	3540 x 2295	Expected C~ 200 10^{-12} F
29			
30 - 31	Capacitance	1555 x 1535	
32 - 33	Planar L x W	3250 x 15	On the film
34 - 35	Planar L x W	3250 x 15	Under the film
36 - 37	TFD Bridge	1395 x 15	For measurements at low T
38 - 39	TFD Bridge	1395 x 15	For measurements at low T
40 - 41	TFD Bridge	1395 x 15	For measurements at low T
42 - 43	TFD Inverted Bridge	1395 x 15	For measurements at low T
44 - 45	TFD Inverted Bridge	1395 x 15	For measurements at low T
46 - 47	TFD Inverted Bridge	1395 x 15	For measurements at low T
48 - 49	Planar L x W	3250 x 15	Under the film
50 - 51	Planar L x W	3250 x 15	On the film
52 - 53	Capacitance	1555 x 1535	

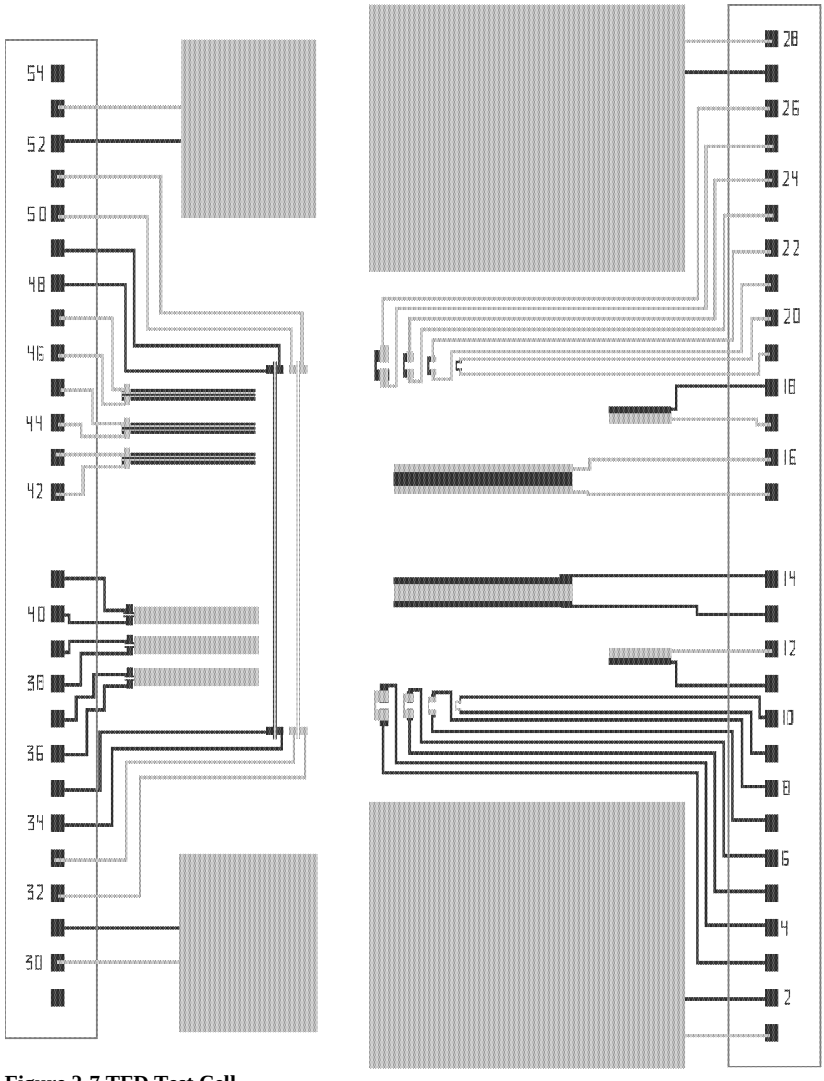

Figure 2-7 TFD Test Cell

Planning of experiment.

As can be seen the problem of optimisation of a-SiN:H thin film with respect to structural and electrical requirements is indeed quite complex. There are tens of characteristics to be measured. Many of them require certain substrate material, certain thickness of the films an so on. This means that for characterisation of a-SiN:H deposited under certain set of PECVD parameters one will need more than one deposition[9]. And here is the question of PECVD parameters. Our PECVD reactor has 6 independently controlled parameters - Pressure in the deposition chamber, RF power (frequency is fixed at 13.56 MHz), Substrate table temperature, 3 independent gas flows - all of which influence the properties of the deposited film. In order to see the influence of the each parameter at least at first order approach one would take minimum three settings for each parameter. This leads to 3^6= 729 possible combinations/needed experiments. Thus amount of needed depositions grows even more.

Historically this problem of huge number of experiments needed is dealt with quite simple - by limiting the number of parameters one will work with and limiting the number of film characteristics one wishes to optimise. This selection - what parameters will not be varied and to which values they will be set - is made on the base of technological experience and analysis of published experimental data. Such an approach is very successful but does not answer one question: Are the films deposited under current parameters set really as good as can be or it is just a local minimum?

Answering such question is of crucial importance in this work. As was mentioned the goal of this work is production of the stable film which meets electrical requirements. This means that we want to be able to change as many deposition parameters as possible during the experiments. And on the other hand we want to control (be able to measure) as much of film properties as possible. One of the possible answer to our concern is the system of experimental design.

Dr. Taguchi's System of Experimental Design[10] [33][11] is aimed to the decreasing of the number of experiments needed for optimisation of one or another characteristics of a product. It is based heavily on the concept of orthogonal arrays which are used for assigning experiments. Such an or-

[9] To be totally correct this number of depositions must be multiplied by number of runs one needs to get the statistical data that allows to say that films deposited under current conditions have certain properties and these properties are reproducible from substrate to substrate, from run to run.

[10] Further in text we will refer to the System of experimental design as SED.

[11] The volume I of the ref.33 devoted to the application of SED and volume II discusses the mathematical basis of SED.

thogonal array allows drastically decrease the number of experiments while observe the influence of particular process parameter level during the change of every other parameter. In a way this is what one could call “screening experiments”. Firstly, with the help of SED one understands how the given property of the product is influenced and how strong this influence is for every process parameter. Based on this date outcome of the experiment with any process parameters set is predicted. Secondly, process parameters levels are chosen so as to get best result.

Area of application of the SED is very wide and still expanding, so more orthogonal arrays are coming in use. Just to demonstrate the power of the SED, let’s get back to our PECVD process: 6 independent parameters with 5 levels each (for higher confidence in curves) lead to $5^6 = 15625$ depositions. With the use of L_{25} (6 parameters, 5 levels) orthogonal array number of experiments is as low as 25. Obviously, good things always come together with bad. Wherever SED will work correctly for the given task depends strongly on inter influence of process parameters. Fortunately, PECVD of Si based thin films is the area where SED works. ELIS-TFCG/IMEC has a history of successful application of SED in a optimisation of SiO_xN_y dielectric films [32,34]. This gives certain level of confidence that SED is applicable in the case of a-SiN:H thin films as well.

There is another aspect to the problem of dealing with huge volumes of experimental data - finding the optimal decision. Flatly, it is finding the global minimum in N-dimensional space where the working surface is superposition of M surfaces (N and M are the number of process parameters and product properties under optimisation respectively). There are two approaches to such a problem: (i) the use of brute force what means going through the all possible parameter sets looking for the best; (ii) the use of some heuristic algorithm which will allow to find the best solution in much shorter time. In my opinion the second approach is much more efficient and as algorithm of search for the optimum “Taboo Search” [35] must be selected. Just a few remarks why:

The main request to any search algorithm one would use in technology is that such algorithm should be able to find “global” minimum on the search surface “even” if there are more than 1 minimum. Historically, the Simulated Annealing method was widely used for technical problems. Being very simple and easy to implement it has major disadvantage - the tendency to converge into the local minimum rather than into global. This disadvantage is inherited with descent strategy of search in which search always moves in the direction of improvement. Thus the result of the search is strongly dependant on the starting point and search surface. Random “moves” implemented in SA can not taken as a cure.

Taboo Search is a recently developed search algorithm which is aimed at always reaching the global minimum. “Taboo” does not really involves any references to the religious or moral considerations, instead it keeps itself busy with imposing and removing certain restriction to guide the search process all over the search surface, looking for the true and only global minimum. There are few kinds of restrictions and rules which allow to utilise much more information provided by SED than traditional SA method.

- Taboo search keeps history, meaning that the new use of the move which lead to the current situation will be forbidden for *n*-iterations even if it appears to lead to the best results - thus search is pushed to the new regions instead of oscillating around local minimum;

- When operating in N-dimensions TS will introduce penalties of frequently used process parameter, meaning that if the current state was reached by changing parameter *k*, next state will be reached without changing parameter *k*, even if it appears to lead to the best results;

- If all the “positive moves” are under some kind of taboo, search will take “negative” moves. Yet the use the “aspiration” may take place at this stage. Aspiration allows to decide on the direction of the current move and/or, if the best move is under taboo, whether or not this taboo can be overridden. Aspiration set of rules can be easily build on the base of Contribution Ratio derived from SED results. In case of SA use this information would be wasted.

- Randomisation[12] can be easily introduced into TS as running search few times with random starting points.

Use of the System of experimental Design together with Taboo Search for the optimisation of a-Si alloys is very effective. Description of the developed software for use in PECVD process optimisation can be found in the Appendix A.

[12] Concession to the SA adepts

Optimisation of a-SiN:H thin films

The goal of a-SiN:H optimisation is the development of the technology processing allowing production of a-SiN:H TFD arrays which comply with electrical and lifetime requirements. As a target we set:

- lifetime as long as possible,
- electrical characteristics are symmetrical and follow the law $I=AV^{\alpha}$, with $\alpha > 7$[13]

Before proceeding with technological experiments we shall determine the "process windows" for every parameter. Such process windows for the first level technological experiments usually chosen on the base of experience with given equipment and literature data. The goals of first level technological experiments are: (i) to create, with minimum experiments, sufficient data bank which will allow to judge on and predict properties of the a-SiN:H films deposited under the different conditions;(ii) as was mentioned in previous section we intend to use System of Experimental Design - but we have to be sure it will work, so second goal is simply testing of SED applicability for a-SiN:H thin films deposition.

Technological experiments: First approach

For the deposition of a-SiN:H we have 5 independent parameters: pressure in the chamber, RF discharge power, substrate temperature, SiH_4 and NH_3 flows[14]. At least three settings for every parameter are needed.

Since nitrogen content in the a-SiN:H films is controlled mostly by NH_3 /SiH_4 ratio and not directly by actual values of gas flows it is possible to set one of the gas flow to some constant level. At this stage we have chosen to fix SiH_4 flow at 8 sccm[3]. By choosing NH_3 flow at levels 60, 120, 160 sccm[3] we vary NH_3 /SiH_4 ratio as 7.5, 15, 20. Selection of the process windows for other parameters was made on the base of experience with silicon nitride films [32].

In this way we have only 4 independent parameters or 3^4=81 experiment to go. With the use of SED and L_9 orthogonal array we can decrease amount of needed experiments to as low as 9. The L_9 array and parameters level assignment are shown in the Table 2 - 6 and Table 2 - 7 respectively. It must

[13] Such selection of the α value is based on requirements to TFD which is supposed to work as a switching element in an array

[14] There is no need for use of N_2O in a-SiN:H deposition process

be noted that in real life amount of experiments is not that low. First of all one needs statistical confirmation of results reproducibility from run to run (3 in our case) and, as can be seen from Table 2-6 , different measurements need different structures and different thickness of a-SiN:H films what leads to further increase in the number of depositions for every parameter set. Yet, the same applies to the straight forward decision and does not change the fact that with the help of SED in this particular case we need 9 times less technological experiments.

Table 2-8 L_9 orthogonal array

Factor	**1**	**2**	**3**	**4**	**5**	**6**	**7**	**8**	**9**
A	1	1	1	2	2	2	3	3	3
B	1	2	3	1	2	3	1	2	3
C	1	2	3	2	3	1	3	1	2
D	1	2	3	3	1	2	2	3	1

Table 2-7 Used PECVD parameters levels

Parameter / Level	1	2	3
Pressure, P, mTorr	350	500	650
RF power, RF, Watt	10	20	30
Substrate temp., T_s, ^oC	220	260	300
NH_3 flow, $sccm^3$	60	120	160

Table 2-6 Types of structures for different measurements

Parameter to measure	Measurement technique / Structure	Comment
Refractive index, thickness, and their uniformity over substrate	Ellipsometry a-SiN:H on c-Si	Thin films (see page 33)
Deposition / Etch rate	a-SiN:H on c-Si	up to n x10^2 nm thick
Absorption integrals	IR spectroscopy a-SiN:H on c-Si	thick films (up to few μm)
N / Si	Auger spectroscopy	as in device (35 - 300 nm)
Optical absorption	a-SiN:H on glass Test cell mask set	thick films (up to few μm)
Electrical characteristics	a-SiN:H on glass Test cell mask set	as in device (35 - 300 nm)
Pinhole density	a-SiN:H on Al on c-Si	as in device (35 - 300 nm)

Table 2-9 Technological experiments: 1st approach L_9 array

Parameter	IP7	IP4	IP2	IP5	IP1	IP8	IP3	IP9	IP6
P	350	350	350	500	500	500	650	650	650
RF	10	20	30	10	20	30	10	20	30
T_s	220	260	300	260	300	220	300	220	260
NH_3	60	120	160	160	60	120	120	160	60
n	1.78	1.78	2.25	1.72	1.73	1.91	1.81	1.82	1.75
n v, %	0.68	18.	16.9	3.0	0.7	3.4	11.9	1.3	1.7
t v, %	2.2	7	7.0	4.2	1.1	3.6	1.2	10.2	1.97
Dep.rate, A/sec	3.34	5.25	4.52	4.65	4.73	5.08	5.41	3.55	5.25
Abs. area N-H	1.4	3.05	1.96	5.51	4.54	3.23	5.21	5.46	7.17
Abs. area Si-H	0.87	0.52	0.6	1.47	0.7	0.81	1.89	1.02	1.69
Abs. area Si-N	11.89	22.96	18.25	36.5	32.33	20.5	40.08	23.28	44.35
% H in Si-H	31	11	18	16	10	15	21	12	14
Si-H/N-H	0.62	0.17	0.31	0.27	0.15	0.25	0.36	0.19	0.24
Width of Si - H_n abs.band	118	118	128	118	101	169	123	142	169
HF edge of Si-H_n abs.band	2319	2278	2278	2250	2222	2306	2278	2250	2250

The results of the first level technological experiments are shown in the Table 2-9.

The reproducibility of these results was tested on the three different runs and data base is constantly updated with the results from any new runs processed in the given process windows. The difference between the actually measured data (for the PECVD parameters set not used in the L_9 array but still in the same process window) and predicted by SED for the same set is varying from around 0.7 % for parameters such as **n**, thickness, deposition / etch rate to up to 3 - 8 % for the IR spectroscopy measurements. Such results of applying SED to the PECVD of a-SiN:H films are very satisfying indeed.

Let us have a more careful look at these results. First of all, from the table above we can extract information on how the change of every particular PECVD parameter influences different film properties. It can be done in two ways - through contribution ratio's (CR) of PECVD parameters to film's properties and simple graphical form - to see details more clearly.

Contribution ratio is in fact some integral characteristic of the process which states that if given property change (with variation of all process parameters through the whole process window) is taken for 100 % then this change was determined by change of *Parameter A* in x_1 %, *Parameter B* in x_2 % and so on[15]. Table 2-10 present the results of CR analysis for the data in Table 2-9:

Table 2-10 Influence of PECVD parameters on final film properties

	n	n v	t v	DR	N-H	Si-H	Si-N	W	HF
P	27	35	11	8	77	58	53	19	28
RF	35	2	24	10	1	33	2	56	25
Ts	19	25	10	44	20	8	43	23	28
NH_3	19	38	55	38	2	1	2	2	19

Legend (Table 2-10): n - refractive index, n v - variation of refractive index over a substrate, t v - variation of the film's thickness over a substrate, DR - deposition rate, N-H - absorption integral for N-H bonds, Si - H - absorption integral for Si-H bonds, Si - N - absorption integral for Si - N bonds, W - width of Si - H_n absorption band and HF - high frequency edge of Si - H_n absorption band.

CR is a very powerful and simple tool when one wishes to determine what parameters is better to use for further optimisation of the film. As an example let us suppose that we need to change variation of the thickness over the substrate. The easiest way to do so is to vary NH_3 flow (biggest CR to t v). But, as Table 2-10 shows, we shall be ready that this will introduce noticeable changes into variation on refractive index and deposition rate, smaller changes into values of n, and some minor changes into the properties associated with IR measurements. Although this is quite valuable information one would wish to know *in which direction* PECVD setting should be changed so as to get desirable change in a film property. In order to answer this we shall use graph showing variation of a-SiN:H properties with the different PECVD parameters levels. These graphs are shown in Figure 2-8 and Figure 2-9

[15] The sum of all x_n is 100 %

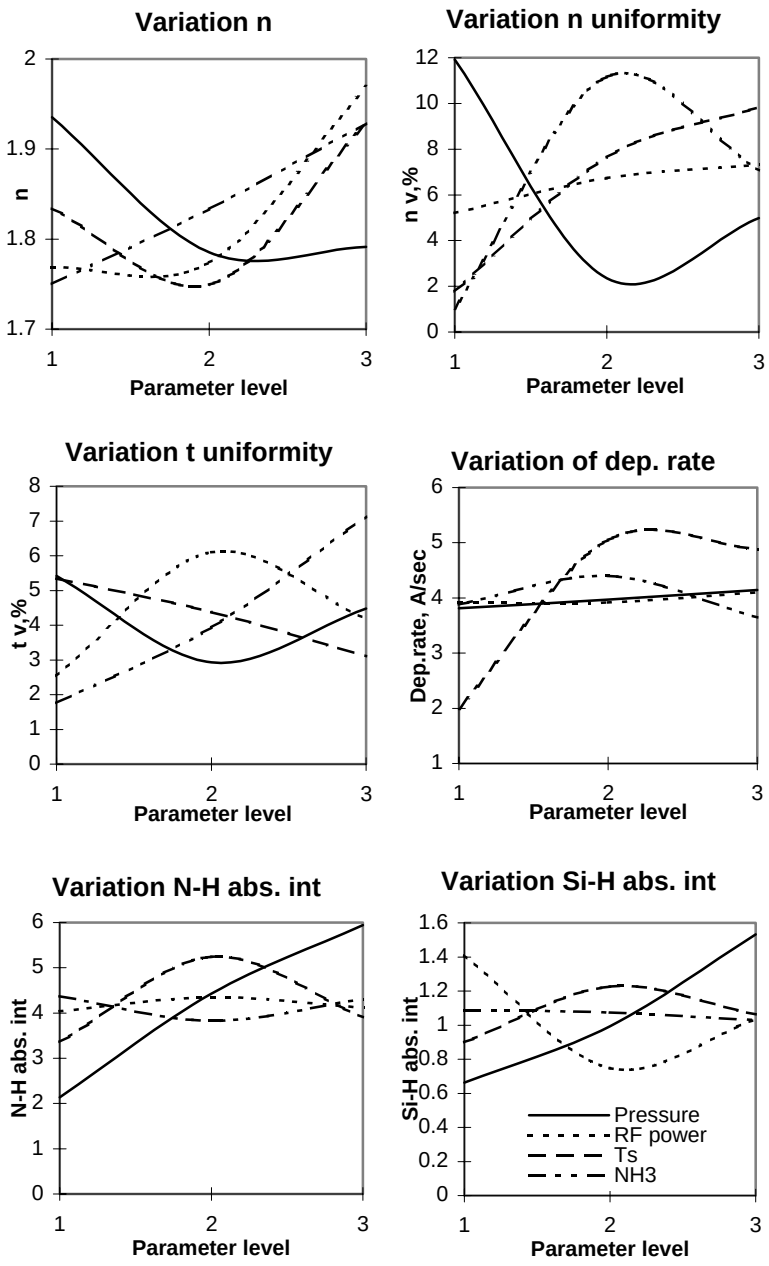

Figure 2-8 Variation of a-SiN:H properties with different PECVD parameters levels

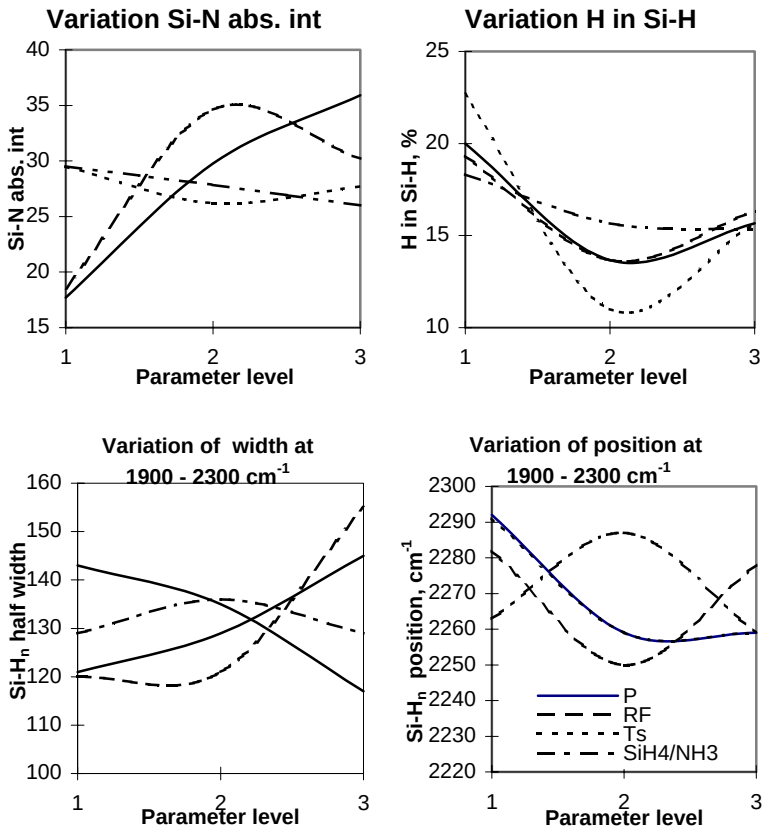

Figure 2-9 Variation of a-SiN:H characteristics with PECVD parameters levels

The last but not least bit of information which can be provided by the SED is possibility to forecast properties of the a-SiN:H obtained under any set of PECVD parameters in the valid process window. For our type of problem we are using hyperbolic aid estimation as opposed to arithmetic one [33]. At the current step we formulate the requirements to the a-SiN:H properties and then search the "experimental data pool" for the nearest fit. Even for the small data pool as in case of L_9 orthogonal array (number of nods equals 81) this is quite time consuming task when done manually. There are two approaches to automation of this task: (i) "brute force" approach - searching every possible combination of input parameters and (ii) heuristic methods - such as "Taboo Search" (see Planning of experiment.) Both of these approaches can be used in the developed software "PECVD optimisation" and both lead to the same search results which are presented below.

Basically now we are looking for the films with highest possible refractive index (100 % weight factor) and still want to have them with the high uniformity in thickness and refractive index over the substrate (give 80 % weight factor to the latter two). Having formulated requirements we can now estimate 10 best possible combinations of PECVD settings - see Table 2-11. Although these films are very good from uniformity n and thickness point of view, the value of refractive index is far too low for the films with intended use in TFD. If one will give up restrictions on uniformity and continue to look for highest possible refractive index one gets another 10 combinations - see Table 2-12. Unfortunately, although the refractive index is fine - it's uniformity as well as uniformity of the thickness is less than satisfactory.

Table 2-11 "10 best" for the n=max, weight=100; n v = min, weight=80; t v = min, weight=80.

P	RF	Ts	NH_3	n	n v, %	t v,%
2	1	1	1	1.6	0.1	1.2
2	1	3	1	1.7	0.5	0.7
2	3	1	1	1.8	0.1	0.6
2	1	2	1	1.5	0.4	0.9
2	2	1	1	1.6	0.2	2
2	3	3	1	1.9	0.8	0.9
2	3	2	1	1.7	0.6	1.3
2	2	3	1	1.7	0.7	1.1
3	1	1	1	1.6	0.3	1.8
2	2	2	1	1.5	0.5	1.6

Table 2-12 "10 best" for the n =max, weight=100

P	RF	Ts	NH_3	n	n v, %	t v, %
1	3	3	3	2.3	16.9	7.02
1	3	3	2	2.2	24.4	3.82
1	3	1	3	2.2	3.29	11.7
3	3	3	3	2.1	7.94	5.8
2	3	3	3	2.1	5.57	3.9
1	2	3	3	2.1	15.6	7.34
1	1	3	3	2.1	12.3	5.41
1	3	3	1	2.08	5.58	1.69
1	3	2	3	2.08	13.4	9.76
1	3	1	2	2.07	5.12	6.53

Real samples produced under the selected parameter sets follow the prediction very well. This means that we either produce TFDs with electrical characteristics satisfying requirements, first of all with α above 7, in a technology not suitable for the large area array production, either we produce fine arrays of the TFDs with low α (4 … 6) coefficient.

The conclusion is that so far we do not have a-SiN:H technology to produce uniform arrays of TFDs with good electrical characteristics.

There is only one way out - we have to modify our process window and by now we have more than enough information which will allow us to so.
Now, when we have finished with the first level technological experiments and about to go to these of the second level, it is good time to formulate the major conclusions we have reached so far:

- Taguchi's SED is working properly in the field of PECVD of amorphous hydrogenated silicon rich silicon nitride thin films;

- Films produced in the current process window are not satisfying the requirements for the large area TFD applications. Nevertheless, first level technological experiments provide enough information on the influence and inter influence of different PECVD parameters on the final film's properties. This provides us solid base for the selection of the process window for the second level technological experiments.

- PECVD parameter process windows must be change in the following fashion. *Pressure*. Pressure has very high influence on almost every characteristic of the film, especially one's derived from IR measurements. Since we are quite satisfied with these characteristics I think that it is reasonable to keep the same process window for this parameter, or even narrow it, deleting the highest pressure value. *Substrate Temperature*. The same kind of motivation (as in previous case) for keeping the substrate temperature in the same range as during the first runs can be applied. Substrate temperature has inferior influence on the characteristics we want to change and yet is second important parameter which determines nitrogen bonding in the film. *RF power*. Process window for the RF power must be extended to higher values. Obtained data allows us to expect that higher levels of RF power will contribute to production of the a-SiN:H films with high refractive index and better thickness uniformity while it's influence on variation of refractive index is extremely low. *NH_3 flow*. NH_3 flow in fact represents the NH_3/SiH_4 process gas ratio. As can be seen we want it to be lower so we will films with low refractive index and thickness variations. But simple decrease of NH_3 flow can not be used, because the work in such process window leads to high deviations of pressure in the chamber from the settled value during

the deposition process. This in turn, leads to the high refractive index variation over the substrate. With understanding that selection of the process window for this parameter is influenced strongly by the used machinery we decrease process gas ratio by simultaneously decreasing NH_3 flow and increasing SiH_4 flow.

Technological experiments: Second approach

For the second level technological experiments we will use L_9 (Table 2 - 6) once again but this time with the different parameter levels assignment summarised in Table 2-13

Table 2-13 Parameter levels assignment table for the second approach technological experiments

Parameter / Level	1	2	3
Pressure, P, mTorr	350	425	500
RF power, RF, Watt	10	40	70
Substrate temp., T_s, ^oC	220	260	300
NH_3 flow, $sccm^3$	30	60	90
SiH_4 flow, $sccm^3$	20	20	20

In the Table 2-14 the experimental results for the L_9 array are shown. It includes data on refractive index, refractive index and thickness uniformity - characteristics which were drastically influenced by the new PECVD parameter levels assignment, - as well as introduces some electrical characteristics of the TFD[16].

Table 2-14 Results of technological experiments second approach

Parameter	IPA	IPB	IPC	IPD	IPE	IPF	IPJ	IPH	IPG
P	350	350	350	425	425	425	500	500	500
RF	10	40	70	10	40	70	10	40	70
T_s	220	260	300	260	300	220	300	220	260
NH_3	30	60	90	90	30	60	60	90	30
n	2.4	1.93	1.88	1.93	2.2	1.94	2.38	2.25	2.13
n v, %	4.17	0.5	0.74	1.0	0.46	0.62	3.78	2.22	1.79
t v, %	14.1	6.5	9.6	6.37	10	2.18	7.02	3.03	4.37
Dep. rate, A/sec	4.85	2.56	2.62	4.85	2.81	3.67	4.22	5.5	3.4
Etch rate, A/sec	1.73	6.4	5.87	12.13	1.62	13.75	2.44	11.78	2.84
I ON	1.110^{-7}	$2.4\ 10^{-11}$	$2.4\ 10^{-11}$	$3\ 10^{-11}$	$8\ 10^{-8}$	$2.4\ 10^{-11}$	$1.9\ 10^{-6}$	$2.3\ 10^{-11}$	$1.1\ 10^{-6}$
α	6.1	6.3	6.2	6.5	7.34	6.23	6.59	6.29	6.4
α v, %	24	2	3	4	12	2	15	3	8
Symmetry	1.04	3.3	3.6	2.64	24	3.5	596	3.3	10

[16] Electrical characteristics included in this table were measured on the single TFDs using TiW /Al electrodes with the a-SiN:H thickness of 100 nm. Current I_{ON} in the table is current measured at V= 30 V. Symmetry then is defined as ratio between currents measured at V= ±30 V.

Following the path we used in the first level technological experiments let us have a look on Contribution ratio's and variation graphs.

Table 2-15 Contribution ratio's for second approach technological experiment

	n	n v,	t v	Dep. rate	Etch rate	I_{ON}	α	α v	Sym-metry
P	30	34	39	17	18	51	33	5	25
RF	30	46	20	34	3	17	19	38	24
Ts	19	14	15	37	27	15	35	12	27
NH_3 flow	21	6	26	12	52	17	13	45	24

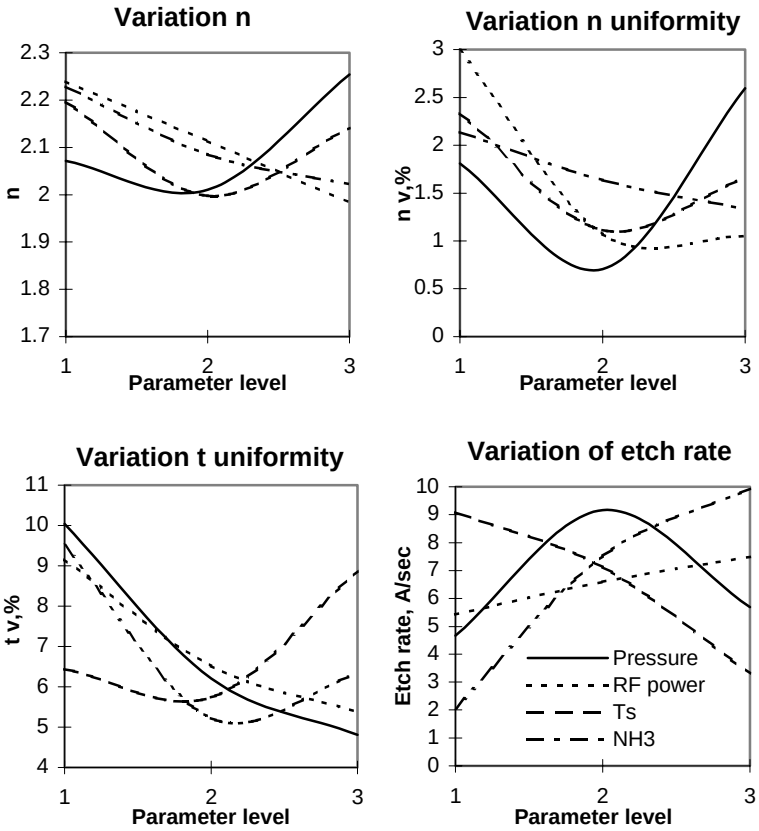

Figure 2-10 Variation of a-SiN:H properties with PECVD parameter levels

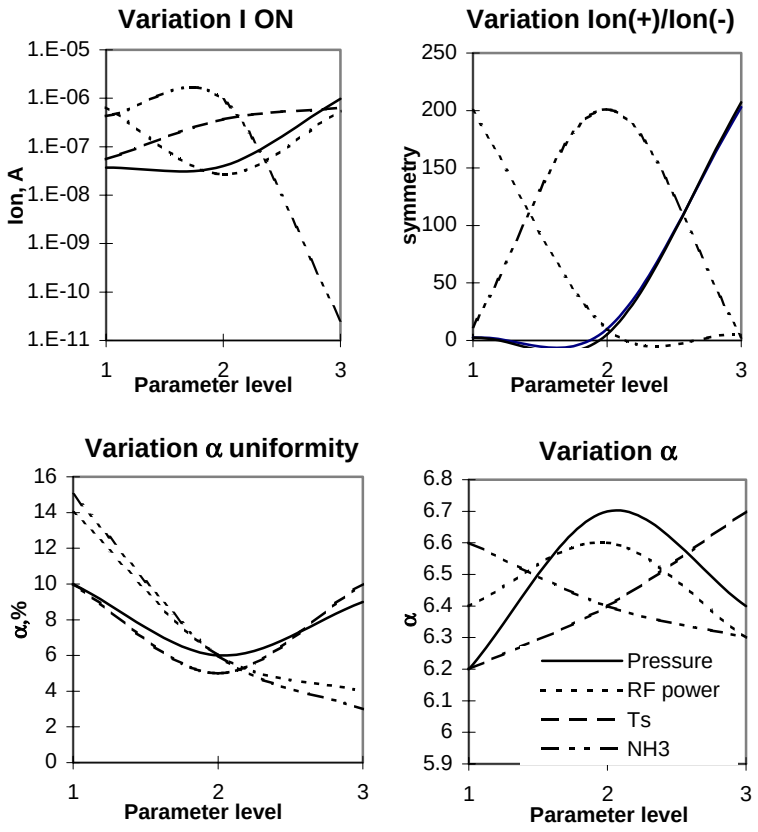

Figure 2-11 Variation of a-SiN:H TFD electrical characteristics with PECVD parameter levels

At this stage we can try to find our optimised films with respect to the electrical requirements (note that we talking now about a-SiN:H electrical properties, not TFD layout or metals for electrodes). Search must be targeted on films which shows maximum value of α and maximum values of refractive index and thickness uniformity. All of these film's characteristics have the same priority. Characteristics which relate to the "process ability" - such as deposition and etch rate - will be dealt with later. So far the criteria for search is formulated as follows:

Search targets
α = max, weight = 100 %
n v = min, weight = 100 %
t v = min, weight = 100 %

The results of the search is presented in the Table 2-16

Table 2-16 "10 best" for the current search targets

P	RF	T_s	NH_3	n	n v, %	t v, %	Ion, pA	α	α v, %	S
2	2	2	2	1.88	0.2	2.36	25	6.8	1.2	8.62
2	**2**	**1**	**2**	**2.07**	**0.5**	**2.66**	**8**	**6.59**	**2.59**	**6.38**
2	2	2	3	1.83	0.2	4.49	0.2	6.75	0.9	13.1
2	3	2	2	1.76	0.3	1.93	63	6.42	0.92	4.78
2	**2**	**3**	**2**	**2.02**	**0.4**	**3.73**	**603**	**7.08**	**2.69**	**4.67**
2	**2**	**2**	**1**	**2.02**	**0.3**	**6.52**	**6 10^3**	**7.05**	**5.67**	**37.8**
2	**2**	**1**	**3**	**2.01**	**0.4**	**5.04**	**0.005**	**6.55**	**2.04**	**9.84**
2	**2**	**3**	**3**	**1.96**	**0.3**	**7.00**	**8**	**7.03**	**2.11**	**7.27**
2	3	1	2	1.94	0.6	2.18	25	6.23	2.00	3.5
2	3	2	3	1.71	0.24	3.69	0.5	6.38	0.81	7.44

Let us not forget that search results presented above is something which was selected on purely formal mathematical basis, determined by the experimental data we have and search targets and weight coefficients we define. System of experimental design, Taboo Search are just the tools one uses to solve problem, but they can not solve this problem because they have no reference to particular “technological experience”. From the point of view of this “technological experience’ there are only few combinations of PECVD parameters in the table above which are of interest for us. These 5 out of 10 combinations are printed in bold font.

Major reasoning beyond such selection is indeed “technological experience” itself. As the Technological experiments: First approach shows films with the refractive index lower than 1.95- 1.90 as well as films with refractive index higher than 2.2 are not suitable for the TFD production. TFD using such films exhibit either too high current in the OFF state or too low current in the ON state. In such situation it does not really matter how good the α is or it’s uniformity. Anyway, if one would use best a-SiN:H possible for production of the TFD electrical characteristics can be tuned with the help of optimisation of TFD layout and build up.

If we would return to analysis the information presented though this chapter we should be able to make the right decision on which films are worth to be used in our TFDs. It looks like that the films with settings 2221 is the best starting point we have so far. Electrical properties of the test TFDs made on

the base of this film are satisfactory but there is still a space for improvement. So the suggestion is to look for somewhat better films in the neighbourhood of the current setting. First of all the changes in RF power and process gas flows must be considered. (Influence of the pressure and substrate temperature is to high to allow them to be used for "tuning" - see CR tables, for example).

Let us first consider the situation when the process RF power will be lower:

2121 vs. 2221 Expected changes in properties

- slight decrease in α
- stronger decrease in α uniformity
- strong increase in ON state current
- decrease in symmetry
- decrease in thickness uniformity
- increase in refractive index
- decrease in refractive index uniformity
- increase in HF edge position of the Si-H_n absorption band
- width at half height of the Si-H_n absorption band stays the same

So basically there is only one positive change with the decreasing of RF power - increase of ON state current. Combined with slightly lower value of α it can lead us to expect higher values of the OFF state current as well. As for other - "negative" changes one can try and compensate them with the increase of NH3 flow. This would lead to the next:

2122 vs. 2121 Expected changes in properties

- decrease in α
- increase in α uniformity
- increase in ON state current
- decrease in symmetry
- increase in thickness uniformity
- decrease in refractive index
- increase in refractive index uniformity
- increase in HF edge position of the Si-H_n absorption band
- increase in width at half height of the Si-H_n absorption band

Such changes are much more favourable for our goals. Although there is the common problem for the last two combinations of lower α and symmetry of TFDs characteristics, it is still worth to try these films in TFD. The base characteristics of the produced films are shown in Table 2-17 and influence of the TFD design (design, metals, a-SiN:H) is illustrated in the Table 2-18

Table 2-17 Base characteristics of the films produced with "best" PECVD parameter sets

Parameter set	n	n v	t v
2221	2.1	1	5.6
2121	2.13	1.7	9.2
2122	2.08	1.6	7

Optimisation of the TFD for the large area array applications is basically includes the steps as:

- selection of a-SiN:H film with appropriate characteristics;
- selection of the metals for electrodes;
- selection of TFD design;
- study of the TFD's electrical characteristics behaviour under the different external influences in order to produce stable TFD.

The analysis of the data presented in the Table 2-18 provides solid base for answering all these questions.

Let us suppose for a minute that we are looking to build an TFD array for the use in LCD displays (the most common use of a-SiN:H TFD arrays nowadays). In case of VGA data-graphic display the requirements to the currents are as follows : $I_{on} > 4\ 10^{-8}$ and $I_{off} < 2\ 10^{-12}$, with $\alpha > 7$. Having in mind these requirements and experimental data presented through this chapter we can pretty easy reach the decision.

Deposition parameters of a-SiN:H thin films. Basically all three selected parameter sets can be used for the current application. But I would stop on the set 2221[17] : P = 425 mTorr, RF power = 40 Wt., substrate temperature = 260 ^{o}C, SiH_4 flow = 20 sccm, NH_3 flow = 30 sccm.

Metals for electrodes. Use of Al electrodes do not lead to the good electrical characteristics of the TFD, most probably due to oxidation of the bottom electrode during the a-SiN:H deposition[18], leading to metal-insulator-semiconductor-metal structure with high operating voltages. Using of TiW for the electrodes looks more attractive. TFDs with TiW/TiW electrodes demonstrate acceptable current-voltage characteristics with only one disadvantage - the values of the OFF state currents are really on the edge. Lower OFF state current is desirable. This goal is achieved with the use of Cr/TiW electrodes based on the fact that Schottky junction height metal-a-SiN:H is

[17] Direct prolonged exposure to the X-rays is quite a harsh stability test for matrix in LCD application indeed. Nevertheless, higher stability of TFDs with 2221 films under x-rays makes me to select it.

[18] Substrates are brought in on the hot table in a normal atmosphere.

Table 2-18 Selection of typical TFD form different runs

Run / Substrate	PECVD set	Metal, top/ bottom	Metal t, nm	a-SiN:H t, nm	Structure
IP1-1				200	Single
IP1-2	2121	Al / Al	100	70	+
IP1-3				35	Bridge
IP3-4,5	2121	TiW/TiW	150	35	Bridge
IP3-6	2121			70	Single
IP3B-4[1)]	2121	TiW/TiW	150	35	Bridge
IP3B-5	2121	TiW/TiW	150	35	Single
IP3B-6	2121	TiW/TiW	150	200	Single
IP4-C2	2121	TiW/TiW	150	35	Bridge
IP4-C2[A]	2121	TiW/TiW	150	35	Bridge
IP4-C5	2122	TiW/TiW	150	35	Bridge
IP4-C5[A]	2122	TiW/TiW	150	35	Bridge
IP4-C5	2122	TiW/TiW	150	35	Bridge
IP4-C6	2221	TiW/TiW	150	35	Bridge
IP4-C6	2221	TiW/TiW	150	35	Bridge
IP6-2	2221	TiW/Cr	150	35	Bridge

higher in case of Cr (Figure 2-12). Cr is not as handy in processing as TiW so best compromise found so far is the use of lift-off technique for forming bottom Cr electrodes and use TiW for the top electrodes.

TFD structure. It looks like bridge structure for the TFD is winning the race, due to three reasons: (i) more symmetrical electrical characteristics; (ii) electrical characteristics are less influenced by external radiation; (iii) twice as thin a-SiN:H films are used in bridge comparing to single TFD, meaning more effective use of the PECVD reactor.

Selection … (Continued)

Electrical characteristics			External influences	Comments
α	U_{on}	U_{off}		
			annealing at 150 C on air, up to 2 hours measuring 0.5,1.2 hours	Current does not reach I_{on} level at voltages less than 30 V before and after annealing
-	-	-		
5.7	±12	10^{-10} A at ±2 V		
7.4	+9-11	10^{-11} A at ±2 V		
7.5	±12	10^{-11} A at ±2 V		
7.1	±13	10^{-10} A at ±4 V		Breakdown voltage 16 - 20 V.
8.2	±20	10^{-12} A at ±2 V		
5.6	±12	10^{-10} A at ±2 V	annealing 150 C on air, 1 hour	See IP4-C2[A]
6.9	±14	10^{-11} A at±6 V		
4.7	-15+10	10^{-11} A at -10+5V	annealing 150 C on air, 1 hour	See IP4-C5[A]
4.5	±15	10^{-11} A at ±7V		
4.0	>±15	10^{-11} A at ±9V	X-ray W anode, 60 kV, 40mA, dose 1 Gy	U_{on} >15V, non symmetrical shift in U_{on}
7.8	±10	10^{-11} A at ±5V	annealing at 150 C on air, up to 2 hours	Annealing cause no changes
7.8	±10	10^{-11} A at ±5V	X-ray W anode, 60 kV, 40mA, dose 2 Gy	Symmetrical shift of U_{on} +1.5V
7.1	±12.5	10^{-12} A at ±5V	annealing at 150 C on air, up to 2 hours	Slight decrease of I_{off}

Full description of the technology process flow for production of control array of TFDs and top glass for VGA data-graphic LCD displays can be found in the Appendix B.

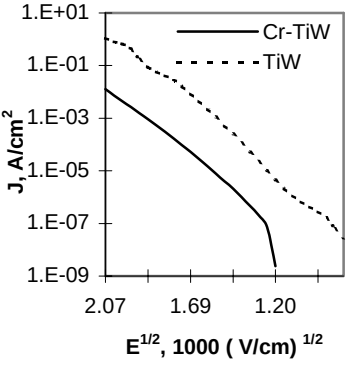

Figure 2-12 Cr/TiW vs. TiW/TiW

Summary

To conclude this chapter I would like mention once again that the major point of this chapter is that now we have a technology processing of a-SiN:H TFD as well as TFD arrays build up from the *material point of view*.

During the course of this chapter

- we have selected some of the a-SiN:H characteristics which are vital for the TFD array production (from our point of view) and appropriate measurements techniques for their control;

- technology of a-SiN:H for TFD applications was discussed and optimised in two steps approach, with the second approach governed by optimisation of a-SiN:H TFD electrical performance.

- Technological experiments are known for the vast amount of data which need to be analysed. In order to decrease the amount of time spent on data analysis System of Experiment Design and Taboo Search techniques were proven to be applicable to the a-SiN:H PECVD process and successfully employed.

- On the base of the experimental data analysis three different PECVD parameter sets were chosen as having the potential to process a-SiN:H films with required characteristics.

- TFD design issues were paid attention to in order to enhance electrical characteristics of the devices.

Chapter Three : a-SiN:H TFD in X-ray environment.

Experiment setup.

Conditions of the operation of a-SiN:H TFD in x-ray environment are principally different from these of LCD. This means that although the work described in the previous chapter has provided solid base for understanding and improvement of TFD it is still only the base and a lot of work still has to be done. The main point of attention shall be electrical performance of the TFD under x-ray irradiation and, if proven necessary, optimisation of the TFD with the respect to both electrical and radiography requirements.

Basically two simple experiments will be needed - firstly, one wishes to know how prolonged exposure to the direct x-rays influences a-SiN:H films of different composition, and, secondly, what will change with simultaneous influence of electrical field and x-rays. First kind of experiments can be conducted using the test cell from the previous chapter (x-ray irradiation and measurements are separated in time) while for the second kind special test cell and irradiation chamber must be developed.

Design of the photolithographic mask set: "X-ray" test cell

Test cell X-ray (Figure 3-1) was designed in order to allow study of the TFD behaviour under the joint influence of electrical fields and x-ray irradiation. Description of the structures used in the test cell is given in the Table 3-1. Bus lines are numbered from left to right from 1 to 10 and lead to the edge of the substrate where contact pads in 2.54 mm pitch are formed. Conductive glue[19] is used for electrical connection. There

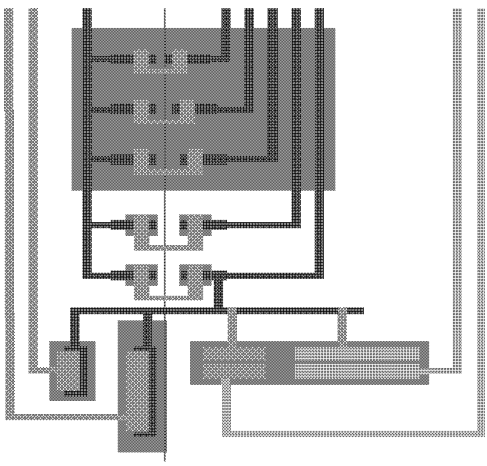

Figure 3-1 X-ray test cell

[19] Post bake at 120°C for 45 min.

Table 3-1 X-ray test cell structure's description

N	Contact pads	Structure	Dimensions	Comment
1	1 - 3	Bridge TFD + Single TFD	50x50 µ 400x200 µ	a-SiN:H is formed, 75µ gap
2	2 - 3	Bridge TFD + Single TFD	50x50 µ 200x200 µ	a-SiN:H is formed, 75µ gap
3	3 - 4	Bridge TFD	50x50 µ	a-SiN:H uniform, 25 µ gap
4	3 - 5	Bridge TFD	50x50 µ	a-SiN:H uniform, 50 µ gap
5	3 - 6	Bridge TFD	50x50 µ	a-SiN:H uniform, 75 µ gap
6	3 - 7	Bridge TFD	50x50 µ	a-SiN:H is formed, 75 µ gap
7	3 - 8	Bridge TFD	50x50 µ	a-SiN:H is formed, 75 µ gap
8	3 - 9	Bridge TFD + Planar	50x50 µ 400x200 µ with 25 µ gap	a-SiN:H is formed
9	3 - 10	Bridge TFD + Planar	50x50 µ 200x200 µ with 25 µ gap	a-SiN:H is formed

are two test cells per 2” substrate.

Structures used in the given test cell can be formally divided (by their purpose) into three groups:

- First group of structures includes bridge TFDs with (2 by) 50 x 50 µ and different gap between the bottom terminals. a-SiN:H is uniform (not formed) thus creating some parallel photoconductor. Goal is investigation of the (i) influence of this photoconductor on the OFF state current of the TFD and (ii) possibility to use such a structure (in fact combining

switching and sensing element in one) as pixel in the digital radiography.

- Second group of structures includes bridge and single - "crossover" TFDs. It is quite reasonable to suggest that symmetry of electrical characteristics of the "sensing" element (as opposite to "switching") shall not be of utmost importance - so we would like to try single TFD as a sensor. Active film - a-SiN:H mostly but not limited to - is formed into 100x100 μ islands.

- Third group of structures includes combination of the bridge TFD plus single TFD and bridge TFD plus planar structure for testing different active films. Basically it is hardware simulation of the single pixel that includes both switching and sensing elements. Such structures are used for the study of the pixel behaviour under x-rays - one wishes to have switching element well defended from changing it's characteristics under the x-ray irradiation while sensing element must have opposite behaviour.

Besides these three groups of structures additional areas of uniform a-SiN:H free of any pattern could be found on the test substrates. These are devoted to the optical measurements aimed at analysis of the density of localised states dynamics.

The photolithographic mask set consists of 5 different masks what allows two possibilities in the production process.

- Mask 1: forming first metal;
- Mask 2: forming a-SiN:H for use in switching TFD;
- Mask 3: forming film for use in x-ray sensor;
- Mask 4: forming a-SiN:H for use in *both* switching and sensing TFD;
- Mask 5: forming top metal

Production using masks 1,2,3,5 - switching and sensing structures are using different a-SiN:H films; production using masks 1,4,5 - the same a-SiN:H is used in switching and sensing structures.

a-SiN:H TFD for LCD applications demonstrated in the previous chapter is the starting point for the current research. The choice of PECVD parameter sets, metals used for lower and top electrodes for the first "x-ray" runs is governed by a-SiN:H TFD for LCD.

X-ray irradiation

X-ray irradiation was carried out with the use W anode tube with possible maximal energy of photons (see typical spectrum in Figure 1-5) from 20 to 60 keV and tube current from 10 to 40 mA. In the used equipment all three settings for the tube (tube voltage, current and the time of irradiation) can be controlled independently. Tube was calibrated by the direct measurements of the total dose leading to the expression for the dose in Gy:

$$\text{Dose } [Gy] = C * I\ [mA] * t\ [sec]$$

where C is a distance from the source dependant constant calculated as:

$1.75\ 10^{-3}$ V *[kV]* - $2.0\ 10^{-2}$ with r^2=0.998 for 4 cm distance

$6.00\ 10^{-4}$ V *[kV]* - $2.5\ 10^{-3}$ with r^2=0.995 for 12 cm distance

Measurements setup is shown in Figure 3-2 and close up to the chamber in Figure 3-3

Figure 3-2 View of the X-ray measurements setup

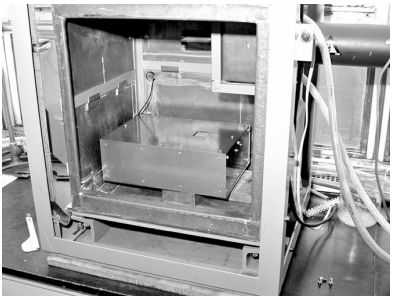

Figure 3-3 Close up: x-ray chamber

a-SiN:H TFD under direct x-ray irradiation.

Under the degradation of the electrical characteristics of the TFD in time we mean either the increase of leakage current in the "off" state either an increase in U_{on} (voltage level at which needed value of "on" current is reached) beyond the levels specified in technical requirements.

It is quite reasonable to expect that processes leading to the degradation of TFD's electrical characteristics in case of AM LCD and AM for X-ray image sensor will be very different. In case of AM LCD TFD degrade due to current flow. From the material point of view, process responsible for this is charge trapping and release on defect sites(such as dangling bonds). This in turn leads to changes in the concentration of neutral and charged defect sites and provide enough energy for altering the local surroundings of the defect site. In the LCD conditions of operation there are no other external influences that could lead to considerable increase in the rate of degradation of a-SiN:H[20].

The situation changes dramatically when one transfers to the X-ray environment. X-ray absorption creates "hot spots" - structure excited areas. Energy freed in charge carrier recombination, is large enough not only for dangling bond defects modification, but also for altering the state of complexes including weak Si-Si bonds, Si-H_n, Si-N, N-H bonds even without current flow through the device. It is clear that in such situation the requirements for the a-SiN:H film's quality (from the point of view of structural network stability) become more severe. So it is reasonable to suggest that the optimisation of the a-SiN:H TFD for x-ray environment must include two steps:

- At the step first, TFD exposed to the prolonged irradiation without any voltage applied to electrodes. Electrical characteristics of the TFD are measured after the irradiation and conclusions on optimising a-SiN:H are made.

- At the second stage both electrical current and x-ray irradiation are involved, measurements of the TFD's electrical characteristics are conducted while TFD is under x-ray irradiation. Such measurements will provide the information for the TFD and TFD array optimisation.

Thus, under the development of the technology process for production stable TFDs for x-ray environment we will follow the same path as we did with the

[20] Temperature of the AM rarely is above 40-60 ^{o}C. As for visual light - first of all, a-SiN:H is not photosensitive, and, it is protected from light anyway by black matrix on pixels.

optimisation of the TFD for AM LCD applications. This means *firstly* production of the films with the minimal density of active defects and, *secondly*, optimising these films with respect to the electrical and environmental requirements.

Static radiation damage

There is more than one set of PECVD parameter levels which allow to produce a-SiN:H TFDs suitable for AM LCD application both from point of view of electrical performance and long term stability (see Technological experiments: Second approach). But this does not guarantee that these TFD will perform equally good in x-ray environment.

As an example one can observe changes in TFD characteristics which were measured before and after it's exposure to the prolonged direct x-ray irradiation. These are show in the Figure 3-4. TFDs based on the a-SiN:H produced with different PECVD parameter sets - in future referred to as technology processing "A" and "B" - were used in such experiments. Overview of the a-SiN:H properties and TFD characteristics is given in the Table 3-2.

The difference between TFDs performance is astonishing, taking into account that TFD "B" received 10^4 times higher radiation dose. While TFD "A" demonstrate non symmetrical increase in the threshold voltage and decrease in the output current, TFD "B" shows just slight decrease in output current. In fact TFD "A" seizes to operate as was defined by technical requirements after receiving only 0.7 Gy dose while electrical characteristics of the TFD "B" are still within the specifications after receiving dose of 7

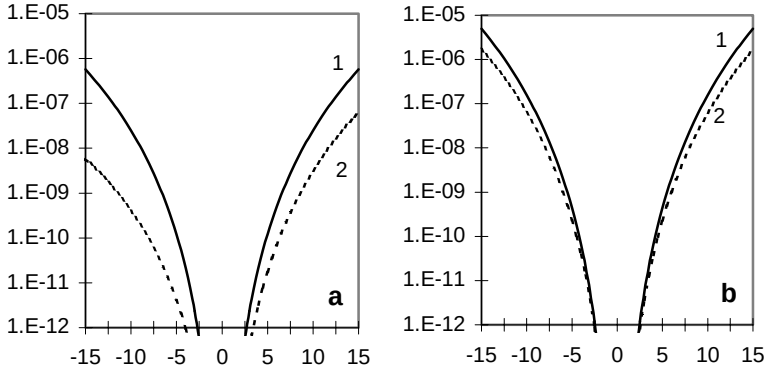

Figure 3-4 Current-voltage TFD characteristics before (1) and after (2) x-ray irradiation: a - TFD produced with technology processing A; b - TFD produced with technology processing B.

Table 3-2 Overview of a-SiN:H properties and TFD parameters - technology processing A and B

Parameter	**TFD "A"**		**TFD "B"**	
Structure of the TFD	Cr/a-SiN:H/TiW 25x25 μ bridge			
PECVD	*value*	*level*	*value*	*level*
P, mTorr	425	2	425	2
RF, Wt	10	1	40	2
Ts, ^{o}C	260	2	260	2
NH_3 flow, sccm	60	2	30	1
SiH_4 flow, sccm	20	-	20	-
Thickness, nm	35		35	
Thickness uniformity over 2", %	93		94	
n	2.08		2.13	
n uniformity over 2", %	98		99	
N/Si	0.61		0.58	
Si-H_n a. b. width, cm^{-1}	136		127	
Si-H_n a. b. position, cm^{-1}	2268		2269	
X-ray dose, Gy	0.7		7000	
Changes in				
α from ⇒ to	7.7 ⇒ 6.6		8.5 ⇒ 8.1	
$+U_{th}$ %	+20		none	
$-U_{th}$ %	+80		none	
$+I_{on}$, times	-98		-2.95	
$-I_{on}$, times	-86		-3	

kGy. In my believe the data presented in Table 3-2 can help us to discuss and answer this question.

a-SiN:H thin film's characteristics look practically identical, TFD performance on their base in normal conditions is practically identical and yet if irradiated TFD's behaviour is different. It is reasonable to assume that structural network of the different a-SiN:H thin is responsible for this.

a-SiN:H thin films produced both with technology processing "A" and "B" have quite high nitrogen concentration. There is a little difference in homogeneity of nitrogen distribution in different films as can be judged from the high frequency edge of the Si-H_n absorption band in IR spectra. But the same absorption band (width at the half height) demonstrate that there is quite a difference in homogeneity of hydrogen distribution - where technology processing "A" leads to production of a-SiN:H films with less homogeneous hydrogen distribution. We can not say that this is comes as a surprise - we have anticipated this while optimising a-SiN:H films for TFD in LCD applications (see page 54). Back then - in LCD conditions of operation - we

did not see the influence of this parameter, but now - in x-ray environment - it gained outmost importance.

Qualitative description of the processes in the structural network of the thin a-Si alloys films under external influence can be outlined as a process of generation of additional defect sites. In a simplified way it's dynamic could be written as:

$$N_g = N_o A\left(\sum_n B_n \exp\left(\frac{E_{in}}{E_{bn}}\right)\right)\ln(t)$$

where A, B_n are constants described below; N_o base concentration of the metastable defects, t is the duration of irradiation, E_{in} and E_{bn} are the energies of external influence and chemical bonds in the material. The physical meaning of the constants is as follows:

I. In fact A equals to the classical criterion of the structural modification efficiency (CSME) [see page 22] for the Si network:

$$\mathrm{CSME} = \frac{(\mathrm{Nos} - \mathrm{Nc})}{\mathrm{Nc}(1 - \mathrm{Ic} - \mathrm{M})}$$

where N_c and N_{os} are the average coordination number and the average number of electrons in the outermost shells of the atoms, respectively, I_c is an averaged coefficient of bond ionicity, M is the factor taking into account the metallic degree of chemical bonds.

II. Second member of the equation for the Ng is in fact probability of the specific chemical bond to be broken, where n goes through the all chemical bonds existing in material. The value of the constant B_n is proportional to the degree of inhomogeneity in the distribution of the specific atoms (nitrogen, hydrogen for example) in the material.

Experimental data on the structure relaxation processes in a-SiN:H could be described using this approach very effectively. It is also in agreement with what have been found earlier for the a-Si:H based thin film transistors (see page 26).

The expression for N_g also allows us to speculate about the possibility of restoring the initial characteristics of the material and TFD. Influence which one uses to restore the initial characteristics should be comparable to the energy flow of influence which caused the degradation. And moreover, energy flow must be targeted which is practically impossible. As soon as con-

siderable amount of hydrogen atoms were send travelling through the material there is no way the initial characteristics could be restored.

One of the most discussed ideas is introduction of additional nitrogen and hydrogen atoms into the film in order to cure new defects. Since we are dealing with the TFD the use additional hydrogen plasma treatment as well as the use of temperatures comparable to the PECVD deposition temperature are out of consideration. In this situation we have tested annealing at the temperatures up to 150 ^{o}C in the forming gas (90 % N_2 + 10 % H_2) for up to 3 hours. Such operation do not lead to the noticeable positive results on the samples after x-ray irradiation - both technology processing "A" and "B" alike.

The only possible decision to increase the stability is through the modification of the used a-SiN:H films. As was demonstrated before the structural units existing in the film, as well as nitrogen and hydrogen distribution in a volume of the film and their bonding with Si will determine the behaviour of the any thin-film device under any external influence. X-ray irradiation is not an exception, and we will continue on our path - first material, then electrical characteristics of the TFD.

Electrical performance of the TFD under direct x-ray irradiation.

Development of the technology processing which allows production of the TFD showing no changes in electrical characteristics *after* being irradiated is hardly enough for digital radiography. In order to build 2D x-ray sensor array we must have knowledge on how exactly TFD's electrical behaviour changes while under x-ray irradiation.

Typical current - voltage characteristics of the 50µm TFD (70 nm a-SiN:H) under x-ray irradiation are shown in the Figure 3-5. X-ray irradiation is carried out with different kV voltage on the tube - directly connected to the maximal value of x-ray photons - and constant photon flow[21]

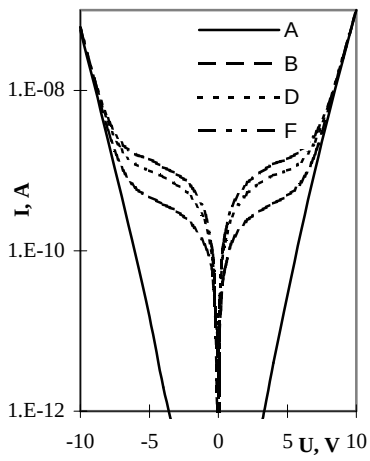

Figure 3-5 Typical I-V characteristics of the TFD under x-ray irradiation. Irradiation: A - none; B - 20 kV/10mA; D - 40kV/10mA; F- 60kV/10mA

[21] For more information on the x-ray spectrum see Figure 1-5

as well as with constant kV voltage and different photon flow.

Figure 3-5 demonstrate clearly that x-ray irradiation causes drastic increase in the OFF state current of the TFD. This increase is several orders of magnitude and tends to follow logarithmic law with tube voltage (maximum photon energy) and linear law with the tube current (photon flow). The difference in the performance between two different structures - single and bridge TFD - is not as well pronounced as in case of AM LCD applications. This fact is illustrated by Figure 3-7 where response curves:

$$I_{response} = \frac{I_{x-rayON}}{I_{x-rayOFF}}$$

of the different TFD are shown.

As can be clearly seen from the presented data current TFD, bridge or cross-over structure, can not be used as a switching element in traditional AM driving schemes for the matrix of x-ray sensor array without total shielding form x-rays. On the other hand, it could be used as a sensing element providing the increase in the response current.

As we were stating all through the previous chapters - TFD characteristics are determined by material itself. So before trying to use current *TFD as a switch* (by building shields for example) we shall look at the a-SiN:H first.

The main goal is to kill response current. Following this goal one would think of using stable a-SiN:H film which would allow production of TFD with low threshold voltage. One of the possibilities is a-SiN:H produced under the next PECVD parameters set:

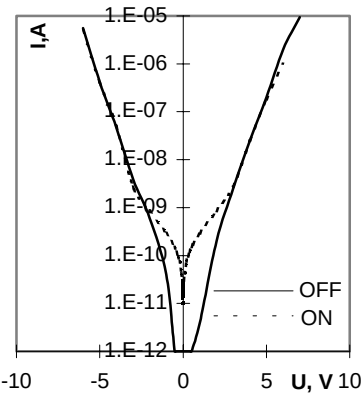

Figure 3-6 Current voltage characteristics of the modified TFD

P - 500 mTorr;
RF - 10 Wt;
T_s - 220 ^oC;
NH_3 flow - 30 sccm;
SiH_4 flow - 30 sccm.

IV characteristics of the TFD using described a-SiN:H under x-ray irradiation are shown in the Figure 3-7. This TFD has lower threshold voltage at the level ~ 2 V and at the voltage 5 V there is no difference in current flowing though the device without or during irradiation. Although the response current is much

lower now it is still present and has considerable values. It could be lowered farther with help of doping for example.

So far we could say that the realisation of the 2D x-ray active matrix sensor array on the base of a-SiN:H is possible. The manufacturing process will include two different PECVD step, where different by properties and thickness a-SiN:H thin films will be deposited. Shielding from x-rays for the switching diodes still will be needed in order to improve the performance of the whole matrix.

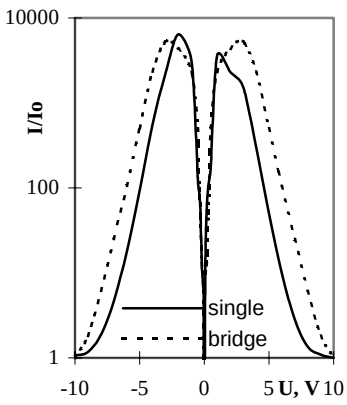

Figure 3-7 Response curves for bridge and single TFD

The use of the a-SiN:H TFD as a sensing element has brighter perspective than in case of the use as a switch provided one could boost its the response to x-rays. This problem is addressed in more detail in Optimisation of the TFD for use as a x-ray sensor.. In this part however I would like to address the design aspect of the sensing TFD.

Behaviour of the TFDs with different structure is almost identical under the x-ray irradiation. Normally, a bridge TFD exhibits a much higher symmetry in IV characteristics in the absence of X-rays than a single TFD (for a single TFD the current at ±15V may differ up to 1 order of magnitude). However, this is not a sufficient reason to prefer the bridge TFD for use as an X-ray detector. The simpler processing technology for an array of single TFDs is a more significant advantage, since one avoids an insulator in between row

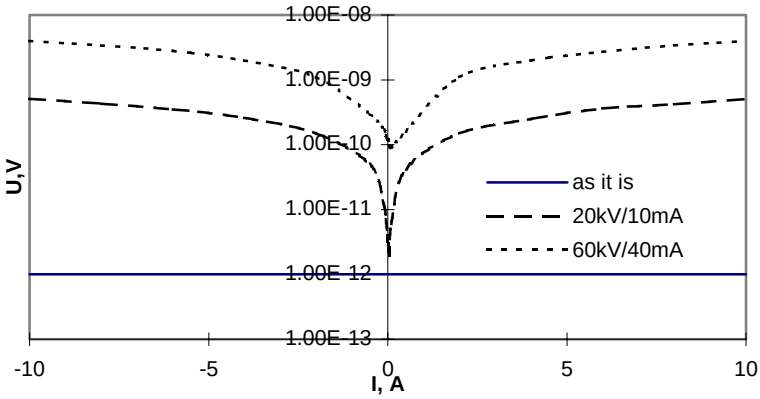

Figure 3-8 Leakage current of the 500 nm $Si0_2$ (area 200x200 µm)

and columns bus bars. And behaviour of the insulator can constitute quite a problem. Regular[22] SiO_2 films of 500 nm thick were tested for this purpose and the results could not be called very promising (Figure 3-8). The leakage current of SiO_2 increases rapidly with the energy of the X-ray irradiation and at voltages higher than 3 V it becomes comparable to the signal to be read out. The only feasible solution in this situation from my point of view is to give preference to a crossover design of the sensing TFD. By making such decision one does not sacrifice much on the performance of the TFD as a x-ray sensor but saves a lot on attempts to solve "leaking SiO_2" problem.

At this stage when we have decided - at first level approach - on the which a-SiN:H films to use (PECVD parameter set "B") and on the design of the TFD (crossover) it is time to see at what extent we can increase the response current of the sensing TFD.

Optimisation of the TFD for use as a x-ray sensor.

Optimisation of the response current of the TFD will be mostly connected with the design and technology issues, such as a-SiN:H thin film thickness, metals used for electrodes, run flow adjustments and so on.

As we have discussed before[23] a-Si is not effective medium for absorbing high energy x-ray photons. But we are using not just a a-SiN:H thin film, we are using TFD on the base of a-SiN:H film. In this case variation of the a-SiN:H thickness results in useful TFD's response current variations. In the Figure 3-9 current voltage characteristics of the TFD using 70 and 1400 nm thick a-SiN:H are shown. TFD based on 1400 nm thick a-SiN:H has clearly superior response characteristics.

But there are some external conditions imposed on our TFD. In this case it is the selection of the driving voltage. If one chooses to stay with low voltage driving electronics (~ 5 V) then the results of the use of thicker a-SiN:H will be as follows:

- Optimal response current is achieved at the electrical field strength of E= 5-7 10^5 V/cm. This is readily achievable while working with 70 nm a-SiN:H but not in case of 1400 nm. Yet the response current of the 1400 nm TFD operated at 5 V (E= 4 10^4 V/cm) is still twice as high as response current of 70 nm TFD operated at optimal electrical field strength.

[22] Routinely used as an insulator in TFCG processing
[23] Table 1-2

- The use of thicker a-SiN:H films leads to suppression of the OFF state current of the TFD. While optimising TFD for LCD applications[24] we had to deal with this problem through the strict selection of the electrode's metal. Now we will have more freedom in selection of metals for electrodes.
- The use of thicker a-SiN:H do not lead to the observable changes in the life-time.

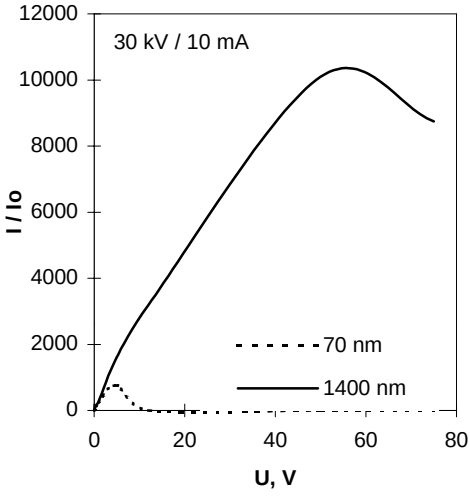

Figure 3-9 Response curves for TFDs with different a-SiN:H thickness

On the other hand, if one would consider to change driving voltage to the values of 50 - 70 V the response current could be enhanced even further while the advantages listed as number two and three would remain.

As for the selected value of thickness - 1400 nm - it is just a good compromise between thickness, build-in-stress and effectiveness of the PECVD reactor use.

Metals used for electrodes may have a dual influence on the response current of the TFD. On the one hand metal used as a top electrode may contribute to the effectiveness of x-ray photon absorption. On the other hand it may contribute through purely design issues. The former will be discussed somewhat later as a part of the discussion on enhancing x-ray absorption efficiency, while now we will focus on design.

Figure 3-10 demonstrates the difference in the current-voltage characteristics of the two TFDs. One is build as followed from LCD optimisation and has Cr/a-SiN:H/TiW structure (goal was to depress OFF state current) while the other has TiW/a-SiN:H/TiW structure. With the thick a-SiN:H we do not have problems with the OFF state current and so can safely use TiW for both

[24] Technological experiments: Second approach

electrodes, have better charge collection efficiency and win on the response current.

The use of the thick a-SiN:H films has one side effect which should be always accounted for in our future considerations. It is in virtue a photovoltaic effect with the strong dependence on the energy of incoming x-ray photons. Figure 3-11 demonstrates this effect, where *a* is a sensing effect and *b* is photovoltaic effect (close up on the voltage). The reason for mentioning this effect here is that is sensing element demonstrates such behaviour a the low bias voltages it will surely influence the pixel performance when such sensor is used in array. And one wants to know as much as possible about the TFD before actually proceeding with arrays of them.

The discussion so far was focused on the design aspects of the a-SiN:H TFD optimisation. But there is more to the problem than just design issues. So in the following paragraphs I will concentrate more on what can we do with material. From my point of view there are two most promising directions - enhancing charge collection efficiency and enhancing a-SiN:H (and/or) TFD x-ray stopping efficiency.

Although the latter sound very pretentious, especially in the part of enhancing stopping efficiency of the material itself, it is very possible indeed because of unique properties of a-Si alloys. When one speaks about enhancing x-ray stopping efficiency of the material one wishes (I know I do) to:

- introduce into structural network of the material a considerable amount (the more the merrier) of much heavier atoms;
- keep the electrical properties of the material after such introduction as intact as possible.

This is not such a problem as it may seem. The whole history of the creation of the *pn*-junction in the amorphous hydrogenated silicon alloys is the history

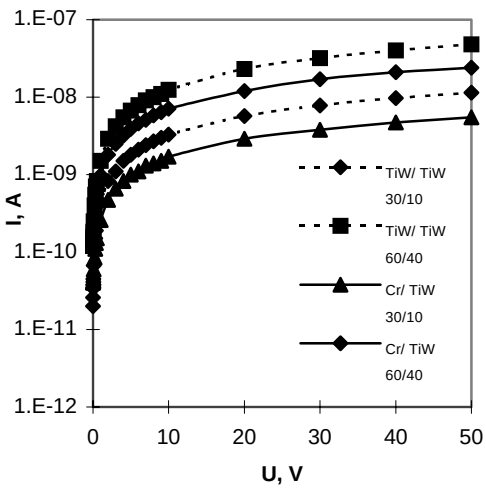

Figure 3-10 Comparison between TiW and Cr for bottom electrode

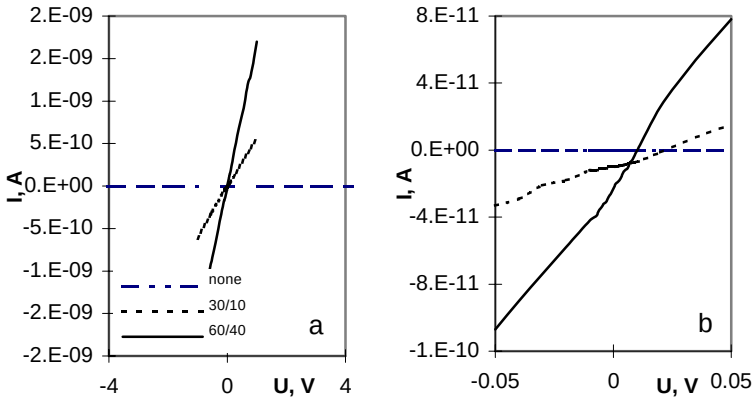

Figure 3-11 Sensing (a) and photovoltaic (b) effects on the a-SiN:H TFD

of the battle with extremely low doping efficiency of the material. For a long time it was believed that amorphous semiconductors can not be doped[25] at all since the local valence requirements are satisfied through bonds rearrangement. Since 1976 when first doped samples were obtained all efforts were putted towards increasing of doping efficiency - and now acceptable level is 1 out 5 dopant atoms is electrically active. In our case the goal is quite the opposite: to *decrease* the doping efficiency much lower than 20 %.

Although there are numerous possibilities for doping of a-Si alloys, including doping during deposition/sputtering, ion implantation and so on, we lack the necessary hardware in house. The only way available for us is to try to prepare sandwiches of a-SiN:H an evaporated metal with combination with some post processing, although there is not much information on the subject could be found in the literature.

Experiments in this area were carried out on the structures such as:

⇒ bottom electrode (Cr/TiW)
⇒ a-SiN:H thickness t_1
⇒ evaporated Au thickness d
⇒ a-SiN:H thickness t_2
⇒ top electrode (TiW/Cr)

where used combinations of thickness were as shown in the Table 3-3

[25] meaning altering conductivity in a wide range through adding donors/acceptors

Table 3-3 Thickness settings for "doping" experiments

N	t_1, nm	d, A[26]	t_2, nm
1	50	2.5 / 5	1350
2	700	2.5 / 5	700
3	1350	2.5 / 5	50

Standard post processing involved intermediate annealing at 260 ^{o}C for 4 hours[27] combined with annealing in a forming gas 90% N_2 +10% H_2 at 350 ^{o}C for 4 hours before the sputtering of the top electrode. The major result of the such approach correlated well with the procedure involved: there is no noticeable influence on the response current of the TFD. The difference in characteristics between “doped” and reference TFD can be seen for settings number two in the Table 3-3 and is in slight depression of dependence of the photocurrent from x-ray tube voltage and in increase of TFD’s threshold voltage.

Talking about charge collection efficiency in the TFD one would refer to the fact that incorporation of nitrogen into the a-Si:H network depresses the charge carriers mobility. So one of the possible ways of increasing the response current of the TFD is to use films with lower nitrogen concentration. But let us not forget that we have use nitrogen in order to enhance the lifetime of the device. While it is true that we can boost up the response current of the TFD by using the films with lower n, we loose much more on the lifetime side. As an example if we compare the response characteristics of the two TFDs discussed earlier (2221 and 2122 see Table 3-2) we will see that the latter demonstrates 15 to 20 % higher response current for all the investigated a-SiN:H thickness, but it’s lifetime characteristics make it impossible to use such TFD in a x-ray sensor array.

There is an another approach which can possible help in the quest of enhancing TFDs response to x-ray. It has less to do with the material properties and more with the design issues while involves the question on physical nature of the sensing phenomena.

As we have seen in Chapter I amorphous silicon is far from being effective x-ray absorbing medium. So as soon as discussion on the use of a-SiN:H TFD for x-ray sensing starts one would suggest that x-ray absorption goes anywhere else (top electrode for example) but not in a-SiN:H thin film[28].

[26] such thickness of the Au film hardly has any physical meaning. What we are talking about here is not a "film” but simple mono atomic layer with number characterising it’s density.
[27] comes automatically with the need of deposition second layer of a-SiN:H (thickness t_2)
[28] A. Natan, A. Sazonov, R. Wiesfield (private communication)

Let us have a careful look at the subject, comparing a-SiN:H TFD developed in this work with a-Si:H TFD with thick Mo electrode developed by group of Dr. Natan (Direct approach., [8]). In the latter case the interaction of x-ray photons with Mo leads to injection of high energy electrons into reverse biased a-Si:H depletion layer where electron multiplication yields a gain. As an experimental data demonstrates the yield increases with the increase of Mo thickness in the range 100 - 500 nm[29] .

In our case the situation is different with all the electrical output being due to x-ray photons absorption in the a-SiN:H film itself. The experimental data presented in this chapter suggest strong support to the statement above. Yet there is another possible experiment with dual goal: providing additional evidence on the physical nature of x-ray sensing effect in a-SiN:H TFD and it's possible enhancement. We are talking about use of a-SiN:H with the thick top electrode for typical irradiation experiments.

The idea behind these experiments is as follow. We are using a-SiN:H to detect low energy x-ray photons. So we could enhance the response of the TFD by stopping more higher energy x-ray photons - in the top electrode. If we would go back to the Figure 3-10 we will see that change from Cr to TiW[30] for the top electrode has lead to the increase in the TFD's response current. One could speculate that what we have observed there has nothing to do with better metal/a-SiN:H interface but is a strong evidence of increased effective x-ray absorption in the top electrode. This needs careful consideration.

For this purpose set of TFDs, with a-SiN:H thickness varied from 35 to 1400 nm and top electrode thickness varied from 100 to 600 nm were processed and measured. Alloy of 10% Ti 90% W was used as a top electrode metal so that obtained data could be correlated to Mo. Also sandwich of Cr (150 nm)/TiW (50 nm) for the top metal was used (Cr in order to get low bus bar resistance).

Unfortunately, as was found for the used energy range, response current of the TFD decreases with the increase of top electrode thickness, losing more than 50 % at TiW thickness of 450 nm compared to TiW thickness of 150 nm. TFD with sandwich top electrode performs exactly as TFD with 150 nm TiW top electrode.

Such behaviour of the TFD response with increase of the top electrode's thickness means that too much of low energy photons are absorbed in top electrode without adding up to the electrical signal of the pixel, while the

[29] after ~ 500 nm considerable self-absorption in Mo is observed.
[30] Higher x-ray absorption efficiency, the same thickness of 150 nm

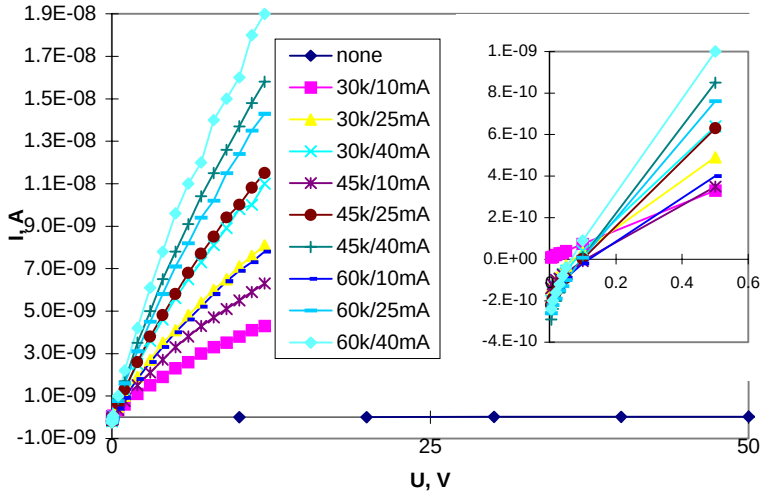

Figure 3-12 TFD's performance under x-ray irradiation

increase in absorption of higher energy photons can not compensate this effect[31].

Taking into account all the experimental data presented above we can now select technology and design for the x-ray sensing a-SiN:H TFD:

- a-SiN:H thin films deposited from mixture of pure SiH_4 and NH_3 at the PECVD parameters settings as: P = 425 mTorr; RF = 40 Wt; T_s = 260 ^oC; NH_3 flow = 60 $sccm^2$; SiH_4 flow = 20 $sccm^2$;
- a-SiN:H thin film thickness at 1400 nm, giving freedom in the selection of the driving voltage;
- electrodes are sandwiches of Cr = 150 nm and TiW = 50 nm with TiW always being innermost metal;
- simple crossover design.

Electrical characteristics of the optimised a-SiN:H TFD under the different levels of x-ray irradiation are shown in the Figure 3-12

[31] But why then two TFDs (a-Si:H with Mo and a-SiN:H) work so differently? The answer is in used energy range: we are working with 20 - 60 keV while measurements for thick Mo were conducted in the range 40 - 100 keV [8] (emission of secondary electrons becomes noticeable from about ~ 60 keV)

Summary

This chapter is devoted to the study of a-SiN:H TFD behaviour under the direct x-ray irradiation. The progress in this process is marked by few milestones:

- Based on the discussion of expected effects we have developed test vehicles for study of TFD behaviour in different situations, namely with and without current flow through device. The test structures included there have allowed us to judge on design of sensing TFD and simulate (in hardware) possible pixel design for the 2D array of the such TFDs.

- During the first stage of experiments we have selected a-SiN:H technology processing which allows us to have stable TFD with a sufficient life span.

- Second stage of experiments gave us valuable knowledge on how exactly our a-SiN:H TFD behaves under the joint influence of the direct x-ray irradiation and electrical field.

- Experimental data obtained in the course of these experiments has allowed us to look for, find and test different approaches to enhancing a-SiN:H sensing TFD response to x-ray irradiation.

- All of the above has lead to developed technology processing for the a-SiN:H x-ray sensing TFD. Electrical performance of a such TFD is at the level with currently used digital radiography systems (Table 1-1 Data sheet on the digital radiography systems currently under development).

Chapter Four : a-SiN:H TFD x-ray sensor array

Prototype of sensor array build-up

Driving strategy

Basically for realisation of the two dimensional array of sensor one needs two different elements in each pixel. One is a sensing element itself (which could be used as storage capacitance to store the data between frames also). The second is a switching element which controls data read out from the pixel. These two elements must have opposite behaviour under the radiation in question: while sensor shall change it's electrical characteristics to the highest degree possible, switch must maintain it's electrical characteristics unchanged.

As we have seen in the previous chapter there was a little attention paid and so a little progress made in optimising a-SiN:H TFD for purpose of switching element under the x-ray irradiation. While "switching" TFD demonstrates much lower sensitivity to x-rays there is still a difference in it's electrical behaviour between situations x-ray ON/ x-ray OFF. This means that such TFD can not be used as a switch in the array of sensors without protection from radiation sufficient to eliminate this difference.

In such situation we have two obvious choices:

- using a-SiN:H TFT as switch, externally accounting for the drift of TFT characteristics in time;

- using x-ray protection shield matrix to defend switch from the radiation.

Both of these options are not good enough and have a common flaw - complex technology processing, not that much simpler than for approaches currently in use. Yet one more reason: when using AM approach we will have row and column bus bars intersection. Row and columns must be isolated - but this not that simple task when speaking about exposure to direct x-ray radiation (Figure 3-8).

Keeping in mind that the goal of this project is cost effective (simple processing, high yield technology) two dimensional x-ray sensor array we have decided to look at the other possibilities - *do we really need switching elements*?

The behaviour of the sensing a-SiN:H TFD under the x-ray irradiation allows us to use other than conventional (active matrix) driving strategy for our array. This specific behaviour (Figure 3-5) of the developed TFD under different levels of direct X-ray irradiation is exploited using the driving scheme shown in Figure 4-1. In this addressing scheme a select signal is applied row by row and the data readout is performed with current sensing operational amplifiers, one for each column [36][32]. In this arrangement we avoid the combination of sensing and switching elements.

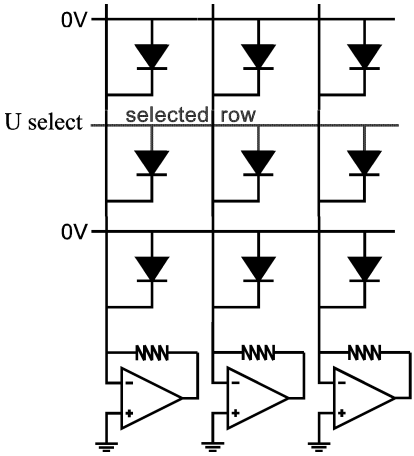

Figure 4-1 Suggested x-ray sensor driving scheme

Requirements for the read out circuits can be determined from SPICE simulations using a model closely representing the real TFD with a-SiN:H thickness of 70 nm and 5 V driving voltage. If we require a readout error less than 10 % in the case where all TFDs in one column are exposed to direct X-ray radiation except the selected one, we get the following offset voltage specifications for the operational amplifiers (Table 4-1). Although these requirements will depend on selected driving voltage for the TFD, TFD performance and so on they still give fairly good idea on what to expect.

Table 4-1 SPICE simulation results on read out circuitry

Pixel pitch, μm	100
X-ray energy, kV	20 - 60
Signal to be read out, A	10^{-12} - 10^{-9}
OA offset voltage, μV	
- 100 rows	500
- 1000 rows	50

Taking into account the above mentioned facts such as:

- a-SiN:H TFD with the good electrical response to x-ray radiation differential to incoming photon flux and energy;

- a little sense in simulating active matrix driving with a-SiN:H TFDs as a switches;

[32] This driving scheme was originally used in a-Si:H scanners

- availability of driving scheme which suits our a-SiN:H TFD behaviour much better;

- promising results of computer simulation of the array;

we have decided to build the demonstrator of cost effective two dimensional x-ray sensor array on the base of a-SiN:H TFD.

Design of photolithographic mask set: Array Test vehicles

Two different test vehicles are used in this part of work. One - "2D2" is the sensor array for use in prototype and the second - "Test array" is the test vehicle for study array related phenomena.

"2D2" sensor array is build to utilise the driving strategy discussed above. 100 rows by 100 columns array with 200μm pixel pitch as well as some test and control structures are formed on the 2" glass substrate. This test vehicle is shown in the Figure 4-2 and its description is given in Table 4-2. Picture in the insert (Figure 4-2) assumes 2 step processing - see Appendix C

Array related phenomena - such as influence of the pixel and array layout on the performance of the system needed the separate test vehicle. "Test Array" includes arrays of different size and layout as well as different pixels lay-outs. It is shown in Figure 4-3 and its description is given in the Table 4-3. In addition to single TFD per pixel (2D2 test vehicle) 4 TFD per pixel and 9 TFD per pixel are included in "Test Array". On the insert to Figure 4-3 one can find different layouts of pixel.

Unusual structure of the paths on the "Test Array" is due to next reasoning. This test vehicle is designed for DC measurement under x-rays. This means that we can access only these rows / columns which were made accessible at the design stage. One wants to be able to measure as many rows / columns as possible but has a finite number of output pads. Paths are long and formed so that any of them can be mechanically damaged (without damaging other paths) so one could create real high impedance state on the rows / columns.

Description of the technology processing for both test vehicles is given in the Appendix C.

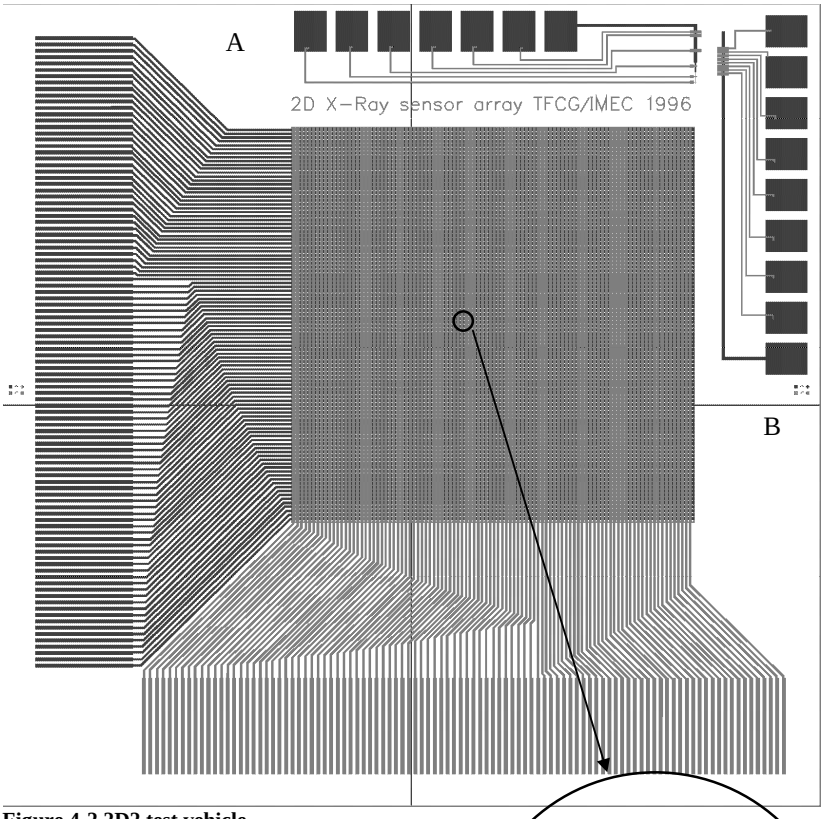

Figure 4-2 2D2 test vehicle

Table 4-2 2D2 included structures

Group	TFD included
A	2 200 x 200 µm TFDs on the same a-SiN:H island separated by 25 µm gap 200 x 200 µm 100 x 100 µm 50 x 50 µm 25 x 25 µm
B	Test column of 8 200 x 200 µm TFD on the same island separated by 25 µm gap

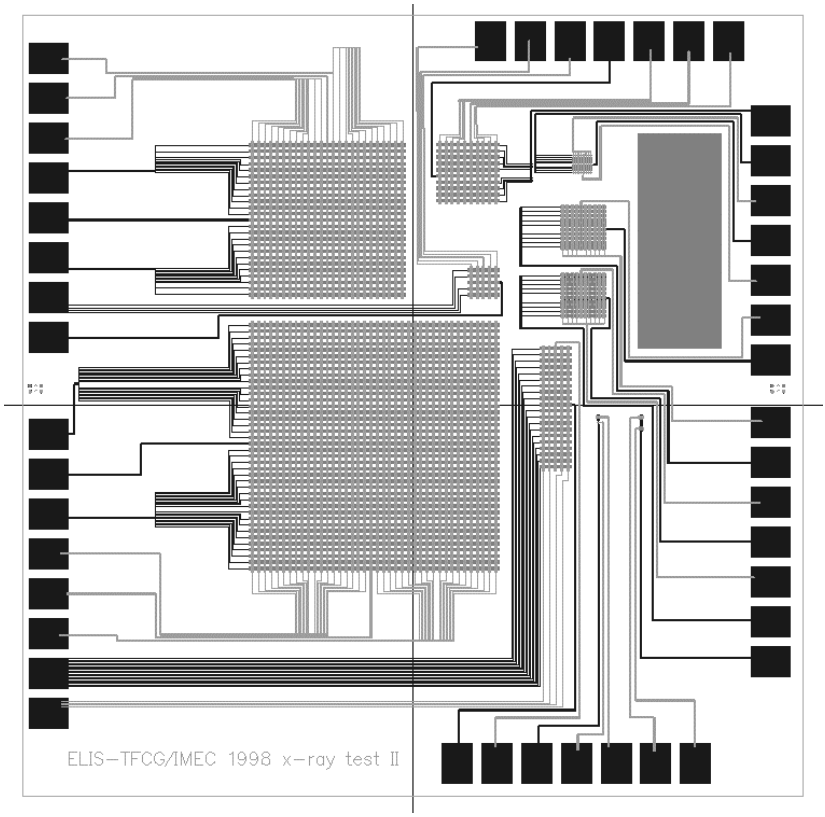

Figure 4-3 Test Array vehicle

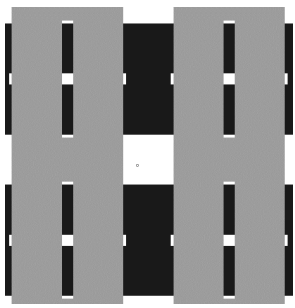

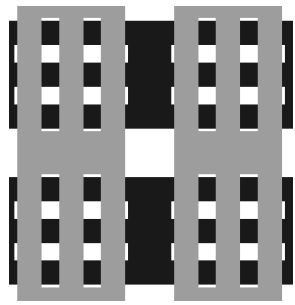

Table 4-3 Test Array test vehicle description

Code	Structure	Dimensions
1	Array	10 x 10 single TFD per 60 x 60 µm pixel 60 µm line to line
2	Array	10 x 10 single TFD per 200 x 200 µm pixel 200 µm line to line
3	Array	10 x 10 4 TFD per 200 x 200 µm pixel 90 µm line to line
4	Array	10 x 10 9 TFD per 200 x 200 µm pixel 90 µm line to line
5	Array	5 x 5 single TFD per 200 x 200 µm pixel 200 µm line to line
6	Single pixel	4 TFD in 200 x 200 µm pixel
7	Single pixel	9 TFD in 200 x 200 µm pixel
8	Single pixel	single TFD in 200 x 200 µm pixel
9	Single pixel	single TFD in 50 x 50 µm pixel
10	Array	20 x 5 single TFD per 200 x 200 µm pixel 200 µm line to line
11	Array	25 x 25 single TFD per 200 x 200 µm pixel 200 µm line to line
12	Array	40 x 40 single TFD per 200 x 200 µm pixel 200 µm line to line

Description of the prototype

Prototype consist of three major subparts:

- First, it is 2D x-ray sensor itself “2D2” test vehicle. This test vehicle is described above and in the Appendix C.

- Second, it is controlling and read out electronics. Development of driving and read out circuits should be fully credited to Geert Van Doorselaer. Full description and layouts could be found in [37] while here we will focus on the aspects important to “electronics-sensor array” relations.

- Third, protective housing in order to defend electronics against x-rays. This housing is simple Pb box with the window in front of sensor array. This window is covered by Al foil transparent to x-rays. The whole structure is reinforced by steel plates.

Overview of the prototype specifications is given in the Table 4-4 and photos in Figure 4 – 4.

Table 4-4 Prototype specifications

Field of view	2.5 x 2.5 cm
Pixel size	200 μm
Number of pixels	100 x 100 (8 columns to be read-out in current design)
X-ray source	W anode, 20 - 60 kV, 10 - 40 mA
Radiation level on detector	
30kV/10mA 4cm	320 mGy /sec
30kV/10mA 12 cm	150 mGy /sec
60kV/40mA 4cm	3.4 Gy /sec
60kV/40mA 12cm	1.3 Gy /sec
Housing	Lead 3 mm/ Steel 1 mm
Life time	more than 10 kGy as measured. There is no diagnostic degradation due to overexposure by direct radiation

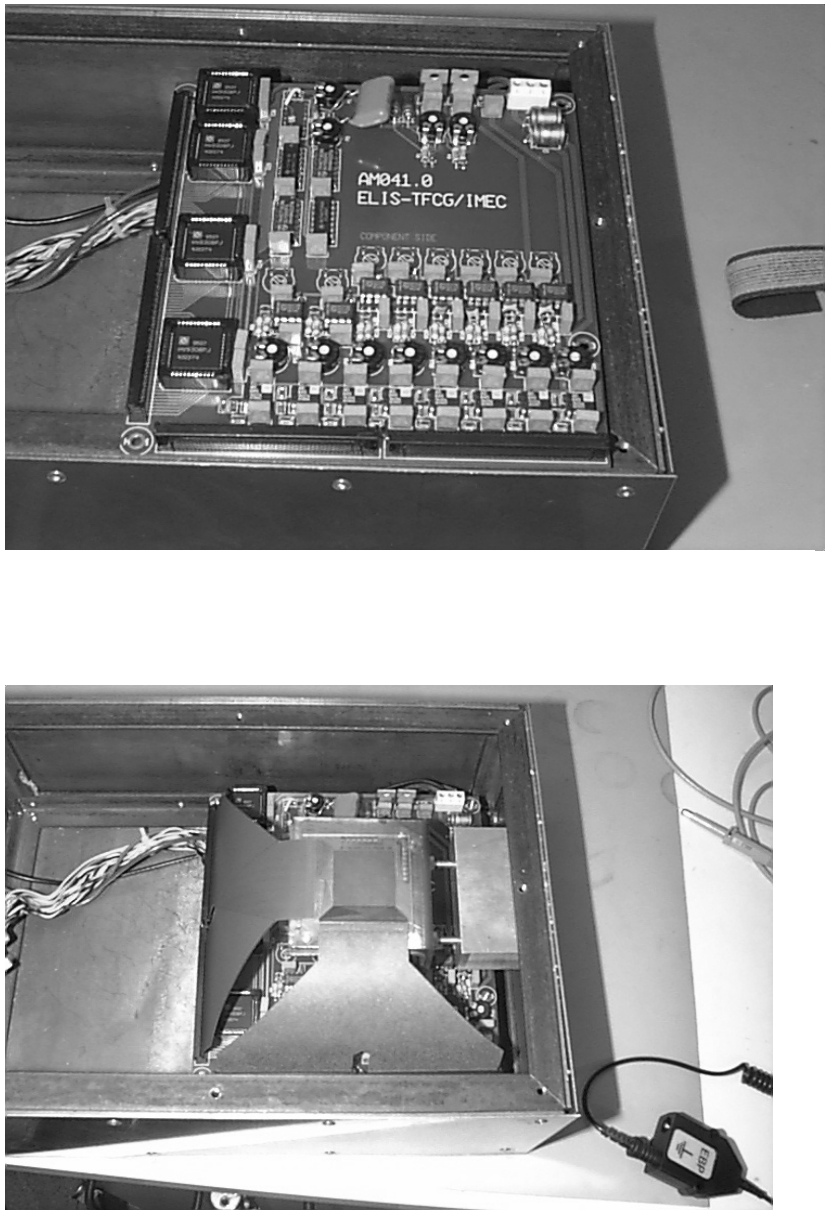

Figure 4-4 2D x-ray sensor array prototype : above - PCB with driving electronics; below - mounted sensor array

Electronic components

Electronic components in the x-ray prototype have dual function. This function is controlling the array and reading out electrical signal. In each frame period all row bus bars must be sequentially and exclusively selected. This is the function of the row drivers. Column read out electronics is responsible for converting small currents from the TFDs on the selected row into voltages.

Custom PCB hosting row drivers and column read out electronics has being designed and fabricated. The interconnection between PCB and the sensor array is based on bend flex material.

Row drivers

Supertex HV93 [38] components are used for the row drivers. These components are normally used in LCD or other display applications. Interfacing is done on TTL levels. Clocks are also generated on the PCB, using the 74LS624 VCO.

Column read out electronics

In the selected driving scheme an Operational Amplifiers (OA) are used for the column signal read out. The requirements of the OA used in the current to voltage conversion circuits are:

- maximal input impedance
- minimal bias current
- minimal offset voltage.

A maximal input impedance is needed for secure reading out of the very small currents. A minimal bias current is needed because bias currents generate additional current noise. And, finally, we need this minimal offset voltage because an offset voltage on the column generates additional currents in the diodes of the not selected rows. Moreover, these additional currents also contribute to generation of 1/f noise.

Analog Devices AD645K [39] OA were used in the prototype. They have a typical and maximum bias current of 0.7 resp. 1.5 pA, a typical differential input impedance of $10^{12}\Omega$ and a maximum offset voltage of 250 μV. Simulations in PSPICE showed that the equivalent input current noise of the circuit is about 12 pA.

Interconnection

For the interconnection bend flex made of 0.1 mm FR4 material was used. FR4 has much lower cost than other flexible materials. At the side of the sensor array a pitch of 0.4 mm was chosen. Here the bend flex was attached to the sensor array substrate with non-isotropic conductive glue. On the PCB however we decided to use ZIF connectors [40] in order to be able to test several sensor arrays on 1 PCB. The ZIF connectors used have a pitch of 1/20 inch (1.27 mm), so a special layout for the bend flex was made.

Measurements on the prototype: Results and discussion.

Matrix and Driving.

Measurements on the prototype which used the row drivers described above had led to quite an unexpected result: currents were measured flowing into and not out of column bus bars. So we have concluded that driving scheme in which non selected rows are kept at low impedance is not capable of correct read out. The roots of *this specific* problem are in the TFD behaviour and not the flaw of selected driving strategy.

As we have seen before (Optimisation of the TFD for use as a x-ray sensor.) the use of thick (1.4µm) a-SiN:H films in the TFD has led to pronounced "photo voltaic effect". This means that irradiated TFD with both terminals connected to the ground still generates current which is subtracted from useful signal. However small the photo current from the single TFD can be – this effect makes the whole difference when we speak about hundreds of interconnected TFDs.

DC measurements with disconnected row drivers[33] gave much more satisfactory results:

- Output current difference between irradiated / non irradiated state of about 5 nA per pixel with equivalent input current noise of less than 50 pA. This means that 100 grey scales are available[34];

- Photo voltaic effect is still visible (due to finite impedance of the rows) however not masking useful signal anymore;

Measurements of the response characteristics of the *TFD in the matrix* to a voltage pulse show that settling time[35] of the read out electronics is about

[33] This means that only one row is selected while other rows see high impedance
[34] True colour video card offer 256 grey scales.

1.5 ms. This leads to the scanning rate of 6 frames per second for 100 rows array if desire full range grey scale picture. This settling time is rather large but considering other read out circuits may help to shorten it. One of the possible decisions could be in the use of an integrator transimpedance amplifier such as the IVC102 [41] instead of linear transimpedance amplifier.

One of the conclusions at this stage that driving scheme for x-ray sensor array described above can not be implemented with the Supertex drivers. Drivers which would suit our purpose must offer:

- Low or high impedance state;
- Low (5 V) and high (12 V) output voltage.

Such drivers were custom designed at TFCG and used in what could be called Prototype II. New measurements in which photo voltaic effect do not mask useful signal anymore allow us to judge on the feasibility of the suggested driving strategy.

The results of measurements could be best illustrated by Figure 4-5 where the dependence of the output signal per pixel is shown as a function of number of rows / columns in the matrix. Output signal per pixel is given as a ratio between current measured from pixel in matrix I_{out} to the output signal of separate (single) test pixel I_o. Such representation of the output signal allows to break free from constant reference to the irradiation levels. As can

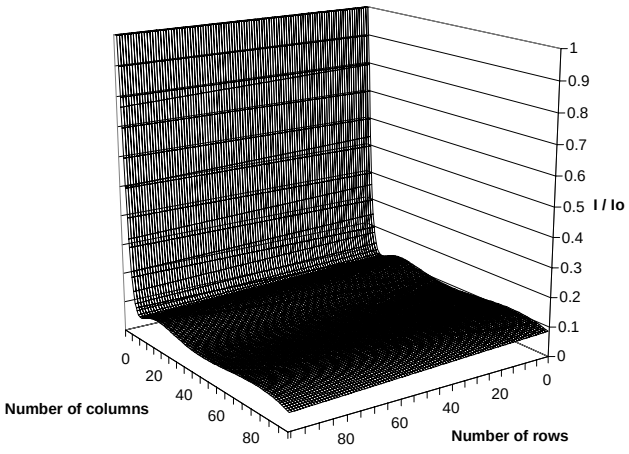

Figure 4-5 Response current of the pixel as a function of the matrix size

[35] To the level 99% of the final value

be clearly seen this ratio decreases with increase of both number of rows and number of columns. However the manner of the decrease is different.

Let us tackle first the decrease of output signal with increase of number of columns. For the matrix which consists of one column and *n* rows the output current in irradiated state will be equal:

$$I_{out} = I_{selected} - \sum_{i=2}^{n} I_{photo}(i)$$

The decrease of the output in this system is mainly due to the photo voltaic effect in non selected TFDs and can be easy compensated. Such compensation is based on reading additional "virtual" row every frame period. While reading *n* physical rows we receive I_{out} from every row. While reading *n+1* row we receive I_{out} in situation when no rows are selected (I_{base}). The actual current from the selected TFD is calculated as a sum of I_{out} and I_{base}. As our experiments show such an approach to solving of "problem of number of rows" works very good and is independent from the "number of columns problem".

"Number of columns problem" originates in the selected driving strategy. Without switching element in every pixel we end up in the situation when pixel "sees" (is exposed to) all the processes in all other pixels. As a result there is column to column interaction which leads to the depression of output current from the single pixel.

With the increasing number of columns *n* output drops in two stages: firstly - following the law ~ 1/*n*; secondly - stabilises at the level ~ 10 times lower than the original value. This "number of columns problem" is integral part of the selected driving strategy. Using the rectangular arrays with low number of columns does not really make sense as a way to overcome this problem[36].

The only possible conclusion can be formulated as follows: if one chooses to use x-ray sensing TFD in suggested driving scheme one shall formulate the requirements for the read out electronics assuming response characteristics of the TFD at the level 10 times lower than measured on the single cell. This means that the use of current driving strategy results in a simple technology processing for the 2D sensor array (2 photolithographic step) and severe requirements to the read out electronics. The use of the conventional active matrix driving strategy results in a complex technology processing for the array but more relaxed requirements to the read out electronics. So selection of the driving strategy will be dependent on for what kind of problem 2D sensor array will be used.

[36] Since the decrease of the output signal goes most intensively between 1 – 10 columns.

Feasibility of the driving scheme is a direct function of the area of application. Basically there are two of these in radiography: medical and industrial (non destructive examinations). While requirements for medical applications are well defined (and governed by the total dose of radiation), industrial application fields are strongly diversified. So for our discussion of feasibility I would use the requirements for digital mammography, medical application field with the most severe radiation dose / resolution requirements (Table 4-5 as compiled from discussions with R&D and medical people). It should be noticed that none of the current digital systems satisfy these requirements.

Table 4-5 Ideal digital mammography detector

Field of view	24 x 30 cm
Pixel size	50 µm
Number of pixels	4800 x 6000
Beam quality	29 to 49 KVP exposure time 30 µs up to 10 sec
Mean radiation level on the detector	12 mR
Exposure range with the image 400/I	0.4 – 160 mR/ 0.2 – 80 mR (speed class 30/60)

Selection of the driving strategy for this application (assuming the same quality of the sensing element) will be governed by:

- *pixel size*. Commercially available radiography systems use pixel size ~ 143 µm. Driving pixel size down to 50 µm presents certain difficulties for the AM approach (having a switching TFT in the pixel means lower sensor square) but not for our approach.

- *Number of pixels and exposure time*. For the AM approach these values are independent, min exposure time determined as a time needed to charge storage capacitors in the pixel. In our approach minimal exposure time is a function of number of rows, radiation must continue until all rows are read. With current prototype system the lower time border is not reachable.

For other medical applications – such as skeleton examinations difference between two driving schemes approaches slowly disappears.

One of the most intriguing questions at this moment can be formulated as “Is there an application field in which 2D a-SiN:H TFD x-ray sensor array in its current state (TFD sensitivity, driving strategy, readout and driving elec-

tronics) could be immediately used?". The answer is "Yes". Although at the current stage we fell short from the medical application requirements (mainly due to tenfold drop in sensor output with current driving scheme) there are at least two fields where such sensor can be used. Firstly, crystallography systems - currently market for Indirect (scintillator / a-Si photo diode) Systems which are not accepted for medical field. Secondly, control and optimisation of sawing of raw material in a lumber industry.

Pixel layout.

Optimisation of the pixel layout can contribute greatly to the response characteristics of the sensor. And major driving force to conduct such an optimisation is in the finding that output signal of the TFD is not directly proportional to the TFD square.

While conducting the optimisation of TFD for x-ray sensing we have measured response characteristics of the TFDs in 25, 50, 75, 100 and 200 pitch. The result of these measurements is that response current drops to the level at about 10 times lower than original with change from 200 x 200 µm TFD to 25 x 25 µm TFD. This is expected result because we work with avalanche multiplication and not photo effect. On the other hand this effect could be used in order to enhance pixel performance.

In order to achieve this goal we used 4 and 9 TFDs connected in parallel per pixel (unlike single TFD per pixel described previously). New pixel layouts could be find in Figure 4-3. The results of the measurements on such pixels are summarised in Figure 4-6, where dependence of the density of the response current is shown as a function of x-ray tube voltage and current. As can be seen there is a little difference in the density of response current in situation single or 4 TFDs per pixel. In situation with 9 TFD we observe noticeable increase of response.

The conclusion which can be directly extracted from this set of experiments is that one can enhance the response characteristics of the pixel by dividing single x-ray sensing TFD into *n* TFDs connected in parallel, where *n* is equal 9 or more.

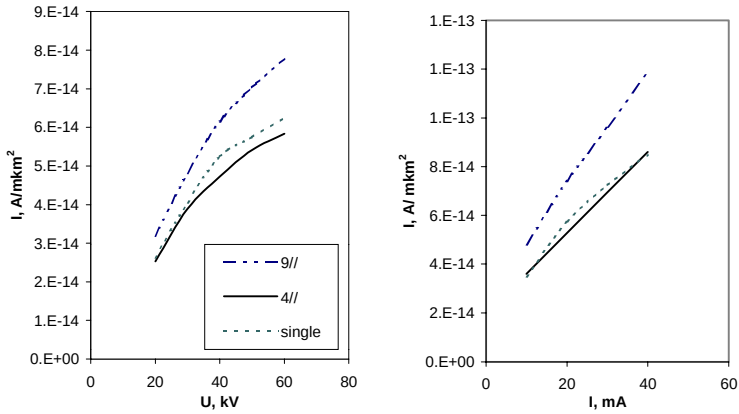

Figure 4-6 Influence of the pixel layout on the response current

Summary

In this Chapter we have discussed the 2D x-ray sensor *array* related problem. The discussion is based on the results of measurements on the developed prototype and includes the next key points:

Novel for digital radiography driving scheme is suggested. This scheme allows fully utilise the specific behaviour of the x-ray sensing a-SiN:H TFD under irradiation. Another major advantage of this scheme is the absence of the switching elements in pixels. This means that one do not need to worry about the behaviour of the switching element under direct x-ray irradiation.

Experimental part is based heavily on the results obtained with the help of two different test "array" vehicles. First of them was designed and produced for the study of the influence of array and pixel size and layout on the performance of the 2D x-ray sensor. The second was used in the prototype of 2D x-ray a-SiN:H TFD sensor array for dynamic measurements. This prototype also features custom row drivers and read out electronics.

Experiments with the different pixel layout have proven the initial assumption that breaking up single sensing TFD per pixel in few connected in parallel would improve response characteristics of the pixel.

The one of major results of this Chapter is practical testing of the suggested simplified driving scheme. Data presented in this Chapter allows to judge on the feasibility and limits of given approach. It also provides sufficient base for comparison between different driving strategies in the digital radiography.

CONCLUSIONS

Experimental data obtained and presented in this work lays solid foundation for the build up of "all a-Si" 2D x-ray sensor array and supports the three major claims formulated below.

"All a-Si" alloys 2D x-ray sensor array is possible.

As a first step we have introduced a-SiN:H as a competitor to the "conventional x-ray sensing materials". While looking back at the moment when this work was started we will see that the use a-Si alloys devices in digital radiography was limited to the information retrieval. This means that well established technology of a-Si:H TFT AM is mostly used for pixel control and read out. Second important application is in indirect systems with conversion of x-rays into visual light. These systems employ a-Si:H photodiodes.

But up to day a-Si alloys are not used for x-ray detection. The reason for this lays in a low stopping efficiency of a-Si to x-rays. As we discuss in the Chapter I if one wishes to efficiently absorb x-ray photons with Si one shall employ "thin" films 3 millimetres thick that is technologically unacceptable. Thus the straightforward decision is not possible. What is possible – and it seems to be a reasonable approach – is to stick with the a-Si films of few μm thick and see how far we can go from this starting point. The assessment of the situation includes the analysis of the radiation spectra and device aspects.

While looking at x-ray spectra it is hard not to notice that the bulk of the photons have an energy much lower than the nominal value. This is to say that x-ray analysis with the 80 keV energy gives us mean photon energy about 37.7 keV. So what one should do is focus on the detection and retrieval of information from the low energy photons. In other words one gets information from the high amount of low energy photons – and these photons can be stopped with sufficient efficiency. At the same time it is accepted that information carried by low amount of the high energy photons (low stopping efficiency) will be lost in the given approach. This draws natural limit on maximum energy of incoming x-ray radiation with which a-Si detection is possible. Targeting detection of photons with specific energy that have the most of information load is the niche for the full a-Si:H alloy 2D x-ray sensor array.

While working with a-Si alloys as an x-ray detector layer one should take extra precautions to assure the lowest loss of signal between the photon absorption and read out circuitry. In our case we have chosen to work with thin

film diode in avalanche multiplication mode to secure stable electrical output even with the small amount of absorbed photons.

Development of technology processing of a-SiN:H TFD dedicated to x-ray absorption.

Development of the technology processing of a-SiN:H TFD to be used as a x-ray sensor is a laborious task. X-ray environment imposes severe and sometimes contradictory requirements to the device. So in the Chapters II and III we :

- Select the system of thin film / TFD measurable characteristics and measuring procedures we use for description and control;
- Use the system of analytical tools that allow to decrease vast amount of technological experiments and yet yield trustful and reproducible results;
- Develop technology processing for 2D TFD array and optimize it with the respect to requirements of the x-ray sensing;
- Optimize design aspects of the TFD.

Such an approach is not specifically tuned to the x-ray applications (except the last steps) and can be successfully employed for the optimization of the a-Si films for different purposes. This is illustrated by development of the technology of a-SiN:H TFD with enhanced performance for LCD applications in the frame of the same approach.

Application of the novel driving strategy to 2D direct x-ray sensor array.

In order to demonstrate practical implementation of a-SiN:H x-ray sensing TFDs we have used driving strategy that is novel for digital radiography. The main advantage of realisation of the array with such driving strategy is the simplicity. With absence of switching elements in the pixels and need of row-to-column insulation the whole array is build up in two photolithographic steps, leading to low cost and high yield process. And not the least important reason is that arrays are produced completely in-house. The results obtained with the help of prototype allow us to judge on the feasibility of the different driving strategies for different application fields, medical as well as industrial.

Further development of this work should include, first of all, boosting the response characteristics of the sensor TFD. The frame for such work was outlined in Chapter III. The main idea is to increase the stopping efficiency

of a-SiN:H thin films. This could be done by introducing large amount of heavy “dopant” atoms without noticeable changes in electrical properties of TFD. This means developing doping procedure with very low doping efficiency, not a very challenging task for a-Si alloys.

Working in this direction will also reinforce the need for accurate x-ray source capable of producing narrow wavelength bands. This need was already acute during the presented work and if not satisfied will hinder further optimization of the sensor TFD. One adding to the other this means that increase in a-SiN:H x-ray sensor performance is determined by availability of highly specialized equipment.

Another subject calling for a careful study is determination of other possible fields of application. The fields of possible application of x-ray are highly diversified and such a study is a laborious task by itself and was not the primary subject of this study.

APPENDIX A: **Implementation of the system of experimental design and taboo search in PECVD optimisation software.**

This appendix is devoted to the description of calculations flow in the *PECVD optimisation* software developed in the frame of this work. It is indeed only the description of calculations flow and nothing more. For the discussion of the methods in use i would refer interested parties to the references [33], [35].

Analysis of orthogonal arrays.

Let us suppose that l_9 orthogonal array (Table A-1) was used in experiment setup and two properties e and f were measured.

Table A-1 l_9 orthogonal array

Factor/ exp. N	1	2	3	4	5	6	7	8	9
A	1	1	1	2	2	2	3	3	3
B	1	2	3	1	2	3	1	2	3
C	1	2	3	2	3	1	3	1	2
D	1	2	3	3	1	2	2	3	1

Table A-2 l_9 analysis for property e

Factor	Level	Mean	Var.
A	1	$(e_1+e_2+e_3)/3$	$[(3 \text{ mean } a_1)^2 + (3 \text{ mean } a_2)^2 + (3 \text{ mean } a_3)^2]/3\text{-cf}$
	2	$(e_4+e_5+e_6)/3$	
	3	$(e_7+e_8+e_9)/3$	
B	1	$(e_1+e_4+e_7)/3$	$[(3 \text{ mean } b_1)^2 + (3 \text{ mean } b_2)^2 + (3 \text{ mean } b_3)^2]/3\text{-cf}$
	2	$(e_2+e_5+e_8)/3$	
	3	$(e_3+e_6+e_9)/3$	
C	1	$(e_1+e_6+e_8)/3$	$[(3 \text{ mean } c_1)^2 + (3 \text{ mean } c_2)^2 + (3 \text{ mean } c_3)^2]/3\text{-cf}$
	2	$(e_2+e_4+e_9)/3$	
	3	$(e_3+e_5+e_7)/3$	
D	1	$(e_1+e_5+e_9)/3$	$[(3 \text{ mean } d_1)^2 + (3 \text{ mean } d_2)^2 + (3 \text{ mean } d_3)^2]/3\text{-cf}$
	2	$(e_2+e_6+e_7)/3$	
	3	$(e_3+e_4+e_8)/3$	

Terms agreement: from now on we will mark “factor c with level 1” as c_1 and “property e measured in experiment 5” as e_5. Calculations of variance of property is going like follow (see Table A-2):

- Calculation of mean values for every factor and level;
- Calculation of variance;
- Calculation of contribution ratio

Value of CF in the table above is calculated as:

$$CF = \frac{\left(\sum_{n=1}^{9} En\right)^2}{9} \qquad \text{(A-i)}$$

Contribution ratio of every parameter now is calculated as contribution of every parameter to the sum of variances (in %).

For the prediction of the value of property e produced at the factor’s levels different from ones in the l_9 array we will use hyperbolic aid approximation. Value of property x is estimated as:

db x= db (mean a_i)+db (mean b_j) + db (mean c_k)+db (mean d_l) -3 db t (A-ii)

$$db(p) = -10\log\left(\frac{100}{p} - 1\right) \qquad \text{(A- iii)}$$

$$p = \frac{100}{1+10^{\frac{db(p)}{-10}}} \qquad \text{(A - iv)}$$

Where i,j,k,l refer to the levels under consideration and t is simple sum of values e from all 9 experiments; formulas A-iii and A-iv are just conversion between decimal / decibel values.

To provide correct estimation one have to choose base set from the l_9 array. Criterion for choosing such a set is that two factors with the highest contribution ratio shall be at the same levels as in the set for which we would like to make an approximation. It is a beauty of orthogonal arrays that there will be always such a base set. So in fact, the base line of the prediction of properties is that we predict influence of two *less* important factors.

To finish our prediction we will need three values:

- X measured value for the base set
- X_x estimated value for the base set (using a - ii)
- X_y estimated value for the set in question (using a- ii)
- Ω correction as

$$X = \frac{1}{1+\Omega} \tag{A-v}$$

Where :

$$\Omega = \left(\frac{100}{X} - 1\right)\frac{\left(\frac{100}{Xy} - 1\right)}{\left(\frac{100}{Xx} - 1\right)} \tag{A - vi}$$

Following this procedure values of any property for any legal parameter set could be estimated.

As for the search of the optimal parameter set we will use taboo search. Search target are defined through two coefficients: *target value* and *weight* for every characteristic of the a-SiN:H thin film and/or TFD on it's base. *Target value* of the final film property can be set to the certain value or to the minimal/maximal value possible in the experimental data pool. *Weight* coefficient is varying from 0 % for "least important" situation to 100 % for "most important". At the *i* iteration the direction of the next step is chosen on the base of *move*.

$$move = \sum_{n=1}^{M} \frac{Weight_n}{BestSoFar_n}\left[\left|C_n - T_n\right| - \left|BestSoFar_n - T_n\right|\right]$$

Where m is amount of the film's characteristics under optimisation, t - target value for the current characteristic, best so far is the best found so far. Move is positive if with the new factor set we get closer to target and negative if we get farther.

Let us look more carefully on the selection process of the best move in the frame of the taboo search.

- Certain *current set* of the l_9 array factors is selected.
- Calculate value of *move* for all the neighbours - *potential sets*.
- Select *best potential move* and appropriate *best potential set*.

- **Key point 1**: if there are no taboos or modifiers on this *best potential move* then
    - Accept the *best potential move* as a *best move*
    - Accept the *best potential set* as a *current set*
    - Taboo this move
    - Update taboo references
    - Update modifiers references
    - **Repeat** from the line 1

Such situation is a most probable in the beginning of the search or on the surface with very nice single global minimum.

- **Key point 2**: if the *best potential move* is under some kind of taboo, then
    - Limit *potential moves* to one which are not under taboo.
    - Search for *best potential move*.

- **Key point 3**: if there are any modifiers
    - Apply modifiers

- **Inspiration**. If the *best potential move* has negative value decide on using inspiration with the possible choices (on the all possible *best potential moves*.):
    - Overriding taboo (and to what extent - in the current setup taboo can be overridden only in case when it will disappear with the next move anyway - with 50 % probability if overriding taboo will lead to the positive value of the *move*)
    - Ignoring modifier (in the current setup if the *potential best move* is heavily penalised, for example, for the frequent use of the factor but this factor has major contribution ratio to the given film's property - ignore with 50 % probability if ignoring the modifier will lead to the positive value of the *move*)
- After decision is made continue as in **key point 1**.

PECVD optimisation software (figure A-I), developed in the frame of this work, utilises this calculation process flow. It includes tools for creating, editing, importing source data for orthogonal array analysis and possibility to search for the optimal PECVD parameters set for the given search targets either with taboo search either with brute force. The control panel of the computer program is shown in the figure A-I.

There is one major point on using *PECVD optimisation* software - as any other software - human thinks, computer works. This basically means that quality of the input data is the responsibility of the operator and will determine the quality of the results of the optimisation. Even if the quality of input data is superb it is often useful to run search few times with targets

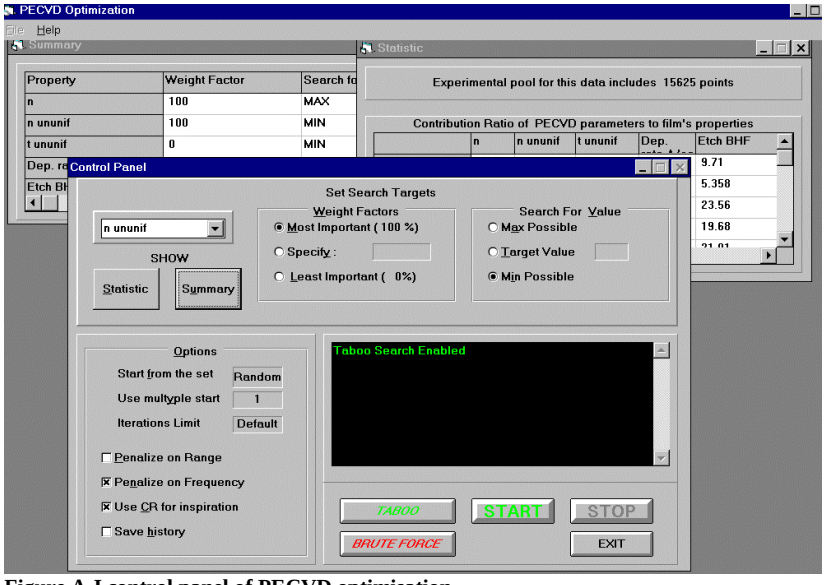

Figure A-I control panel of PECVD optimisation

defined through different film characteristics. This sometimes gives new insights on what is going on.

APPENDIX B: **a-SiN:H TFD based active matrix for 2x2" LCD: technology processing description.**

Production of liquid crystal display involves not only forming array of switching elements (TFD in our case) but also additional steps, such as integration of the pixel electrodes. Material usually used for the pixel electrodes is ITO and it's processing includes 4 hours baking step at 400 ^{o}C. So one should insure that processing of ITO will not interfere with TFD characteristics in case when pixel electrodes are formed after forming TFD and processing of TFD will not influence ITO 's characteristics in the case when pixel electrode is formed first. Major concerns here are (i) will TFD processed at 260 ^{o}C withstand 400 ^{o}C bake and (ii) protection of ITO layer from the different influences during the processing of TFDs. At the same time we would like to have as little photolithographic steps as possible.

Results of some experiments on the sheet resistance of the ITO are presented in figure B-1.there also other comments on the subject:

- Increasing of baking time of ITO/Cr sandwich at 400 ^{o}C to 4 hours leads to decrease of sheet resistance of ITO to 1.72 10^2 Ohm/ . On one hand it's not such a big difference but on the other keep the process compatible with other processes at TFCG without making it more complicated;

- Forming Cr on ITO with wet etch is not very reproducible process and the best thing for that is lift-off technique;

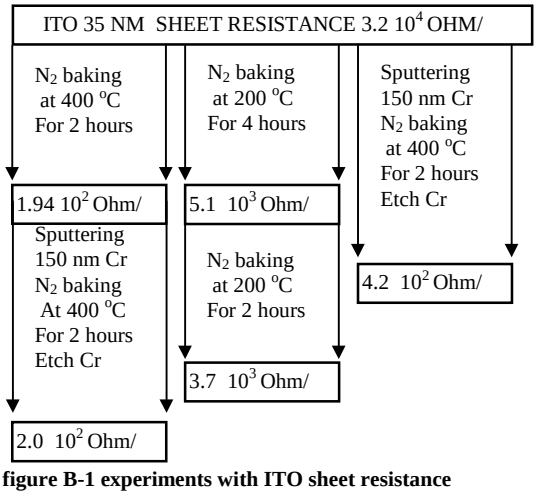

figure B-1 experiments with ITO sheet resistance

- Lift-off technique is also preferable if we refer to the photoresist which is influenced by Cr etching. This influence cause difficulties in removing photoresist so more careful control needed. With use of lift-off we eliminate this problem.

So as a conclusion for these experiments we can state that:

1. Neither baking ITO at 200 C nor baking TFD at 400 C is not an option. TFD must be formed after the forming of ITO pixel electrode.

2. ITO pixel electrode should be defended from influences of different etchings during the processing so possible decision is removing Cr from pixel at the very last moment.
3. Lift-off technique is preferable for forming pixel electrodes.

Technology processing.

Step 1: cleaning of substrates
Material : 2"x2"x0.032" corning 7059 glass substrates.
Tagging : the tag is "a" and "t" followed by a number for the am substrate and top glass with columns respectively.
Cleaning : see cleaning substrates /TFCG knowledge base.

Active matrix

Step 2: forming rows and pixel electrodes (image reversal)

- photoresist : AZ5218-e.
- illumination : 10 s through mask "row and pixel electrode"; 2 min reversal bake on the hot plate at 120°C; 10 s without mask from the front side.
- developing : 35 s.
- control 1 : special attention should be paid to the clean gaps between pixel electrode and rows above/below ; good separation of the two bottoms electrodes of the TFDs.
- material : ITO/Cr
- thickness : 35/150 nm.
- purpose : forming of the rows, bottom electrodes of the TFDs and pixel electrodes. Use of the ITO/Cr sandwich allows to decrease amount of masks needed. Cr on pixel electrodes defends the pixel ITO properties being altered during the processing.
- application : sputtering, in one step without taking substrates on air after the ITO sputtering.
- look : shining metal, just like a perfect mirror.
- patterning: 1 min USA in acetone

- control: no shortages between pixels, rows, TFD's electrodes.
- bake: 4 hours at 400 ^{o}C in N_2 flow

Step 3: forming a-SiN:H.

- material : a-SiN:H
- thickness : 35 nm.
- purpose : forming of the active areas of TFDs and protection of Cr row lines.
- application : PECVD, 260 ^{o}C
- look : golden yellow (on Cr)

  patterning :
- photoresist : s1400-31.
- illumination : 10 s through mask "a-SiN:H".
- developing : 1 min 30 s.
- control: photoresist is only on rows with small rectangles covering TFD's bottom electrodes.
- post-bake.
- etching : 1 min in HF 10 (horizontal, static)
- control: there is no a-SiN:H on pixel electrodes.
- stripping.
- control: quick check - photoresist on a-SiN:H is almost the same colour as a-SiN:H itself.

Step 4: forming TFD's top electrodes.

- material : TiW
- thickness : 150 nm.
- purpose : forming of the TFD's top electrodes.
- application : sputtering
- look : shining metal, just like a perfect mirror.

  patterning :
- photoresist : s1400-31.

- illumination : 10 s through mask "TFD's top electrodes".
- developing : 1 min 30 s.
- control: there is only photoresist left on small rectangles over the TFD's bottom electrodes.
- post-bake.
- etching : 45 sec in H_2O_2 at 50 ^oC, 15 sec rinse in H_2O_2 at room temperature (horizontal, static).
- control: all area but TFDs is clear from TiW.
- stripping.
- control: there is no photoresist on substrate.

Step 5: open contacts to row electrodes (image reversal)

- photoresist : AZ5218-e.
- illumination : 10 s through mask "open contacts"; 2 min reversal bake on the hot plate at 120°C; 10 s without mask from the front side.
- developing : 35 s.
- control: there are 64 clean openings on rows contact areas.
- etching : 1 min in HF 10 (horizontal, static)
- control: clean white Cr on contact areas
- stripping.
- control.

Step 6: external contacts

- material : TiW/Au.
- thickness : 50/200 nm.
- purpose : shunt the contacts to the outside.
- application : sputtering.
- look : shining gold.

patterning :

- photoresist : s1400-31.
- illumination : 10 s through mask "open contacts".

- developing : 1 min 30 s.
- control: there is only photoresist left on the external contacts.
- post-bake.
- etching : Au on sight 30±5 min in KI/I_2. The TiW must be completely visible. TiW on sight 30 sec.
- control: the matrix must be completely free of golden spots.
- stripping.
- control: the external contacts look like fine golden lines.
- control: check the test TFDs characteristics.

Step 7: removing Cr from pixel electrodes.

- purpose: remove Cr from pixel electrodes so we have there only ITO
- etching: Cr etching ~ 35 min (horizontal, static)
- control: pixel electrodes must be free of any Cr spots. (when etching is ok pixel electrodes hardly could be visible on glass substrate)

Step 8: black polyimide covering

- purpose : improving optical performance of the display.
- application and patterning : see black polyimide covering / TFCG knowledge base.
- illumination : mask "black matrix".
- control: in the matrix the pixel surface must be free of polyimide.

Top substrate

Step 9: forming columns electrodes.

- material : ITO.
- thickness : 150 nm.
- purpose : forming of the vertical bus bars.
- application : sputtering.
- look : transparent with a brownish shade.

- patterning :
- photoresist : s1400-31.
- illumination : 10 s through mask "columns".
- developing : 1 min 30 s.
- control
- post-bake.
- etching : HF 250 25 min (vertical, static)
- control: check the resistance between two points on the substrate.
- stripping.
- control

Step 10: external contacts

- material : TiW/Au.
- thickness : 50/200 nm.
- purpose : shunt the contacts to the outside.
- application : sputtering.
- look : shining gold.
- patterning :
- photoresist : s1400-31.
- illumination : 10 s through mask "open contacts" (alignment on structures).
- developing : 1 min 30 s.
- control: there is only photoresist left on the external contacts.
- post-bake.
- etching : Au on sight 30±5 min in KI/I_2. The TiW must be completely visible.
- TiW on sight 30 sec.
- control: the substrate must be completely free of golden spots.
- stripping.
- control: the external contacts look like fine golden lines.

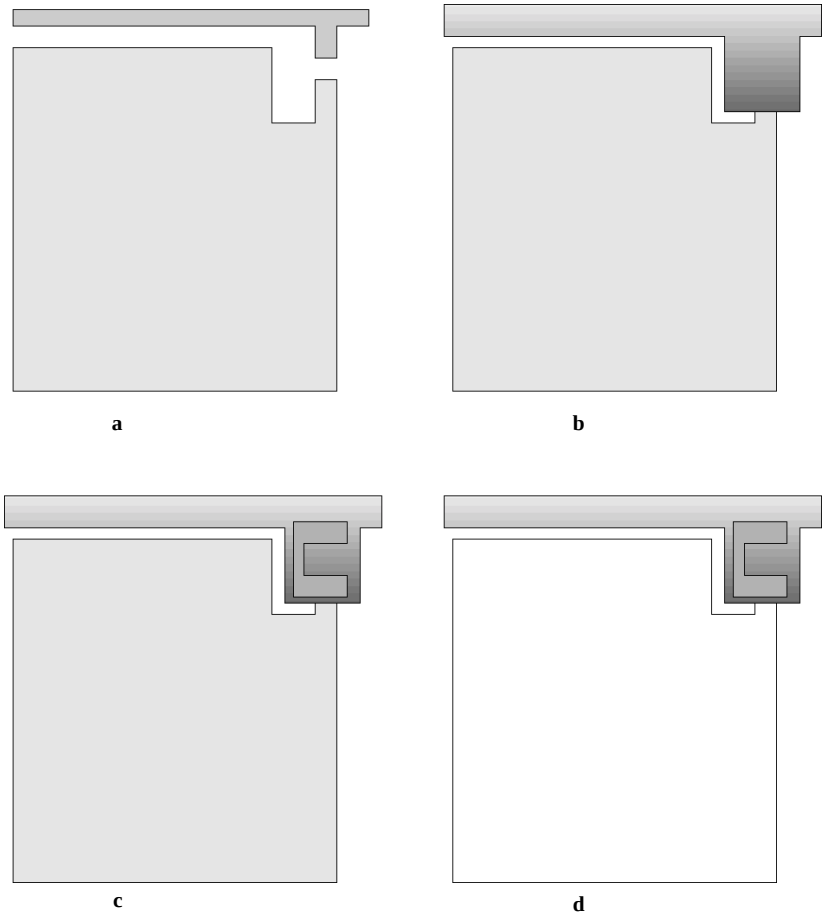

Figure B-2 forming pixel of LCD. A - step 2; b -step 3; c - step 4; d - step 7

This technology processing flow is illustrated in figure B-2.

Few runs were processed along these lines and electrically tested with the good results. Photograph of the array is shown on the figure B-3.

APPENDIX C**: a-SiN:H TFD x-ray sensor array technology processing**

Both test vehicles are processed with alike technology which includes very few photolithographic steps. This process is inspired in big part by technology developed for LCD described in Appendix B. The only difference is that we switch to wet etching of Cr for both row and column bus bars.

Technology processing for x-ray sensor array

Step 1: cleaning of substrates
Material : 2"x2"x0.032" corning 7059 glass substrates.
Tagging : the tag is "X" followed by a number.
Cleaning : see cleaning substrates /TFCG knowledge base.

Step 2: forming row bus bars

- material : Cr/TiW
- thickness : 50/150 nm.
- purpose : forming of the row bus bars.
- application : sputtering, in one single vacuum cycle.
- look : shining metal, just like a perfect mirror.

  patterning :
- photoresist : S1818.
- illumination : 7.5 s through mask "Row".
- developing : 30 s.
- control
- etching : 45 sec in H_2O_2 at 50 ^oC; rinse; 9 minute in Cr etchant at 50 ^oC; rinse scrupulously - otherwise there will be residue visible after a-SiN:H deposition. (horizontal, static)
- control
- stripping.

Step 3: forming a-SiN:H.

- material : a-SiN:H
- thickness : 1.4 μm.
- purpose : forming of the active areas of TFD
- application : PECVD, 260 ^{o}C
- look : dark yellow (wet sand on metal)

  patterning :
- photoresist : AZ4562.
- illumination : 10 s through mask "a-SiN:H".
- developing : 30 s - on sight.
- control: photoresist is only on rows
- post-bake.
- etching : RIE
- control: there is no a-SiN:H anywhere but on rows
- stripping.

Step 3: forming column bus bars

- material : TiW/Cr
- thickness : 50/150 nm.
- purpose : forming of the column bus bars.
- application : sputtering, in one single vacuum cycle.
- look : shining metal, just like a perfect mirror.

  patterning :
- photoresist : S1818.
- illumination : 7.5 s through mask "Column".
- developing : 30 s.
- control
- etching : 9 minute in Cr etchant at 50 ^{o}C; rinse scrupulously;
- Stripping

- etching TiW 45 sec in H_2O_2 at 50 ^oC; rinse;(horizontal, static) using Cr as a mask

As our experience shows the technology processing for the sensor array can be even simpler without affecting the characteristics of the array (SEE RESULTS). It is possible to come down to ***two photolithographic steps***, if sputter top metals without forming a-SiN:H in advance. Then, after forming Cr, TiW and a-SiN:H could be formed by single step by RIE using Cr as a mask. The only drawback of such processing is that RIE is performed in two steps (but still in the same vacuum cycle) and takes somewhat more time. But comparing to saving one photolithographic step it is a minor drawback indeed.

References

1. Rowlands J., Kasap S., Amorphous Semiconductors Usher in Digital X-ray Imaging, Physics Today, Nov., 1997, pp. 24 - 30
2. Spahn M., Alexander J., Gmeinwieser J., Amorphous Silicon Solid State Detectors And Their Future Use In Medical x-ray Imaging, Electromedica V.65, N1, 1997, Pp.37-41
3. Volk M., Strotzer M., Alexander J., Gmeinwieser J., Frund R., Seitz J., Manke C., Spahn M., Feuerbech J., Flat Panel x-ray Detector Using Amorphous Silicon Technology: Reduced Radiation Dose For The Detection Of Foreign Bodies, Investigative Radiology, V.32, N7, 1997, Pp.373-377
4. Jeromin L.S., Lee D., Nakagawa T., Ugai Y., Aoki S., Application Of A-S Active Matrix Technology In A X-Ray Detector Panel., Sid Digest Volume XXVIII, 1997, Pp 91 - 94
5. Brauers A., Conrads N., Frings G., Schiebel U., Powell M.J., Glasse C., X-ray Sensing Properties Of A Led Oxide Photoconductor Combined With An Amorphous Silicon TFTs Array , Mrs Symp. Proc. V507, 1998, Pp. 321-326
6. Kinno A., Atsuta M., Tanaka M., Sakagichi T., Ikeda M., Suzuki K., Development Of A Large Area Direct Conversion X-Ray Image Detector, Proc. Idw'98, 1998, Pp. 159-162
7. Rodriks B., Lee D., Hoffberg M., Cheung L., Williams C., Dittrich D., Imaging Performance Of A 14x17 Se + TFTs Direct Radiography System, Proc. Icps'98, 1998, Pp.319 - 323
8. Park B., Murthy R.V.R.,Sazonov A., Nathan A., Chamberlain S.G., Process Integration Of A-Si:H Schottky Diode And Thin-Film Transistor For Low-Energy X-Ray Imagine Applications , Mrs Symp. Proc. V507, 1998, Pp. 237-242
9. Golikova O., Semiconductors V 25 N 9 1991, 1517
10. Popov A. I., Michalev N., Shemetova V.K., "Structural Modification Of Some Glassy Chalcogenides",Phil.Mag.B V 47 N 1 1983, 73 - 81
11. Popov I. A., Semiconductors, V 30 N 3 1996, 258
12. Adler D., Physical Properties Of Amorphous Materials, Plenum Press, 1985
13. Bruecsch P., Phonons: Theory And Experiments Ii, Springer Verlag, 1986
14. Payton D. N.,. Visher M, Phys. Rev. V 154 1961, 802
15. Gautman G., D. Joydeep, R. Swati , Barua, Appl. Phys. Lett. V 55 N 19 1989, 1975
16. Kazurov B.,. Voronkov E, Popov I. Tchernorotov BP, Elect. Ind. N3 1993, 25
17. . Chen Y, Clough F.J., Sankanara E.M., Narayanan, Eccleston W., Milne W, Proc. Eurodisplay'96, 1996, 21

18. Shanon J.M, Hartman W., Jacobs J.M., Kuntzel J. H., Kwint J.P.M., Pitt M.G., Et Al., Tfd-R: Improved, Stable 2-Terminal Devices For State-Of-The-Art Am-Lcd, Proc.14th Int.Display Res. Conf., 1994, 373 -376
19. Howard W.E "Active-Matrix Techniques For Displays", Sid Seminar,V.2, 1986, P. 7.2/1-38
20. Ohira K.Et Al, Analysis Of High Resolution Active-Matrix Lcd With Sin_x - Diode Array", Proc. Japan Display'89, 1989, P.452
21. Aivazov A.A., Budagyan B.G. Et Al "Growth Process, Structure And Thermal Sability Of A-Sin:H Films", J. Non-Cryst.Sol., V. 146, 1992, P.190
22. Aivazov A.A., Budagyan B.G., Meltin M.N. "Influence Of Structural Inhomogenity On Conductivity And Relaxation Processes In A-Si:H And A-Sin:H" Phys Semic., V. 26, N.9, 1992, P. 890
23. Konuma M."Flim Deposition By Plasma Techniques", Springer-Verlag, Berlin Heidelberg New York, 1992.
24. Sawin H.H, "A Review Of Plasma Processing Fundamentals", Solid State Technology, Aprl 1985, P. 211 - 216.
25. Chapple-Sokol J.D.,. Pliskin W.A,. Conti R.A,. Tierney E, Batey J., "Energy Considerations In The Deposition Of High Quality PECVD Silicon Dioxide", Proceedings Of The Eight Symposium On Plasma Processing, Montreal, Canada, Mei 1990, P. 593 - 604.
26. Rand M.J.,. Wonsidler D.R"Optical Absorption As A Control Test For Plasma Silicon Nitrid Deposition" - Solid-State Science And Technology, - Jan. 1978, - P.99
27. Kniffer N,.Schroder B,. Geiger J "Vibrational Spectroscopy Of Hydrogenated Evaporated Amorphous Silicon Films", J. Non-Cryst. Sol, 58 (1983), P.153
28. Hydrogen In Disordered And Amorphous Solids, Ed. G. Bambakidis And R.C. Bowman, Nato Asi Series B, V136, Plenum Press, N.Y., 1986, P. 428
29. Aivazov A.A. Et Al. "Analysis Of Ir Spectra Of A-Sin:H Alloys On The Basis Of The Induction Model", Physics And Technology Of Semiconductors, Eng.Tr -28/6 (Jun 1994),-P.781
30. Landford W.A., Rand M.J., " The Hydrogen Content Of Plasma Silicon Nitride", J. Appl.Phys., 49 (4) 1978, P.2473.
31. Aivazov A.A., Budaguan B.G., Stryahilev D.A., "Investigation Of Inhomogeneities In A-Sin:H Alloys By Infrared Spectroscopy", J.Non-Cryst. Sol., 167 (1994) P.185
32. Lernout J., Optimisatie En Karakterisatie Van Pecvd Siliciumoxinitridelaen - Toepassing In Een Dunne Film Multichipmodule Op Silicium., Ph.D.Thesis., University Of Gent, 1998,Pp. 36 - 47
33. .Taguchi G, System Of Experimental Design (Kraus International, New-York, 1988)
34. De Baets J., Van Calster A., Et Al Silicon Oxinitride Layers For Device Passivation, Proc. Of Elec.-Chem Soc., Toronto 1992, Pp 192-200

35. Glover F., Laguna M., Taboo Search *In* Modern Heuristic Techniques For Combinatorial Problems, Ed. C. Reevs, Mcgraw-Hill Book, 1995
36. Morozumi S. et al “Completely integrated contact type linear image sensor”, IEEE Trans.Elec.Dev., 32 (8), 1995, pp.1546 – 1550
37. Popov I, Van Doorselaer G., Prototype of 2D direct x-ray sensor array on the base of a-SiN:H TFD, Research report, TFCG/IMEC, 1997
38. Supertex, http://www.supertex.com/databook/ch12/pdf/HV93.pdf
39. Analog Devices, http://www.analog.com/products/sheets/AD645.html
40. AMP Flexible Film Products Catalog 82007 (1986) pp. 30 – 31
41. Burr-brown; http://www.burr-brown.com/products/datasheets/IVC102.html